

# Lawrence Berkeley National Laboratory

## Recent Work

### Title

NEUTRON AND GAMMA MISSION IN FISSION

### Permalink

<https://escholarship.org/uc/item/2b04v1rd>

### Authors

Nifenecker, H.  
Signarbieux, C.  
Babinet, R.  
[et al.](#)

### Publication Date

1973-07-01

Presented at the Third Symposium on the  
Physics and Chemistry of Fission,  
Rochester, New York, August 13-17, 1973

LBL-1950

RECEIVED  
LAWRENCE  
RADIATION LABORATORY

AUG 8 1973

LIBRARY AND  
DOCUMENTS SECTION

NEUTRON AND GAMMA EMISSION IN FISSION

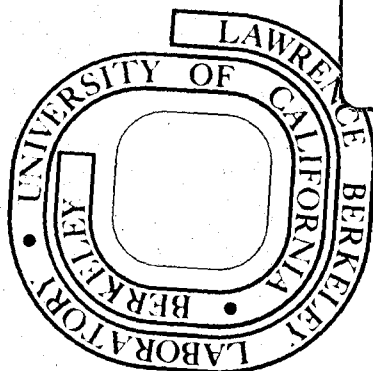
H. Nifenecker, C. Signarbieux,  
R. Babinet, and J. Poitou

July 1973

Prepared for the U. S. Atomic Energy Commission  
under Contract W-7405-ENG-48

TWO-WEEK LOAN COPY

This is a Library Circulating Copy  
which may be borrowed for two weeks.  
For a personal retention copy, call  
Tech. Info. Division, Ext. 5545



LBL-1950

cd

34c

## **DISCLAIMER**

This document was prepared as an account of work sponsored by the United States Government. While this document is believed to contain correct information, neither the United States Government nor any agency thereof, nor the Regents of the University of California, nor any of their employees, makes any warranty, express or implied, or assumes any legal responsibility for the accuracy, completeness, or usefulness of any information, apparatus, product, or process disclosed, or represents that its use would not infringe privately owned rights. Reference herein to any specific commercial product, process, or service by its trade name, trademark, manufacturer, or otherwise, does not necessarily constitute or imply its endorsement, recommendation, or favoring by the United States Government or any agency thereof, or the Regents of the University of California. The views and opinions of authors expressed herein do not necessarily state or reflect those of the United States Government or any agency thereof or the Regents of the University of California.

## NEUTRON AND GAMMA EMISSION IN FISSION\*

H. Nifenecker<sup>†</sup>Lawrence Berkeley Laboratory  
University of California  
Berkeley, California 94720

and

C. Signarbieux, R. Babinet and J. Poitou

CEN Saclay  
France

A Review

Abstract

Some of the characteristics of neutron and gamma emission in fission are reviewed. Recent measurements of the average number of neutrons as a function of fragment masses  $m$  and total kinetic energy  $E_k$  show distinctive differences with previous ones. The reasons for these discrepancies are analyzed and it is shown that, at present, the use of large neutron detectors yields safer results than that of small neutron detectors. The energy necessary for the emission of one additional

\*Work performed under the auspices of the U. S. Atomic Energy Commission.

<sup>†</sup>On leave from CEN Saclay.

Third Symposium on the Physics and Chemistry of Fission, Rochester, New York, August 13-17, 1973.

neutron is discussed and shown to be of the order of 8 MeV, in the case of the  $^{252}\text{Cf}$  spontaneous fission. This includes the effect of the observed correlation between neutron multiplicity and total  $\gamma$  ray energy. This correlation cannot be explained on the basis of neutron binding energy variations alone and is interpreted as an effect of the spins of the fragments.

The gross features of the  $\gamma$  ray emission by fission fragments (time, energy, angular distributions) are summarized. These features appear to be in agreement with a statistical de-excitation of the fragments provided angular momentum effects are suitably taken into account.

The variances of the excitation energies of the fission fragments as a function of  $m$  and  $E_k$  are obtained from the observation of neutron number distributions. Here again it is shown that, at present, the use of large neutron detector is the safer technique. The knowledge of these variances allow an improved estimation of the difference between the total energy release in fission and the minimum potential energy of the scission configuration. This difference is found to be at most of the order of 7 MeV in the  $^{252}\text{Cf}$  of spontaneous fission.

One of the basic assumptions of the "fission band" model of W. Nöremberg<sup>(41)</sup> is strongly supported by the observation of 1.7 MeV difference in the total kinetic energy of fissions giving rise to odd Z-odd Z and even Z-even Z pairs of fragments. This model also accounts for many of the aspects of the neutron and  $\gamma$  emission in fission.

## Introduction

Rather than being a general survey of all experimental evidence on the neutron and gamma emission in the fission process, this paper will focus on some of the recent detailed measurements relative to this subject. In the first section we shall examine the average neutron numbers as measured as a function of both mass and kinetic energy of the fission fragments. Although recent measurements do not show new qualitative features they quantitatively differ from previous ones, especially with respect to the value of the energy carried away per neutron. The disagreement may be traced to different experimental approaches; one set of experiments makes use of low efficiency plastic scintillators and the other of high efficiency loaded liquid scintillators. We shall discuss the relative advantages and drawbacks of these two techniques. In the second section we shall examine some of the detailed measurements of gamma-ray energy, gamma-ray multiplicity and gamma-ray angular anisotropy which have been carried out as a function of the energy, mass or charges of the fragments. Combining the neutron, gamma and fragments kinetic energy measurements the measured energy release in fission can be compared with predictions of mass tables. We shall present evidence of even-odd effects when the neutron, gamma emission and the fragments kinetic energies are measured as a function of the charges of the fragments. We conclude this section with a discussion of the angular momenta of the fragments. In the third section we shall discuss the detailed measurements of the variances of the neutron number distribution in view of the large discrepancies observed between the results obtained in experiments using low efficiency and high efficiency neutron detectors, respectively. We show how the variances of neutron number can be transformed into variances of the excitation energies of the fragments. In the last section we shall discuss the

significance of the even-odd effects and the possible use of the variance measurements for testing different theories of fission.

I. Variations of the average neutron number as a function of mass and kinetic energy of the fission fragments

At the time of the Salzburg conference most of our knowledge of the average neutron number variations as a function of mass and kinetic energy of the fragments were obtained using low efficiency neutron detectors<sup>(1,2,3)</sup>, with the noticeable exception of the measurement made by Whetstone<sup>(4)</sup> on the Californium spontaneous fission. In an effort to resolve the existing discrepancies between some of those experiments in the case of the neutron induced fission of  $U^{236}$ , Maslin et al.<sup>(5)</sup> and Boldeman et al.<sup>(6)</sup> used a large gadolinium loaded scintillator as a high efficiency neutron detector. On the other hand, we have obtained<sup>(7)</sup> the neutron number distributions in the spontaneous fission of  $Cf^{252}$  and, thereby, their first moments; our results are to be compared to those of S. L. Whetstone<sup>(3)</sup> and H. R. Bowman et al.<sup>(1)</sup> Figure 1 shows the variations of the average neutron number  $\bar{\nu}(m)$  as a function of the mass of the fragments as obtained in these experiments. Although the general trends of the representative curves  $\bar{\nu}(m)$  are similar in all measurements, quantitative discrepancies as high as 30% can be noticed on the figure. The situation is hardly better when one considers the variations of the average neutron number  $\bar{\nu}(E_k)$  as a function of total kinetic energies of the fragments as can be seen on Fig. 2 where the results obtained by H. R. Bowman et al.<sup>(1)</sup>, S. G. Whetstone<sup>(3)</sup>, and ourselves are compared. This situation gives rise to a wide range of values of the energy carried away per neutron from the 6.6 MeV/n advocated by H. R. Bowman et al.<sup>(1)</sup> to the 18.5 MeV/n claimed by E. E. Maslin.<sup>(5)</sup> The origin of these discrepancies seems to rest mostly in the different methods used to take

into account the following factors:

— The assumed geometrical efficiency of the detector which depends, sometimes critically, on the assumptions made regarding the neutron energies and angular distributions

— The efficiency of detection of neutrons penetrating the detector

— The energy and mass resolution and possible asymmetry of the fission fragments detection system

— For the large liquid scintillator, the dead-time corrections and the possible multiple firing of the phototubes

— The recoil correction which has to be used for the determination of the masses and kinetic energy of the fragments. This correction has recently been studied in detail by A. Gavron<sup>(8)</sup> and found to be most sensitive for small efficiency detectors.

As shown by Terrell<sup>(9)</sup> the low efficiency neutron detector experiments are much more sensitive to the first two factors. For example, the use of the superposition of two Maxwellian shapes for the center of mass neutron energy spectrum increases the number of neutrons measured in the direction of the emitting fragment by 10% as compared to the value obtained with only one Maxwellian distribution. If the detector subtends an angle of  $90^\circ$  the increase is reduced to 0.4%. When a large liquid scintillator is used in a  $4\pi$  geometry to measure total number of neutrons the efficiency problem is obviously minimized, being reduced to the question of neutron detection efficiency. Monte-Carlo simulations have shown that, as expected, this last quantity is itself almost insensitive to center of mass energy spectra provided the radius of the detector is greater than approximately 30 cms. It, therefore, appears that, provided the last two factors of possible systematic errors could be satisfactorily dealt with, the total



number of neutrons measurements carried out with large  $4\pi$  detectors should be used to check the more error-prone determinations of average number of neutrons emitted per fragment. It has been pointed out by Fraser<sup>(2)</sup> that neutron evaporation could lead to a non-colinearity of the fragments paths. This lack of colinearity could cause an unwanted selectivity in the detection of the fragments in double time of flight or double energy experiments. This effect can be overridden by using an asymmetrical disposition of the fragments detector with respect to the fission source. This condition is especially easy to fulfill by measurements of the total number of neutrons where the fission fragments direction needs not be defined, thereby allowing for a compact source-fragment detector geometry. Such a geometry has the additional advantage of increased signal to background ratio. As far as mass and energy resolutions are concerned the performances obtained with the most widely used double-energy technique provide mass and energy resolution of around 4 a.m.u. and 2 MeV, respectively (FWHM). These figures are small enough compared to the physical widths of the structures appearing in the fission process to allow a satisfactory correction for resolution effects. This is in contrast with the situation in the pioneering work<sup>(1,3)</sup> in this field where experimental energy widths as high as 20 MeV were estimated.

A. Gavron has recently<sup>(8)</sup> shown that the very fact that a neutron is detected in a preferential direction requires that the masses and kinetic energies of the fragments be corrected for recoil effects. This recoil correction appears to be especially important when the kinetic energy dependence of neutron numbers is studied. The magnitude of this correction is shown in Fig. 3 and appears to be able to account for most of the differences observed between the high and low efficiency measurements. In  $4\pi$  neutron counting this correction does not exist and in the high efficiency  $2\pi$  measurements it is drastically reduced.

It is outside the scope of this paper to go into details about dead-time corrections and optimization of the large liquid scintillators operation. We found it most satisfactory in our work to use the following conditions: (1) a 200 nsec fixed dead-time, (2) low voltages on the phototubes, and (3) summation of the pulses of the phototubes after equalization of their gain. As pointed out by several authors<sup>(10,11)</sup> it is possible to confirm that the dead-time and background corrections have been made properly and that the detector worked correctly. Let  $\bar{v}$  and  $\sigma^2(v)$  be the mean value and the variance of the neutron number distribution of the source. Let  $\bar{q}$  and  $\sigma^2(q)$  the same quantities relative to the distribution obtained after correction of the experimental one for background and dead-time but before the efficiency correction. Let  $\epsilon$  be the efficiency of the detector. Then

$$\bar{q} = \epsilon \bar{v}$$

and

(I.1)

$$\sigma^2(q) = \epsilon^2 \sigma^2(v) + \epsilon(1 - \epsilon) \bar{v}$$

Substituting for  $\epsilon$

$$\frac{\sigma^2(q)}{\bar{q}^2} - \frac{1}{\bar{q}} = \frac{\sigma^2(v)}{\bar{v}^2} - \frac{1}{\bar{v}} \quad (\text{I.2})$$

The first member of equation (2) must then be independent of the efficiency of the neutron detector. Figure 4 shows to what extent this condition can be realized in an actual system. It is fulfilled for efficiencies lower than 80%. For higher efficiencies the influence of afterpulses in the phototubes and of multiple-firing of the discriminators starts to be felt. It is noteworthy that the observed invariance of expression (2) is an indication that delayed gamma-rays

from the fission fragments do not impair the measurements. In a more detailed check of the operational and correction procedures in the total number of neutrons measurements we found that the results obtained for the values of both the means  $\bar{\nu}_T(m, E_k)$  and the variances of  $\sigma^2(\nu_T: m E_k)$  of the neutron number distribution measured as a function of the mass and total kinetic energy of the fragments agreed within statistical accuracy for two experiments where the detectors efficiency were 80% and 55%, respectively. Finally, an independent check of the validity of the measurements of total number of neutrons with  $4\pi$  high efficiency liquid scintillators is provided by the agreement between those measurements and those recently<sup>(12)</sup> carried out with  $^3\text{He}$  counters placed in a paraffin moderator. This rather lengthy justification of the use of large neutron detectors for measurements of total number of neutrons was felt useful in view of recent doubts<sup>(13)</sup> which have been raised in their behalf. In particular, it has been argued that these experiments gave unreasonably high values of the energy necessary to emit one additional neutron. The variation of the average total of neutrons emitted by both fragments as a function of their total kinetic energy is very nearly linear. The inverse of the slope of this variation  $\langle \frac{d\nu_T}{dE_k} \rangle^{-1}$  has been found to be 16.7 MeV/neutron by J. N. Boldeman et al.<sup>(6)</sup> in the thermal neutron induced fission of  $^{236}\text{U}$  and, by us, to be 13.0 MeV/neutron in the case of the spontaneous fission of  $^{252}\text{Cf}$ . However, these quantities should not be interpreted as the energy necessary for a given pair of fragments to emit one more neutron. This is mostly because different mass distributions are obtained for different total kinetic energies. The argument can be put on a more quantitative basis with the help of relations similar to those already used by Terrell.<sup>(9)</sup> First, the slope  $\langle \frac{d\nu_T}{dE_k} \rangle$  can be expressed as a function of the variance  $\sigma^2(E_k)$  of the total kinetic energy and of the co-variance of  $\nu_T$  and  $E_k$

$$\left\langle \frac{dv_T}{dE_k} \right\rangle = \frac{C(v_T, E_k)}{\sigma^2(E_k)} \quad (I.3)$$

Then, up to first order in the variations of  $E_k$  and  $v_T$  as a function of fragments masses the over all co-variance  $C(v_T, E_k)$  can be expressed as a function of the mass averaged value of the conditional co-variances  $C(v_T, E_k : m)$  of  $v_T$  and  $E_k$  for a fixed mass by

$$C(v_T, E_k) = \left\langle \frac{dv_T}{dm} \right\rangle \left\langle \frac{dE_k}{dm} \right\rangle \sigma^2(m) + \overline{C(v_T, E_k : m)} \quad (I.4)$$

Due to the small variation of  $v_T$  as a function of  $m$  the first term of the second member of equation (4) can be neglected so that

$$C(v_T, E_k) = \overline{C(v_T, E_k : m)} \quad (I.5)$$

A relation similar to equation (3) holds between quantities measured at a fixed mass ratio of the two fragments so that

$$C(v_T, E_k : m) = \left\langle \frac{dv_T}{dE_k} \right\rangle_m \sigma^2(E_k : m) \quad (I.6)$$

Assuming a negligible correlation between the values of  $\left\langle \frac{dv_T}{dE_k} \right\rangle_m$  and  $\sigma^2(E_k : m)$  for different mass values, one can then write that

$$\left\langle \frac{dv_T}{dE_k} \right\rangle_m^{-1} = \left\langle \frac{dv_T}{dE_k} \right\rangle^{-1} \frac{\overline{\sigma^2(E_k : m)}}{\sigma^2(E_k)} \quad (I.7)$$

In the case of  $Cf^{252}$  using resolution corrected values of  $\sigma(E_k : m) = 9.2$  MeV and  $\sigma(E_k) = 11.33$  MeV one obtains an approximate value of

$$\left\langle \frac{dv_T}{dE_k} \right\rangle_m^{-1} = 8.6 \text{ MeV/neutron}$$

This figure can be considered to be a determination of the energy necessary to emit one additional neutron and can be compared with estimates based on neutron binding energies, kinetic energies and, as will be seen later, on gamma-neutron competition. We shall make this comparison in the next section using the more detailed values of  $\left\langle \frac{dv_T}{dE_k} \right\rangle_m^{-1}$  computed for each mass of the heavy fragment. Figure 5 shows the result of this comparison.

As compared with total number of neutrons measurements the study of neutron emission by each individual fragment presents the added difficulty of detector efficiency variations with the angular and energy distributions of the neutrons. We shall assume that the fission events are sorted out according to the mass  $m$  of the fragment flying towards the neutron detector and to the total kinetic energy  $E_k$  of the two complementary fragments. The average number of detected neutrons for a given fission configuration is then equal to

$$\bar{q}(m, E_k) = \epsilon(m, E_k) \bar{v}(m, E_k) + r(M - m, E_k) \bar{v}(M - m, E_k) \quad (I.8)$$

where  $\bar{v}(m, E_k)$  and  $\bar{v}(M - m, E_k)$  are the average number of neutrons emitted by the fragments moving towards and away from the neutron detector, respectively.

$\epsilon(m, E_k)$  and  $r(M - m, E_k)$  are the probabilities of detection of these neutrons.

A similar relation holds when the fragment of mass  $M - m$  moves towards the detector, namely

$$\bar{q}(M - m, E_k) = \epsilon(M - m, E_k) \bar{v}(M - m, E_k) + r(m, E_k) \bar{v}(m, E_k) \quad (I.9)$$

Provided the set of forward and backward efficiencies  $\epsilon(m, E_k)$  and  $r(m, E_k)$  the average numbers of neutrons emitted per individual fragment  $\bar{v}(m, E_k)$  can be obtained. The sets of efficiencies can be computed by means of a Monte-Carlo simulation.<sup>(14)</sup> They depend on the fragment velocity and the center of mass neutron energy spectrum. We have already noticed that, in the case of large neutron detectors, the forward efficiencies were not sensitive to the assumption made for the center of mass neutron energy distribution. However, in this case, the ratio of the backward to the forward efficiencies can be as high as 20% and the quantities  $r(m, E_k)$  cannot, by any means, be neglected. We have found that

the efficiencies provided by the Monte-Carlo simulation were slightly but consistently overestimated by 2 to 3%. Thus, a constant normalization factor was applied to them so that the over all average total number of neutrons per fission could be reproduced.

The values of the average neutron numbers per fragments  $\bar{\nu}(m, E_k)$  were found to vary by less than 2% over their entire range when two different assumptions were made on the neutron spectra; in one case we assumed a constant temperature Maxwellian spectrum, and in the other we used the actual spectra as determined by H. R. Bowman et al.<sup>(1)</sup> The sum  $\bar{\nu}(m, E_k) + \bar{\nu}(M - m, E_k)$  of the average neutron numbers emitted by two complementary fragments should be equal to the average total neutron numbers  $\bar{\nu}_T(m, E_k)$  as determined in the  $4\pi$  geometry experiments. This agreement was obtained by Whetstone,<sup>(3)</sup> Maslin et al.<sup>(5)</sup> In our experiment the agreement is better than 2% for the all range of masses and kinetic energies. This seems to be a good check of the efficiency correction procedure.

Up to now we have not considered the possible existence of an isotropic component in the neutron angular distribution. This component has been first suggested by Skarsvag et al.,<sup>(15)</sup> Fraser et al.,<sup>(2)</sup> and Kapoor et al.<sup>(16)</sup> It is shown in Appendix I that in the case of a large detector subtending a  $90^\circ$  angle from the neutron source and assuming a constant detection efficiency for all neutrons entering the detector, the neglect of the isotropic component is equivalent to its sharing in equal parts between the two fragments. On the contrary, with a small neutron detector, the sharing will depend on the fragments and neutron velocities. This could give rise to differences between the results of the two types of measurement of up to 5%.

The variations of the average number of neutrons emitted by complementary fragments of selected masses as a function of their total kinetic energy  $E_k$  are

shown on Fig. 6. It can be seen that, while the variations of the total number of neutrons with  $E_k$  are very nearly linear, this is not so for the number of neutrons emitted by one of the fragments. Thereby, for a given mass split, the fraction of excitation energy taken up by one of the fragments cannot be held as constant.

## II. Gamma-ray emission and energy balance in fission

The emission of gamma rays by fission fragments is not as well known as their neutron emission. This is the consequence of several experimental difficulties:

— The need to discriminate between fission  $\gamma$  rays and  $\gamma$  rays produced following neutron capture or inelastic scattering

— The time-distribution of fission  $\gamma$  rays which covers a wide range from less than  $10^{-11}$  s to several microseconds. This circumstance makes difficult the comparison between experiments using different arrangements

— The moderate amount of anisotropy in the angular distribution of the fission  $\gamma$  rays, which makes it much more difficult to measure the relative share of each fragment in the  $\gamma$  emission than it is in the case of neutrons.

The first difficulty is usually overcome by the conjunction of a time discrimination between the gamma rays originating from the fission fragments and those produced in neutron capture or inelastic reactions and a careful collimation of the  $\gamma$  ray beam. For total gamma ray energy measurements, large liquid scintillators of the type described in Sec. I can also be used with the advantage of a very high efficiency; in this case a satisfactory correction for neutron parasitic effects can be made, provided a simultaneous measurement of neutron multiplicity. (17)



To deal with the two last difficulties a knowledge of both distribution in time and angular distribution of the fission  $\gamma$  rays is needed. In the following we first summarize this knowledge.

### II.1. Angular distribution of fission $\gamma$ rays

There are two causes of anisotropy in the fission  $\gamma$  rays angular distribution. The first one is a Doppler effect similar to what is observed in the neutron case. An isotropic distribution of  $\gamma$  rays in the fragment referential will give rise to a distribution in the laboratory system of the form:

$$W_D(\theta) = W_0 \left( 1 + (2 + r) \frac{v}{c} \cos\theta \right) \quad (\text{II.1})$$

where  $v$  is the velocity of the fragment,  $c$  the velocity of light,  $\theta$  the angle with respect to the fragment direction and  $r$  a small correction term accounting for the change in energy of the  $\gamma$  rays. This Doppler anisotropy obviously disappears when the two fragments are not distinguished by the experimental set up or when they are stopped before the  $\gamma$  emission takes place. On the other hand, it can be used to determine the share taken by each of the two complementary fragments<sup>(18,19)</sup> in the total  $\gamma$  ray emission and to obtain information on the time dependence of that emission.<sup>(20)</sup>

The other cause of anisotropy of the fission  $\gamma$  rays is a consequence of a preferential orientation of the fragments' spins with respect to their direction of flight. J. B. Wilhelmy et al.<sup>(21)</sup> have measured the angular distribution of several  $2^+ \rightarrow 0^+$  transitions in the ground state bands of several even-even fission isotopes. They found a preferential emission of the E2 radiations along the direction of the fragment with anisotropies ranging between 8.3% and 33.4%. Because

of possible attenuation effects in the platinum catcher they used, these values are to be considered as lower limits for the actual anisotropies. These anisotropies can only be explained if the initial spins of the fragments are preferentially oriented perpendicular to the fragments' paths, in agreement with the results of the early analysis of the gross angular distribution of fission  $\gamma$  rays by M. M. Hoffman.<sup>(22)</sup> In more recent experiments the anisotropy of the whole fission  $\gamma$  ray spectrum has been studied as a function of fragments kinetic energies, mass ratios, masses and as a function of  $\gamma$  ray energy. These experiments all dealt with the slow neutron induced fission of  $^{235}\text{U}$ . Figure 7 shows the results obtained by O. I. Ivanov et al.<sup>(23)</sup> in their study of fission  $\gamma$  anisotropy as a function of total kinetic energy and mass ratio of the fragments. The figure shows a definite increase of anisotropy with the total kinetic energy of the fragments for all mass ratios studied. On the other hand, the anisotropy seems insensitive to the mass ratio of the two fragments. This last result has been confirmed by P. Armbruster et al.<sup>(20)</sup> Using the collimator technique pioneered by S. V. Johansson<sup>(24)</sup> these authors have been able to study the anisotropy of the  $\gamma$  rays emitted between 10 ps and 100 ps after fission as a function of the fragment's mass. Their results are shown on Fig. 8 ; they show some structure but no definite trend except for a tendency to higher anisotropies in the heavy fragment mass range which averages around 20% as compared to 14% for the light fragment. When measured as a function of  $\gamma$  ray energy between 0.1 and 1.2 MeV the anisotropy<sup>(20)</sup> do not show strong departure from an average value of 13%. This is only slightly less than the values obtained by J. B. Wilhelmy et al.<sup>(21)</sup> for pure E2 transitions. It therefore appears that measured anisotropies of fission  $\gamma$  rays indicate that those  $\gamma$  rays are mostly of the E2 type with a

possible admixture of between 10% and 20% of dipolar radiation. This conclusion holds for  $\gamma$  energies between 0.1 and 1.2 MeV as quoted above. As a concluding remark concerning the question of anisotropy of  $\gamma$  ray emission by the fission fragments it is worthwhile noting that the neglect of this effect in some of the measurements of  $\gamma$  ray energy emitted in fission could lead to errors of about 5%; this holds not only for absolute values but also for relative ones, especially when the fragment's kinetic energy is retained as a parameter in the measurement.

## II.2. Time dependence of $\gamma$ ray emission by the fission fragments

The gross time dependence of  $\gamma$  emission by the fission fragments of  $^{235}\text{U}$  has been most thoroughly investigated by H. Albinsson.<sup>(25)</sup> Using the collimator technique this author studied the rate of production of fission  $\gamma$  rays between 10 and 200 picoseconds. He found that the corresponding decay curve could be well represented by the sum of three exponentials corresponding to half-lives of 7.5 ps, 18 ps, and 60 ps with intensities, relative to the total gamma radiation emitted within 1 ns after fission, of 35%, 25%, and 10%, respectively. P. Armbruster et al.,<sup>(20)</sup> by a comparison of observed  $\gamma$  ray anisotropy when both fragments were allowed to fly and when one of them was stopped in the fission source backing concluded that, in the latter case, the average velocity of the stopped fragment had to be reduced to 27% of its original value to account for the observed residual Doppler anisotropy. They show that, assuming a single time constant  $T$  for the decay curve of the  $\gamma$  emission the reduction factor  $f$  is equal to

$$f = \frac{t_c}{T + t_c}$$

where  $t_c$  is the characteristic slowing down time in the source backing. In their experiment P. Armbruster et al.<sup>(20)</sup> estimated this slowing down time to be approximately 1.7 picosecond. One then finds that if the fastest time components were those reported by Albinsson the reduction factor would amount to approximately 4%. To explain the observed reduction factor one is then led to assume the existence of a fast component with minimal relative intensity of 23% corresponding to an infinitely short half-life. This component is most probably responsible for the attenuation of the  $\gamma$  ray anisotropy for measurements carried out between 0 to 1 ns after fission with respect to those relative to the 10 ps-100 ps range. It is thus probably of the dipole type. H. Albinsson<sup>(26)</sup> has measured the gross features of the  $\gamma$  ray energy spectra corresponding to the three decay constants reported earlier. The bulk of the  $\gamma$  rays corresponding to the 7.5 ps half-life has an energy centered around 1 MeV. At this energy both the single particle lifetime estimates for E1 and M1 transitions and the collective estimates for E2 transitions are much shorter than 7.5 ps. On the other hand, this value lies very close to the single particle estimate for E2 transitions. The same can be said about the energy spectra associated to the 18 ps time component. The 60 ps component displays a strong peak around 200 keV which very probably corresponds to E2 rotational transitions similar to those reported in the work of E. Cheifetz et al.<sup>(27)</sup> in the Californium fission case.

From the preceding and the average multiplicity of about four gamma rays per fragment a qualitative picture can be drawn of the average cascade of  $\gamma$  rays emitted by the fragments. A first transition, mostly of the electric dipole type with an average energy greater than 1 MeV is followed by two E2 transitions of a non collective type; the cascade then terminates with an average of about one transition in the ground state rotational band when it exists.

In some cases, after what can be considered as the prompt  $\gamma$  emission, delayed  $\gamma$  rays can be emitted. W. John<sup>(28)</sup> estimated that approximately 20% of the total  $\gamma$  ray number or 7% of the total  $\gamma$  ray energy was emitted between approximately 100 ns and 2000 ns after fission of  $^{252}\text{Cf}$ .

The picture for  $\gamma$  ray emission by fission fragments presented above is certainly oversimplified; it should be modified, in particular, according to the measured photon-multiplicities or total  $\gamma$  ray energies which are, now reviewed.

### II.3. Multiplicities and energies of the fission $\gamma$ rays

A very careful measurement of total  $\gamma$  energy and photon average energy in the fission of  $^{252}\text{Cf}$ ,  $^{240}\text{Pu}$ , and  $^{236}\text{U}$  was reported at the Vienna conference by V. V. Verbuiski et al.<sup>(29)</sup> Their results are shown in Table I, together with the average neutron numbers. The values relative to the long range particle accompanied fission also present in Table I are taken from the work of G. Mehta et al.<sup>(30)</sup> except for the average energy per fission which has been assumed equal in binary and ternary fission.

Table I

Type of Fission	$E_{\gamma}$ (total)	Average energy per photon	$\gamma$ multiplicity	$\bar{\nu}_T$
$^{235}\text{U} + n$	6.51	0.97	6.69	2.42
$^{239}\text{Pu} + n$	6.82	0.94	7.25	2.83
$^{252}\text{Cf}$ Sp. L.R.A.	5.99	0.88	6.7	3.052
$^{252}\text{Cf}$ Binary Sp.	6.84	0.88	7.75	3.756

The measurements of Verbinsky et al.<sup>(29)</sup> refer to a period extending up to approximately 10 ns after fission and a  $\gamma$  energy range from 0.14 to 10 MeV.

Pleasanton et al.<sup>(19)</sup> report measurements of total  $\gamma$  ray energies and multiplicities in time ranges of 5 ns, 70 ns, and 275 ns after the slow induced fission of  $^{235}\text{U}$ . Their values are shown in Table II and are in very good agreement with the  $^{235}\text{U}$  figures of Verbinsky. From Table II it can be seen that the delayed  $\gamma$  contribution in the case of the induced fission of  $^{235}\text{U}$  would account for approximately 24% of the total number of  $\gamma$  rays and 14% of the total  $\gamma$  ray energy. The last figure is more than twice the corresponding one reported by John et al.<sup>(28)</sup> for the spontaneous of californium 252. In summary, we find that the total  $\gamma$  ray energy emitted in fission lies around 7.5 MeV with an absolute uncertainty of about 0.5 MeV for most of the known cases. This value of 7.5 MeV can be compared with that obtained in statistical computations such as the recent one by E. Nardi et al.<sup>(31)</sup> of approximately 6 MeV in the  $^{252}\text{Cf}$  spontaneous fission case. Although the difference between the expected value and the observed one is much less than some years ago it is still significant. Table I shows that positive correlation exists between the  $\gamma$  ray multiplicities and the total number of neutrons per fission.

Such a correlation had been observed by S. G. Johansson<sup>(24)</sup> when he first determined the  $\gamma$  multiplicity as a function of the mass of the emitting fission fragments of  $^{252}\text{Cf}$ . John<sup>(28)</sup> added a delayed component to Johansson's results and obtained the curve shown on Fig. 9. Similar data have been obtained in the slow neutron induced fission case by H. Albinsson et al.<sup>(32)</sup> using the same collimator technique as S. G. Johansson and by F. Pleasanton et al.<sup>(19)</sup> using the Doppler anisotropy technique. The results obtained by both groups are shown on Fig. 10. Although the two experiments agree qualitatively and both show a pronounced saw-tooth structure the rates of variation of the  $\gamma$  multiplicities as a function of

Table II. Average  $\gamma$  multiplicities and total  $\gamma$  energies as a function of time after the slow neutron induced fission of  $^{235}\text{U}$ .

$\gamma$ energy	Time interval ns	$\bar{N}_{\gamma T}$ ( $\gamma$ /fission)	$\bar{E}_{\gamma T}$ (MeV/fission)
0.09 - 10 MeV	~ 5	6.51	6.43 $\pm$ 0.3
0.03 - 10.4	~ 70	8.1	7.0 $\pm$ 0.7
0.03 - 10.4	275	8.6	7.4 $\pm$ 0.7

fragment mass are different. This difference cannot be attributed in its entirety to the different time range after fission studied in the two experiments, since, if it were so, the values obtained by F. Pleasanton should always be in excess to those obtained by H. Albinsson. The correlation between  $\gamma$  ray and neutron emission is best visualized by plotting the points corresponding to the various couples  $(E_\gamma(m), \nu(m))$  on the  $(E_\gamma, \nu)$  plane. This is done on Fig. 11 for both californium and  $^{236}\text{U}$  cases. In preparing Fig. 11 we have used Albinsson's data for  $^{236}\text{U}$  and the relative yields given by John divided by a normalization factor of 1.55 so that comparison could be made with the total  $\gamma$  ray energy measurements on  $^{252}\text{Cf}$  which will now be examined.

The variations of total  $\gamma$  energy or yields as a function of the total kinetic energy of the fragments have been measured by H. Albinsson et al.,<sup>(33)</sup> F. Pleasanton et al.,<sup>(19)</sup> and G. V. Valskii et al.<sup>(34)</sup> in the slow neutron induced fission of  $^{235}\text{U}$ . A good agreement is observed between the results obtained by the three groups. We show on Fig. 12 the results obtained by H. Albinsson. Using a large liquid scintillator as a  $4\pi$   $\gamma$  ray detector<sup>(35)</sup> we obtained the variations of total  $\gamma$  ray energy as a function of total fragment kinetic energy for the spontaneous fission of  $^{252}\text{Cf}$ . These variations are also shown on Fig. 12. The correlation between the total  $\gamma$  ray energy (or multiplicity) and the total number of neutrons measured as a function of total fragment kinetic energy can be examined as done before for the fragment's mass related values. This is done in Fig. 13. This figure and Fig. 12 strongly suggest that a linear relation exists between the  $\gamma$  ray energy and the number of neutrons emitted in fission. The straight lines appearing in Fig. 12 and 13 correspond to the assumption that

$$\bar{E}_\gamma(m, E_k) = [0.75 \bar{\nu}(m, E_k) + 2]_{\text{MeV}} \quad (\text{II.1})$$



in the  $^{252}\text{Cf}$  case and

$$\bar{N}_\gamma(m, E_k) = [1.1 \bar{V}(m, E_k) + 1.75] \quad (\text{II.2})$$

in the  $^{236}\text{U}$  case.

The extent to which such relations are accurate can be estimated from more detailed measurements where the  $\gamma$  ray energies or multiplicities are studied as a function of both the masses and the kinetic energies of the fragments. Using the large liquid scintillator we have measured<sup>(35)</sup> the total  $\gamma$  energy emitted in fission as a function of total kinetic energy and mass ratio. The results are shown on Fig. 14 where the variations of total  $\gamma$  energy as a function of the fragment's total kinetic energy are displayed for a choice of mass ratios. It can be seen from the figure that the variations are very nearly linear. In Fig. 15 we show the variations of the average total  $\gamma$  energy and of the slopes  $\langle \frac{dE_\gamma}{dE_k} \rangle$  of the above mentioned linear variations as a function of mass ratio (or mass of the light fragment). It can be seen that the variations of those quantities are less than 10% except at symmetry. Since the variations in the slopes  $\langle \frac{dv_T}{dE_k} \rangle$  as a function of fragment mass as shown in Fig. 5 are themselves less than 10%, it follows that equation (II.1) could be accurate within 20% for the whole mass and kinetic energy range. However, this conclusion might be an oversimplification. The results obtained by F. Pleasanton et al.<sup>(19)</sup> seem to indicate that this is the case. Figure 16 taken from the work of these authors shows the variations of the  $\gamma$  energy emitted by one fragment as a function of total kinetic energy for a choice of masses of the fragment. It can be seen on the figure that for some heavy fragments the emitted  $\gamma$  energy tends to increase with kinetic energy and is, thereby, anticorrelated with the number of neutrons emitted by

this fragment. This tendency sometimes leads to values of  $\gamma$  ray energy emitted by one fragment well under a half neutron binding energy for fission events where the fragment emits about two neutrons. Such a behavior is very difficult to understand.

#### II.4. Energy balance in fission

The observed variations of total  $\gamma$  ray energy as a function of total fragment's kinetic energies have a bearing on the computation of energy balance in fission. For example, from equation (II.1) one sees that the energy necessary to emit one supplementary neutron will be approximately 0.75 MeV higher than the sum of the neutron binding and center of mass kinetic energies. A comparison between the computed and observed energies carried away per neutron is made on Fig. 5. The agreement is fair and the energy carried away per neutron ranges around 8.5 MeV. It is seen, however, that the experimental value lies consistently higher than the computed one especially for light fragment masses higher than 105. This will be explained in the following section in terms of a not accounted for tailing of the kinetic energy resolution function. The detailed measurements of average neutron numbers  $\bar{\nu}(m, E_k)$ , of total  $\gamma$  ray energies  $E_Y(m, E_k)$  and of center-of-mass neutron kinetic energies  $\bar{\eta}(m, E_k)$  as a function of mass and kinetic energies of the fragments allow equally detailed computations of the total energy  $Q(m, E_k)$  released in fission:

$$Q(m, E_k) = E_k + \bar{\nu}_1(m, E_k)[\bar{B}(m, E_k) + \bar{\eta}(m, E_k)] + \bar{\nu}_1(M - m, E_k)[\bar{B}(M - m, E_k) + \bar{\eta}(M - m, E_k)] \\ + \bar{E}_Y(m, E_k)$$

where  $\bar{\nu}_1(m, E_k)$  is the average number of neutrons emitted by fragment of mass  $m$ ,  $\bar{\eta}(m, E_k)$  is the average center-of-mass kinetic energy of these neutrons,  $\bar{B}(m, E_k)$  is the mean binding energy of these neutrons as obtained from a suitable averaging of mass-table values,  $E_Y(m, E_k)$  is the total  $\gamma$  ray energy emitted by the two

complementary fragments,  $m$  is the mass of one of the fragments,  $M-m$  the mass of the complementary one.

The values of  $Q(m, E_k)$  should be independent of the total kinetic energy  $E_k$ . The extent to which this condition is fulfilled provides a very useful check of the coherency of the experimental data. This check can be made in the case of the spontaneous fission of  $^{252}\text{Cf}$  with the help of Fig. 14. On this figure both the  $\gamma$  ray energies obtained from direct measurement and those obtained with the assumption of energy balance are displayed for several masses. The condition that total energy release be independent on  $E_k$  is equivalent to the requirement that the variations of the above quantities be parallel. This appears to be the case, for most masses, within statistical accuracy. However, although the two quantities plotted on Fig. 14 display parallel variations their absolute values differ. The magnitude of the disagreement is shown on Table III where the differences between the experimentally determined energy release and the values obtained from the Garvey *et al.*<sup>(36)</sup> mass tables are displayed. The experimental values are 1 to 2 MeV higher than the computed ones. Recent evidence<sup>(37)</sup> seem to indicate that fragments total kinetic energies could indeed be overestimated by such an amount.

#### II.5. Even-odd effects on fission energetics

The energy release in fission can be expressed from the masses of the fissile species and of the fragments. For example, in the case of the spontaneous fission of  $^{252}\text{Cf}$

$$Q(N, Z) = M(154, 98) - M(N, Z) - M(154-N, 98-Z)$$

expresses the total energy release for a fission giving rise to a fragment with  $Z$  protons and  $N$  neutrons. When the fissile nucleus has an even charge the

Table III. Comparison of experimental and computed energy releases in the fission of  $^{252}\text{Cf}$ .

A	$Q(A)_{\text{Garvey}}$	$Q_{\text{Exp.}} - Q_{\text{Garvey}}$
90	203.33	1.22
91	204.39	1.61
92	205.81	1.62
93	205.83	1.65
94	206.45	2.20
95	207.78	1.13
96	209.03	0.06
97	208.92	1.11
98	209.71	0.37
99	209.84	0.56
100	210.45	0.30
101	211.04	0.99
102	212.58	-0.47
103	212.55	0.97
104	213.11	1.35
105	214.32	0.93
106	215.73	0.91
107	216.01	2.5
108	217.47	1.32
109	218.21	1.74
110	219.36	1.57
111	220.64	2.01
112	222.82	0.63
113	223.66	2.07
114	225.05	1.92
115	226.65	1.62
116	228.31	2.33
117	229.40	3.6
118	230.97	2.25
119	231.63	2.19
120	231.93	1.95
121	232.47	2.05
122	233.75	0.0
123	233.14	1.30
124	232.95	2.63
125	233.02	7.37
126	232.97	-4.2

fragments have both either an odd or an even charge. Because of the pairing energy of the protons it then follows that a fission giving rise to two even-charge fragments will be, on the average, 2.5 MeV more energetic than a fission giving rise to two odd-charge fragments. Studies of the variations of average total kinetic energies, neutron and gamma emission as a function of the fragments charges can therefore provide information on the partition of this even-odd energy difference; such information cannot be obtained from mass measurements. We have measured the average total  $\gamma$  ray energy, total neutron number emitted in the fission of  $^{252}\text{Cf}$  as well as the fragments total kinetic energy as a function of the charges of the fragments. Since no detailed report of this work has been made earlier we now shortly describe the experimental technique involved as well as some aspects of the data analysis.

In the neutron multiplicity and total  $\gamma$  ray energy measurements, a californium fission source was placed near a silicon/lithium drifted x-ray detector at the center of a diametrical hole managed into a big gadolinium-loaded liquid scintillator. For each detected fission event the pulse height of the coincident pulse produced in the scintillator was analyzed as well as the pulse height delivered by the x-ray detector; the number of neutrons detected by the scintillator was counted between 1  $\mu\text{s}$  and 36  $\mu\text{s}$  after fission. The three quantities were then stored on an event-by-event basis on a magnetic tape. The fission events were detected either by the requirement of a coincidence between an auxiliary fragment detector and the x-ray detector or by the requirement of a coincidence between the x-ray detector and the liquid scintillator. In the later case it was also required that at least one neutron be counted in the 35  $\mu\text{s}$  gate. We have been able to show that the two techniques for detecting fission events

were equivalent. In the later case both fragments could be stopped in the source and the Doppler broadening of the x-rays emitted by the fragments was thereby minimized. In that case the resolution of the x-ray detector was 350 eV at 35 keV.

The fission fragments x-ray spectrum obtained in this experiment is shown on Fig. 17.

The kinetic energy determination made use of data obtained by E. Cheifetz et al. <sup>(27)</sup> in the course of their study of  $\gamma$  rays emitted by fission fragments. In one of their experimental set-ups the  $^{252}\text{Cf}$  source was deposited on a solid state detector, which detected one of the fragments. The other fragment was detected in another solid-state counter. Both fragment detectors were operated in coincidence with an x-ray detector positioned behind the source. The pulse heights delivered simultaneously by the three detectors were stored on event-by-event basis on a magnetic tape. When the data were processed only events where the x-ray had been emitted by the stopped fragments were considered. From the two pulse heights provided by the fragment detectors the total kinetic energy of the fission event was obtained using the calibration scheme first proposed by H. W. Schmitt. <sup>(38)</sup> In this experiment the resolution of the x-ray detector was approximately equal to 1 keV.

The data from the two experiments were processed in a similar way. The number of counts corresponding to each x-ray amplitude bin was determined as well as the corresponding average values of the interesting quantities ( $\gamma$  ray energy, neutron multiplicity and total kinetic energy). Thus, if  $X_i$  is a particular x-ray bin we obtained

$$N(X_i), \bar{E}_\gamma(X_i), \bar{\nu}(X_i), \bar{E}_k(X_i)$$

In the following we shall denote by  $\bar{A}(X_i)$  the measured average value of the quantity A corresponding to the x-ray amplitude  $X_i$ . Let  $y(Z,A)$  the number of fissions producing a fragment of charge Z and a value A of the quantity under study. Let  $Y(X_i,A)$  the number of fission producing an x-ray pulse in channel  $X_i$  and the same value A of the quantity under study. For each fission producing a fragment of charge Z we assume that we count a pulse in the x-ray channel  $X_i$  with the probability  $R(Z,X_i)$  which corresponds to the elemental response of the detector. Then the charge yields  $y(Z,A)$  can be obtained from the observed yields  $Y(X_i,A)$  by minimizing the sum of squares

$$\chi^2 = \sum_{i=1}^n W_i (Y(X_i,A) - \sum_Z R(Z,X_i) y(Z,A))^2$$

The solution of the least-squares equation then expresses the charge yields as linear functions of the channel yields

$$y(Z,A) = \sum_i B(Z,X_i) Y(X_i,A) \quad (\text{II.3})$$

The matrix elements  $B(Z,X_i)$  depend exclusively on the weights  $W_i$  and the response matrix elements  $R(Z,X_i)$ ; they do not depend on A.

A relation similar to equation (II.3) obviously holds for any linear function of the yields

$$L(y(Z,A)) = \sum_i B(Z,X_i) L(Y(X_i,A))$$

In particular if

$$N(X_i) = \sum_A Y(X_i, A) \quad Y(Z) = \sum_A y(Z, A)$$

$$N(X_i) \bar{A}(X_i) = \sum_A A Y(X_i, A) \quad Y(Z) \bar{A}(Z) = \sum_A A y(Z, A)$$

we can write that

$$Y(Z) = \sum_i B(Z, X_i) N(X_i) \quad (\text{II.4})$$

$$Y(Z) \bar{A}(Z) = \sum_i B(Z, X_i) N(X_i) \bar{A}(X_i) \quad (\text{II.5})$$

The equations (II.4) and (II.5) are identical to those which would result from a least-square analysis of the quantities  $N(X_i)$  and  $N(X_i) \bar{A}(X_i)$ , respectively. Thus, the charge yields  $y(Z)$  and average values  $\bar{A}(Z)$  can be obtained from only two least-squares treatments operating on the channel yields  $N(X_i)$  and on the products  $N(X_i) \bar{A}(X_i)$  of the channel yields by the channel average values. This analysis was applied to the experimental data in order to obtain the charge dependent yields  $Y(Z)$ , average total  $\gamma$  ray energies  $\bar{E}_\gamma(Z)$ , neutron multiplicities  $\bar{\nu}(Z)$  and average total kinetic energies  $\bar{E}_k(Z)$ .

Since the  $k$  x-ray emitted by fission fragments are mostly produced by electron conversion processes, their yields are expected to depend strongly upon the nuclear characteristics of the fragments, and this has been confirmed in numerous experiments. The question then arises of the extent to which the values of average  $\gamma$  energies, neutron multiplicities and total kinetic energies obtained in experiments such as described above are not seriously biased. Since, if such a bias exists, it is not probable that it acts identically on different fragments, it is possible to check its existence by comparing the values of  $\bar{E}_\gamma(Z)$ ,  $\bar{\nu}_T(Z)$ ,



and  $\bar{E}_k(Z)$  obtained for a pair of complementary charges  $Z$  and  $98-Z$ . This comparison can be made on Fig. 18, 19, 20. Figure 18 shows the variations of the measured total  $\gamma$  energy as a function of the charges of the fragments. It can be seen that the complementary condition is fulfilled within statistical accuracy for almost all charges. Also apparent on the figure is a clear even-odd effect on  $\bar{E}_\gamma(Z)$ . As can be seen on Fig. 19 the complementary condition is not always fulfilled for the variations of total number of neutrons  $\nu_T(Z)$ . We have superimposed on Fig. 19 the variations of the total number of neutrons as a function of mass  $\bar{\nu}_T(m)$  as obtained in experiments such as those referred to in Sec. I. The mass and charge scales of the figure reflect the charge to mass ratios of the fission fragments. It can be seen that, whenever the complementary condition is fulfilled the values of  $\bar{\nu}_T(Z)$  lie close to the corresponding values of  $\bar{\nu}_T(m)$ . The complementary condition is not fulfilled for the charge pairs 45-53, 44-54, 46-52 and several pairs with a light fragment's charge smaller than 39. It appears that in those pairs one of the values of  $\nu_T(Z)$  lies close to the corresponding value of  $\nu_T(m)$  while the other has a smaller value. We have assumed that the value closer from  $\nu_T(m)$  was not biased by the x-ray emission process. Figure 21 shows the values of  $\nu_T(Z)$  obtained when keeping the highest of the two observed values of  $\bar{\nu}_T(Z)$  and  $\bar{\nu}_T(98-Z)$ . No even-odd effect is apparent on the figure.

The values of  $\bar{E}_k(Z)$  show an even-odd effect for both heavy and light fragments. Values for complementary charges differ by 0.5 to 1 MeV. This is mostly a consequence of the existence of a high background under the x-ray peaks, due to interactions of high energy gamma-rays with the detector. Figure 22 shows the values of  $E_k(Z)$  obtained when keeping the highest of the two observed values of

$\bar{E}_k(Z)$  and  $\bar{E}_k(98-Z)$ . Also shown for comparison are the values of  $\bar{E}_k(m)$  obtained in a double fragment kinetic energy measurement. It is clear that the even-odd effect observed on the values of  $\bar{E}_k(Z)$  reflects itself in the modulations appearing on the  $\bar{E}_k(m)$  curve.

In summary, while the calculated difference in energy release between fission events with two even-charge fragments and those with two odd-charge fragments is

$$\Delta Q = Q_e(Z) - Q_o(Z) = 2.7 \text{ MeV}$$

It is found experimentally that:

the difference  $\Delta v_T$  in the total number of neutrons is less than 0.04 corresponding to a difference in excitation energy  $\Delta E_\gamma$  smaller than 0.3 MeV, the difference in total gamma-ray amounts to  $\Delta E_\gamma = 0.66 \pm 0.05$  MeV and the difference in fragments total kinetic energy amounts to  $\Delta E_k = 1.58 \text{ MeV} \pm 0.1 \text{ MeV}$ . The sum  $\Delta \bar{E}_\gamma + \Delta \bar{E}_\gamma + \Delta \bar{E}_k$  is then equal to  $2.24 \pm 0.45$  MeV. Within statistical accuracy it is in agreement with the computed value of 2.7 MeV.

## II.6. De-excitation mechanism of the fission fragments

We should like, in the following, to summarize the experimental results on the fragments de-excitation which have been presented above and discuss whether these results can be explained in a coherent theoretical frame. We shall mostly concentrate on the features of the gamma-ray emission by the fission fragments. However, we must bear in mind that the neutron energy spectra appear to be satisfactorily accounted for by a standard evaporation theory, provided the level densities used in the calculation properly include shell effects. Such calculations have been performed, among others, by E. Nardi et al.<sup>(31)</sup> and Fig. 23

shows a comparison between the experimental and computed values of the average center of mass kinetic energies of the neutrons. Those computations made use of the technique developed by L. Moretto,<sup>(39)</sup> where both Strutinsky shell corrections and pairing are taken into account for the determination of level densities.

In an attempt to explain the striking correlation between  $\gamma$  and neutron emissions by the fission fragments Johansson<sup>(24)</sup> made the hypothesis that the  $\gamma$  rays corresponded mainly to vibrational transitions through which the fragments could lose the deformation they had at scission. The high proportion of E2 radiation in the fission  $\gamma$  spectrum seemed to confirm this point of view. However, very strong objections stand against this hypothesis. It seems to be well established experimentally that at least 70% of the total  $\gamma$  ray energy is emitted more than one picosecond after fission while the neutrons are emitted in a time shorter than  $10^{-14}$  seconds. We have shown earlier that the fastest  $\gamma$  ray transitions were probably E1 in character since they tend to decrease the angular anisotropy. It thus appears that the collective  $\gamma$  ray transitions, if they exist, occur after neutron emission. The  $\gamma$  ray emission should reflect the state of the system at this time and not at the time of scission. The hypothesis assumes that most of the initial excitation energy of the fragments is tied into deformation. After neutron emission most of this deformation energy has been dissipated and the remaining fraction, if it exists, has no reason to be proportional to the initial value. Rather it should be a complicated function of vibrational levels damping, neutron and  $\gamma$  widths at energies in the neighborhood of the neutron binding energy. Furthermore, the success of the evaporation theory of neutron spectra points to an effective damping of the deformation energy of the fragments in times less than  $10^{-18}$  sec. The last objection to Johansson's hypothesis is that the lifetimes of the possible vibrational transitions should be at least an order of magnitude

shorter than the observed ones, which, as stated earlier, are close to E2 single particle estimates.

The alternative to Johansson's hypothesis is to assume that the de-excitation of fission fragments is governed by the statistical theory. Using the shell plus pairing model Nardi et al.<sup>(31)</sup> were not able to reproduce the variations of the  $\gamma$  ray energy as a function of fragment's mass. Their model did not fully include the influence of the spin on the level density. Such models predict some correlation between the neutron and the  $\gamma$  ray emission by the fragments. This correlation reflects mostly the increase in the binding energy of the last emitted neutron when the number of neutrons emitted by the fragment increases. From the mass tables it is seen that, in the fission fragments region, an increase of one unit in the number of emitted neutrons produces an increase of approximately 0.3 MeV in the binding energy of the last neutron, which should be reflected by an increase of 0.15 MeV of the  $\gamma$  ray energy. This effect is certainly present in the experimental data, but it leaves, in the case of  $^{252}\text{Cf}$ , an increase of  $\gamma$  ray energy of approximately 0.6 MeV for each additional emitted neutron unexplained.

When the average number of emitted neutron is less than one the variations of the  $\gamma$  ray energy emitted by the fragment should reflect the effects of two opposite trends. For the cases where the increase in excitation energy of a given fragment does not allow the opening of an additional neutron channel the  $\gamma$  ray energy should increase with excitation energy. On the contrary when the excitation energy sweeps through the region of opening of an additional neutron channel the  $\gamma$  ray energy should drop abruptly. Therefore, for low values of  $\bar{\nu}$  such as those which can occur in the slow neutron induced fission of  $^{235}\text{U}$

additional correlation or anticorrelation of the total  $\gamma$  ray energy with neutron number could be observed. Correlation is to be expected if the variance of the excitation energy distribution is large.

Statistical computations which treat the influence of pairing in a phenomenological way by introducing the effective excitation energy have had some success in reproducing the trend of the variation of the  $\gamma$  ray energy emitted as a function of the fragment's mass. Such a calculation has also been performed by E. Nardi et al.<sup>(31)</sup> However, the physical justification of such phenomenological models is not clear and it is possible that the introduction of an effective excitation energy simulates the effect of the spins of the fission fragments which will be discussed later. Furthermore, these models cannot account for the observed increase in  $\gamma$  ray energy with excitation energy for fragments of given masses.

That spin considerations should enter into statistical computation of  $\gamma$  ray emission by the fission fragments stems from the following considerations:

1) Most evaluations of the spins of the fragments before neutron emission indicate that these spins are approximately  $6\hbar$  to  $8\hbar$  higher than the ground state spins. Neutron emission is not expected to decrease that spin by more than one unit of angular momentum. When the fragments are left with an energy only slightly higher than a neutron binding energy they have still from 5 to  $7\hbar$  units of angular momentum to dissipate. Further neutron emission which would leave the residual nucleus in the vicinity of its ground state is thus expected to be strongly inhibited except for odd-odd nuclei. To obtain level with spin differing from the ground state one by more than 5 units of angular momentum requires the coupling of at least two unpaired nucleons, and thus the breaking of a pair in both even-even and odd-A nuclei. The observed even-odd difference in total  $\gamma$  ray energy

emitted in fission is easily explained in that context. From the experimental value of 0.66 MeV for this difference, we can derive the increase of  $\gamma$  ray energy emitted in fission induced by angular momentum effects. If we assume that there is no increase for odd-odd fragments, and that the increases are equal in the other cases we find that angular momentum effects should add 2 MeV to the  $\gamma$  ray energy release in fission. The total  $\gamma$  ray emitted in fission would then lie between 7.5 and 8 MeV, in reasonable agreement with experiment.

2) The dominantly E2 character of the fission  $\gamma$  ray as well as their relatively high multiplicity cannot be understood when compared with the features of neutron capture gamma-ray spectra without the assumption that  $\gamma$  emission by the fission fragment is strongly influenced by the absence of available states for E1 transitions.

After neutron emission has taken place the residual fragment is left with an average energy of approximately 4 MeV, and an average spin of approximately  $6\hbar$ . In these conditions electric dipole emission should not be inhibited and we can assume it takes place with an average energy of approximately 1.5 to 2 MeV. This emission should not reduce the spin of the fragment significantly and thereby leaves it with an excitation energy of approximately 2 to 2.5 MeV and an average spin exceeding  $5\hbar$ , that is, in the region of the "yrast" line. However, the "yrast" line should not be considered as the ground state rotational band but rather as the intrinsic levels "yrast" region at which energy the density of levels of given spin and parity can be treated statistically. In this "yrast" region E2 transitions dominates, because of spin and parity limitations, until the ground state band is reached. In this picture the E2 transitions reduce the spin of the fragment by the maximum possible amount, that is two units of

angular momentum. The average energy of the E2 transitions of approximately 1 MeV thus represents the average energy which is necessary to reduce the spin of the fragment by 2 units along the path followed by the system in the (E,I) representation. It is interesting to see what this simple picture would predict if the initial spin of the de-exciting nucleus is increased. The nucleus would enter the yrast region at a higher energy and would then decay along this region until it reaches the ground state. On the average when the spin is reduced to its former value the de-excitation scheme would be the same as in the lower initial spin case.

In particular, it is possible to predict how the feeding of the rotational states of the ground state band will vary as a function of initial spin. Let  $Y(I, I_M)$  be the feeding intensities of the ground state band when the initial spin is  $I_M$ . With the initial spin increase to  $J_M$  the intensities  $Y(I, J_M)$  will accordingly be

$$Y(I, J_M) = aY(I, I_M) + b$$

the constant term  $b$  reflects the possible direct feeding of the ground state band when the nucleus goes through states with angular momenta between  $J_M$  and  $I_M$ . Comparison of the feeding intensities are usually made by normalizing them to the intensity of the  $2^+ \rightarrow 0^+$  transition. Then

$$\frac{Y(I, J_M)}{Y(2, J_M)} = \frac{aY(I, I_M) + b}{aY(2, I_M) + b} = \frac{Y(I, I_M) + b/a}{Y(2, I_M) + b/a}$$

and

$$\frac{Y(I, J_M)}{Y(2, J_M)} - \frac{Y(I, I_M)}{Y(2, I_M)} = \frac{b/a}{Y(2, I_M) + b/a}$$

the quantity  $b/a$  is small since it represents the ratio of the feeding probability of the highest members of the rotational band to that of the  $2^+$  state. It is, then, seen that the difference between the two reduced feeding intensities is approximately a constant. Figure 24 which was taken from J. B. Wilhelmy et al.<sup>(21)</sup> shows that for both fission and  $(\alpha, xn)$  reactions the experimental data seem to agree with that picture. It should be noted that when  $b/a$  increases the above formulation leads to a feeding through the highest states as the ground state band which corresponds to the situation in  $(HI, xn)$  reactions.

The consequence of this oversimplified model of the  $\gamma$  de-excitation of fission fragments is that the increase of  $\gamma$  ray energy with excitation energy which have been reported would be the consequence of an increase of the average spin of the fragments with their excitation energy. Using the experimentally determined increase of 0.6 MeV in  $\gamma$  energy for each additional neutron, a value of 8 MeV for the energy necessary to emit one more neutron and a difference of 2 spin units for 1 MeV additional  $\gamma$  energy one finds that the average spin of the fission fragments should increase by one unit for an increase of excitation energy of approximately 7 MeV. Such a result does not contradict that of J. B. Wilhelmy et al.<sup>(21)</sup> who found that the increase in spin of the fragments was less than 2 for a decrease of the total kinetic energy of approximately 15 MeV.

P. Armbruster et al.<sup>(20)</sup> have pointed out that such a behavior of the spins of the fragments could be explained in the frame of the collective model of fission suggested by W. Nöremberg.<sup>(40,41)</sup> This model also predicts the observed preferential orientation of the fragments' spins in the plane perpendicular to the fission direction. On the contrary, the statistical theory of fission as outlined by P. Fong<sup>(42)</sup> cannot account for the features of the  $\gamma$  ray emission mentioned earlier. It could be



advocated, in this case, that the fragments acquire most of their spin by Coulomb excitation after scission; this would, however, lead to unreasonably low values of spins at scission.

### III. Variances of the excitation energies of the fission fragments

With the exception of the pioneering work of S. G. Whetstone<sup>(3)</sup> it is only recently that detailed measurements of the variances of the number of neutrons emitted in fission have been carried out. In the following we shall assume that the neutrons are all emitted by the fragments, after fission has taken place. One should, however, bear in mind the possible existence of an isotropic component in the fission neutrons which could seriously impair the results and interpretation of variance measurements. With that assumption we write the probability that  $\nu_1$  neutrons are emitted by one of the fragments and  $\nu_2$  by the other as a bi-variate distribution  $P(\nu_1, \nu_2)$ . We have shown elsewhere<sup>(43)</sup> how it is possible, in principle, to derive this distribution from the probability  $Q(g_1, g_2)$  that  $g_1$  and  $g_2$  neutrons are detected simultaneously by two suitably arranged detectors. Such a program is not feasible, however, because of the statistical errors in the definition of the observed distribution  $Q(g_1, g_2)$  and because of our uncertain knowledge of the efficiencies of the neutron detectors. We must therefore content ourselves with the extraction of some significant features of the distribution  $P(\nu_1, \nu_2)$  from the experimental data. Such features are, for example, the five lowest moments of this distribution defined as follows:

$$\bar{\nu}_1 = \iint \nu_1 P(\nu_1, \nu_2) d\nu_1 d\nu_2$$

$$\bar{\nu}_2 = \iint \nu_2 P(\nu_1, \nu_2) d\nu_1 d\nu_2$$

$$\sigma^2(\nu_1) = \iint (\nu_1 - \bar{\nu}_1)^2 P(\nu_1, \nu_2) d\nu_1 d\nu_2$$

$$\sigma^2(\nu_2) = \iint (\nu_2 - \bar{\nu}_2)^2 P(\nu_1, \nu_2) d\nu_1 d\nu_2$$

$$C(v_1, v_2) = \iint (v_1 - \bar{v}_1)(v_2 - \bar{v}_2) P(v_1, v_2) dv_1 dv_2$$

We have dealt with the determination of the two first moments in Sec. I. We have seen that, as soon as the masses of the fragments are measured, a single measurement with one neutron detector provided the values of the two average numbers of neutrons. Similarly only two independent measurements are necessary to determine the three second-moments. As in Sec. I two different techniques have been used in that purpose. The low efficiency technique makes use of two small neutron detectors in conjunction with two fragments detectors.<sup>(44)</sup> When the two neutron detectors are on the same side of the fission source the ratio of the rate of quadruple coincidences to the square of the rate of triple coincidences is equal to:

$$\frac{\langle \epsilon v_1 \epsilon (v_1 - 1) \rangle}{\langle \epsilon v_1 \rangle^2}$$

where it is assumed that both neutron detectors have the same efficiency  $\epsilon$ . It is further assumed that this efficiency does not depend on the neutron multiplicity at least when the fragments mass and kinetic energies are specified. One then obtains:

$$\frac{\langle v_1(v_1 - 1) \rangle}{\langle v_1 \rangle^2} = \frac{\langle v_1^2 \rangle}{\bar{v}_1^2} - \frac{1}{\bar{v}_1} = \frac{\sigma^2(v_1)}{\bar{v}_1^2} - \frac{1}{\bar{v}_1} + 1$$

A similar relation holds when the complementary fragment flies in the direction of the neutron detector, allowing to obtain  $\sigma^2(v_2)$ .

When the two neutrons are situated on opposite sides of the source one then obtains, in the same manner as above

$$\frac{\langle \epsilon_1 v_1 \epsilon_2 v_2 \rangle}{\langle \epsilon_1 v_1 \rangle \langle \epsilon_2 v_2 \rangle} = \frac{\langle v_1 v_2 \rangle}{\bar{v}_1 \bar{v}_2} = \frac{C(v_1 v_2)}{\bar{v}_1 \bar{v}_2} + 1$$

This technique assumes a complete separation of the neutrons emitted by the two fragments due to the fragments velocity. It is subject to the same causes of uncertainty that have been mentioned for the average number of neutron measurements. The consequences of these uncertainties are, however, amplified here. We show that this is so for the co-variance measurement. Let  $M$  be the measured ratio of coincidence rates. Then

$$C(v_1, v_2) = \bar{v}_1 \bar{v}_2 (M - 1)$$

The relative error is thus approximately given by

$$\frac{\Delta C(v_1, v_2)}{C(v_1, v_2)} = \frac{\Delta \bar{v}_1}{\bar{v}_1} + \frac{\Delta \bar{v}_2}{\bar{v}_2} + \frac{\Delta M}{M - 1} \quad (\text{III.1})$$

The first two terms of the second member of Eq. (III.1) do not lead to unacceptable errors on the co-variance, they include effects such as errors in the efficiency determination or mass and kinetic energy resolution. The last term includes principally two effects: the first effect is related to the fragment recoil correction, which was found by A. Gavron<sup>(8)</sup> to be very important in average neutron number measurements. Starting from Gavron's considerations we show in Appendix II that the dominant term in the error on the co-variance is

$$\Delta C(v_1, v_2) = \frac{4 E_k}{M_1 + M_2} \left( \frac{M_2}{M_1} + \frac{M_1}{M_2} \right) \left( \frac{v \cos \theta}{v_F} - 1 \right) \frac{E_k - \bar{E}_k}{\sigma^2}$$

where  $E_k$  is the total kinetic energy,  $M_1$  and  $M_2$  the masses of the fragments,  $v$  the laboratory velocity of the neutron,  $v_F$  that of the fragment,  $\sigma^2$  the variance and  $\bar{E}_k$  the mean value of the kinetic energy distribution.

Inserting realistic values for the different parameters one obtains:

$$\Delta C(v_1, v_2) \# 0.03(E_k - \bar{E}_k)$$

it is seen that for  $E_k - \bar{E}_k = 10$  MeV  $\Delta C(v_1, v_2) \# 0.3$  a value which will be seen to be of the same order of magnitude as the co-variance itself.

The second important cause of error in the co-variance measurements stems from the dependence of the efficiencies on the neutron multiplicities. It is also shown in the appendices that if one assumes a linear dependence of the efficiency on  $v_1$

$$\epsilon_1 = \bar{\epsilon}_1 + a(v_1 - \bar{v}_1)$$

$$\epsilon_2 = \bar{\epsilon}_2 + b(v_2 - \bar{v}_2)$$

the co-variance is given by the modified equation

$$\frac{C(v_1, v_2)}{\bar{v}_1 \bar{v}_2} \left( 1 + \frac{k M v_T}{\bar{\epsilon}_1 \bar{\epsilon}_2} \right) = M - 1$$

where we have assumed

$$k = a \bar{\epsilon}_1 = b \bar{\epsilon}_2$$

Since

$$M \# 1$$

we obtain

$$\Delta C(v_1, v_2) \# \frac{a v_T}{\epsilon_2} C(v_1, v_2)$$

Qw.

For higher multiplicities the average neutron energy decreases so that the efficiency decreases and  $a$  is negative. The magnitude of  $a$  depends on the experimental set up and is difficult to evaluate, however, a ratio of  $\frac{a}{\epsilon}$  of around 0.1 could be found and would lead to a 40% error on the co-variance. Since published results<sup>(44)</sup> on the variances of the neutron multiplicity distributions which made use of low efficiency detectors do not account for the above two causes of error they appear strongly in doubt. However, if an accurate treatment of the experimental data became available the small neutron detector technique would be the easiest and most elegant way of measuring the moments of the neutron number distributions.

The measurements making use of large neutron detectors, although rather cumbersome, are essentially free from the errors mentioned in the case of small neutron detectors. They require a knowledge of both backward and forward neutron detection efficiencies. Two independent measurements are necessary to obtain the three second moments of the neutron number distributions, but, in contrast with the low efficiency case, the two measurements must be considered together; this is a consequence of the finite values of the backward efficiencies.

The first measurement uses a  $4\pi$  geometry and provides the variance of the total number of neutrons for the different kinetic energy and mass ratios of the fragments. If  $\epsilon(m, E_k)$  is the computed efficiency of the neutron detector  $\sigma^2(v_T: m E_k)$  the unknown variance and  $\sigma^2(g_T: m E_k)$  the measured one then:

$$\sigma^2(v_T: m E_k) = \sigma^2(g_T: m E_k) \epsilon^{-2} + \epsilon^{-1}(1 - \epsilon^{-1}) \bar{g}_T$$

where  $\bar{g}_T$  is the average number of detected neutrons and  $m$  the mass of one of the two complementary fragments.

The second measurement uses a geometry such that the neutron detector subtends less than a  $2\pi$  solid angle as viewed from the fission source. It has been shown<sup>(43)</sup> that the variances of the observed distributions could be expressed in terms of the five first moments of the bi-variate distribution  $P(v_1, v_2)$

$$\begin{aligned} \sigma^2(g: m E_k) &= \epsilon^2(m, E_k) \sigma^2(v: m E_k) + r^2(m, E_k) \sigma^2(v: m_C, E_k) \\ &+ 2\epsilon(m, E_k) r(m, E_k) C(v_1, v_2: m, E_k) \\ &+ \epsilon(m, E_k)(1 - \epsilon(m, E_k)) \bar{v}(m, E_k) + r(m, E_k)(1 - r(m, E_k)) \bar{v}(m_C, E_k) \\ \sigma^2(g: m_C, E_k) &= \epsilon^2(m_C, E_k) \sigma^2(v: m_C, E_k) + r^2(m_C, E_k) \sigma^2(v: m E_k) \\ &+ 2\epsilon(m_C, E_k) r(m_C, E_k) C(v_1, v_2: m E_k) \\ &+ \epsilon(m_C, E_k)(1 - \epsilon(m_C, E_k)) \bar{v}(m_C, E_k) + r(m_C, E_k)(1 - \epsilon(m_C, E_k)) \bar{v}(m, E_k) \end{aligned} \quad (\text{III.2})$$

Here the quantities labeled by the mass  $m$  corresponds to the case when the fragment of mass  $m$  is flying towards the neutron detector and those labeled by

$m_C$  to the case when the complementary fragment flies towards the detector.

The notations used in Eqs. (III.2) are such that

$$\sigma^2(v_1: m E_k) = \sigma^2(v: m E_k)$$

$$\sigma^2(v_2: m E_k) = \sigma^2(v: m_C, E_k)$$

$$\bar{v}_1(m, E_k) = \bar{v}(m, E_k)$$

$$\bar{v}_2(m, E_k) = \bar{v}(m_C, E_k)$$

The variance of the total number of neutrons is related to the three second moments of the distribution  $P(v_1, v_2)$  by

$$\begin{aligned} \sigma^2(v_T: m E_k) &= \sigma^2(v_1 + v_2: m E_k) = \sigma^2(v_1: m E_k) + \sigma^2(v_2: m E_k) + 2 C(v_1, v_2: m E_k) \\ &= \sigma^2(v: m E_k) + \sigma^2(v: m_C, E_k) + 2 C(v_1, v_2: m E_k) \end{aligned} \quad (\text{III.3})$$

The Eqs. (III.2) and (III.3) can then be solved simultaneously to provide  $\sigma^2(v_1)$ ,  $\sigma^2(v_2)$ , and  $C(v_1, v_2)$  since the average values  $\bar{v}_1$  and  $\bar{v}_2$  are known.

As a more detailed account of both the experimental technique involved and the results is given in another communication to this conference<sup>(45)</sup> we shall now deal only with two specific questions, namely the comparison between total kinetic energy and total number of neutrons variances and the extraction of excitation energy variances from the neutron multiplicity measurements.



1) Variations of the total number of neutron distributions

The variances of the total number of neutrons have been measured as a function of both the mass of one of the fragment and the total kinetic energy. The values obtained are written  $\sigma^2(\nu_T: m E_k)$ . For a given mass split we define the average value of these quantities as

$$\overline{\sigma^2(\nu_T: m E_k)} = \int_{E_k} \sigma^2(\nu_T: m E_k) p(E_k) d E_k$$

Using the relations found in Appendix III the variance of the total number of neutrons measured for a given mass split and for all possible kinetic energies is given by

$$\sigma^2(\nu_T: m) = \left\langle \frac{d\nu_T}{d E_k} \right\rangle_m^2 \sigma^2(E_k: m) + \overline{\sigma^2(\nu_T: m E_k)} \quad (\text{III.4})$$

the quantities  $\sigma^2(\nu_T: m)$  and  $\overline{\sigma^2(\nu_T: m E_k)}$  as obtained from the experiment are plotted on Fig. 24 for the case of the spontaneous fission of  $^{252}\text{Cf}$ . It is possible to use Eq. (III.4) to compute the values of the kinetic energy variance  $\sigma^2(E_k: m)$ . If the values of  $\left\langle \frac{d\nu_T}{d E_k} \right\rangle_m$  obtained in the experiment and shown on Fig. 5 were used one would, then, obviously obtain values of  $\sigma^2(E_k: m)$  equal to those that can be determined from the fission yield curves alone. This is because Eq. (III.4) stands as an identity in such a case, provided only that the regression of  $\nu_T$  on  $E_k$  is linear. If, on the other hand, one uses the values of  $\left\langle \frac{d\nu_T}{d E_k} \right\rangle_{\text{calc.}}$  which have been calculated from the neutron binding and kinetic energies and from the rate of change in  $\gamma$  ray energy as a function of  $E_k$  one obtains another set of values for  $\sigma^2(E_k: m)$ . Both sets are shown on Fig. 25. It can be seen that the

two sets diverge, especially for masses which range between the most probable mass and symmetry. This divergence reflects the one observed on Fig. 5 for the two corresponding sets of values of  $\langle \frac{dv_T}{dE_k} \rangle_m$ . Figure 25 suggests that kinetic energy resolution effects were not completely accounted for; inspection of the fragment yields show that a low energy tailing appears for the masses where the experimental and calculated values of  $\langle \frac{dv_T}{dE_k} \rangle_m$  diverge. It is probable that such a tailing has an experimental origin. If this is true the values of  $\sigma^2(E_k: m)$  computed from the values of  $\sigma^2(v_T: m)$  as indicated above would be better estimates of the true total kinetic energy variances than the values obtained directly from the fragment yields curves. It is interesting to see that the rise of  $\sigma^2(E_k: m)$  near symmetry does not occur for the calculated values which stay remarkably constant. On the other hand, it is well known that tailing of the fragment energy resolution functions will result in a shift of the experimental masses towards symmetry and in an increase of the variance of the total kinetic energy for the more symmetrical fragments pairs. Since the neutron and gamma-ray results should not be very sensitive to this tailing it is possible that, in the future, they will be used to correct the kinetic energy data.

## 2) Variations of the excitation energies of the fission fragments

We have seen that experiment could provide the values of the variances  $\sigma^2(v_1: m E_k)$ ,  $\sigma^2(v_2: m E_k)$  and the co-variances  $C(v_1 v_2: m E_k)$  of the neutron distributions for selected values of one of the fragment's mass and of total kinetic energy. These quantities cannot be immediately transformed into fragment's excitation energy variances because of the neutron evaporation process. Even if a fragment is produced with given mass, charge and excitation energy, a

finite variance of the number of neutrons will be observed due to the statistical nature of this evaporation process.

Since, as will be shown below, we are chiefly interested in the excitation energy variances for fixed masses and charges of the fragments and since the experimental quantities are measured as a function of masses or charges alone it is also necessary to determine in what respect the experimental data are representative.

We first examine this question. Using the formulas of Appendix III we can write that

$$\begin{aligned} \sigma^2(v_1: m E_k) &= \left\langle \frac{dv_1}{dZ} \right\rangle_{m, E_k}^2 \sigma^2(Z: m E_k) + \frac{m}{Z} \sigma^2(v_1: m Z E_k) \\ \sigma^2(v_2: m E_k) &= \left\langle \frac{dv_2}{dZ} \right\rangle_{m, E_k}^2 \sigma^2(Z: m E_k) + \frac{m}{Z} \sigma^2(v_2: m Z E_k) \\ C(v_1 v_2: m E_k) &= \left\langle \frac{dv_1}{dZ} \right\rangle_{m, E_k} \left\langle \frac{dv_2}{dZ} \right\rangle_{m, E_k} \sigma^2(Z: m E_k) + \frac{m}{Z} C(v_1 v_2: m Z E_k) \end{aligned} \quad (\text{III.5})$$

We shall assume that the isotopic widths  $\sigma^2(Z: m E_k)$  and the slopes  $\left\langle \frac{dv_1}{dZ} \right\rangle_{m, E_k}$  do not depend sensitively on the total kinetic energies so that Eqs. (III.5) would also hold when the total kinetic energy variable is disregarded.

Neutron emission is very sensitive to shell effects so that it has more physical grounds to express the rates of variation of average number of neutrons as a function of the charge and neutron number of a nucleus than as a function of its number of mass. Let us then consider the slopes  $\left\langle \frac{dv_1}{dZ} \right\rangle_N$  and  $\left\langle \frac{dv_1}{dN} \right\rangle_Z$  which express the rate of variation as a function of charge (or neutron number) of the

average number of neutrons emitted by a fragment having a fixed number of neutrons (or of protons). Then since  $m = N + Z$

$$\left\langle \frac{dv_1}{dZ} \right\rangle_m = \left\langle \frac{dv_1}{dZ} \right\rangle_N - \left\langle \frac{dv_1}{dN} \right\rangle_Z \quad (\text{III.6})$$

and for example

$$\sigma^2(v_1: m) = \left( \left\langle \frac{dv_1}{dZ} \right\rangle_N - \left\langle \frac{dv_1}{dN} \right\rangle_Z \right)^2 \sigma^2(Z: m) + \frac{m}{Z} \sigma^2(v_1: m Z) \quad (\text{III.7})$$

On the other hand, the slope of the representative curves  $\bar{v}_1(m)$  which have been presented in Sec. I can be written as

$$\left\langle \frac{dv_1}{dm} \right\rangle = \left\langle \frac{dv_1}{dZ} \right\rangle_N \frac{dZ}{dm} + \left\langle \frac{dv_1}{dN} \right\rangle_Z \frac{dN}{dm}$$

assuming that the charge density is the same in the fragments as in the fissile nucleus, we obtain for  $^{252}\text{Cf}$  fission

$$\left\langle \frac{dv_1}{dm} \right\rangle = 0.39 \left\langle \frac{dv_1}{dZ} \right\rangle_N + 0.61 \left\langle \frac{dv_1}{dN} \right\rangle_Z$$

typical values of  $\left\langle \frac{dv_1}{dm} \right\rangle$  range around 0.1. It appears reasonable to assume that for most of the cases  $\left\langle \frac{dv_1}{dZ} \right\rangle_N$  and  $\left\langle \frac{dv_1}{dN} \right\rangle_Z$  have the same sign since the closed shells at 50 protons and 82 neutrons occur in the same mass region. Then the first term of the second member of Eq. (III.7) is maximum for  $\left\langle \frac{dv_1}{dN} \right\rangle_Z = 0$  and

$$\left\langle \frac{dv_1}{dZ} \right\rangle_N \neq 0.25$$

Taking a value of  $\sigma^2(m: Z) \approx 0.25^{(46)}$  we obtain for

$$\left( \left\langle \frac{dv_1}{dZ} \right\rangle_N - \left\langle \frac{dv_1}{dN} \right\rangle_Z \right)^2 \sigma^2(Z: m)$$

a maximum value of 0.015. This value is approximately 1% of the observed values of  $\sigma^2(v_1: m)$  and less than 10% of the values of  $\sigma^2(v_1: m E_k)$ . We conclude that for most masses the existence of a charge distribution for the fragments should not impair the conclusions which could be drawn from the study of the variances of neutron number measured only as a function of total kinetic energy and masses.

We now turn to the extraction of the excitation energy variances. Insofar as the formulas of Appendix III can be applied, we can write that

$$\begin{aligned} \sigma^2(v_1: m E_k) &= \left\langle \frac{dv_1}{dE_1} \right\rangle_{m, E_k}^2 \sigma^2(E_1: m E_k) + \mathcal{M}_{E_1} \sigma^2(v_1: m E_k E_1) \\ \sigma^2(v_2: m E_k) &= \left\langle \frac{dv_2}{dE_2} \right\rangle_{m, E_k}^2 \sigma^2(E_2: m E_k) + \mathcal{M}_{E_2} \sigma^2(v_2: m E_k E_2) \\ C(v_1 v_2: m E_k) &= \left\langle \frac{dv_1}{dE_1} \right\rangle_{m, E_k} \left\langle \frac{dv_2}{dE_2} \right\rangle_{m, E_k} C(E_1 E_2: m, E_k) \\ &\quad + \mathcal{M}_{E_1 E_2} C(v_1 v_2: m E_k E_1 E_2) \end{aligned} \tag{III.8}$$

The second terms of the second members of Eqs. (III.8) represent the contribution of the evaporation process to the neutron number variances and co-variances. In particular, the term  $C(v_1 v_2: m E_k E_1 E_2)$  measures the correlation between the numbers of neutrons emitted by two complementary fragments of fixed masses and excitation energies. Except for possible weak spin effects,

the two evaporation processes should not be correlated and therefore

$$C(v_1 v_2: m E_k E_1 E_2) \neq 0$$

The inverses of the slopes  $\langle \frac{dv_1}{dE_1} \rangle_{m, E_k}$  and  $\langle \frac{dv_2}{dE_2} \rangle_{m, E_k}$  are the energies necessary for the fragment to emit one additional neutron. These can be computed, as indicated previously, from the mass tables, average neutron numbers and kinetic energies, and from the variations of the  $\gamma$  ray energy with neutron number.

The two excitation energies  $E_1$ ,  $E_2$  and the total kinetic energy  $E_k$  are obviously related by energy conservation requirement:

$$Q(m) - E_k = E_1 + E_2 \tag{III.9}$$

The value of  $Q$  is not strictly defined by the knowledge of the masses of the fragments because of their charge distribution. Using again the relations of Appendix III one can write

$$\begin{aligned} \sigma^2(E_1: m, E_k) &= \left\langle \frac{dE_1}{dQ} \right\rangle_{m, E_k}^2 \sigma^2(Q: m) + \frac{m}{Q} \sigma^2(E_1: m, E_k, Q) \\ \sigma^2(E_2: m, E_k) &= \left\langle \frac{dE_2}{dQ} \right\rangle_{m, E_k}^2 \sigma^2(Q: m) + \frac{m}{Q} \sigma^2(E_2: m, E_k, Q) \end{aligned} \tag{III.10}$$

$$C(E_1 E_2: m, E_k) = \left\langle \frac{dE_1}{dQ} \right\rangle_{m, E_k} \left\langle \frac{dE_2}{dQ} \right\rangle_{m, E_k} \sigma^2(Q: m) + \frac{m}{Q} C(E_1 E_2: m, E_k, Q)$$

Because of Eq. (III.9) we have

$$\left\langle \frac{dE_1}{dQ} \right\rangle + \left\langle \frac{dE_2}{dQ} \right\rangle = 1$$

We assume that  $\langle \frac{dE_1}{dQ} \rangle = \langle \frac{dE_2}{dQ} \rangle = \frac{1}{2}$  in order to estimate the first terms of the second members of Eqs. (III.10). This choice maximizes this corrective term for the third equation. Using the mass tables and the data relative to the charge distribution of the fission fragments one can see that  $\sigma^2(Q; m)$  fluctuates between  $1 \text{ MeV}^2$  and  $12 \text{ MeV}^2$ .<sup>(47)</sup> Retaining this last number one sees that the corrective terms in the co-variance are at most equal to  $3 \text{ MeV}^2$ . Expressed in neutron number these quantities are approximately equal to  $0.05 n^2$  which is of the order of 10% of the observed values. In the following we have neglected this effect and have, therefore, assumed that, for a given value of  $m$  and  $E_k$  the total excitation energy  $E_1 + E_2$  was determined. In that case one has evidently

$$\sigma^2(E_1; m E_k) = \sigma^2(E_2; m E_k) = -C(E_1 E_2; m E_k)$$

and the system III.10 can be solved. Fig. 26 shows the variations of the variances  $\sigma^2(E_1; m E_k)$  obtained as explained above with the total kinetic energy  $E_k$  for a choice of masses of the light fragment. The experimental data had been smoothed before the background and efficiency corrections were made. The estimated errors on the curves presented in Fig. 26 are of the order of 20%. The parabolic behavior of the variances appear to be well established. Fig. 27 shows the variations of the variances averaged over  $E_k$  as a function of  $m$  as well as the value of the maximum variance for each mass. Lastly, Fig. 28 which is taken from Ref. 48 shows the values of the variances and co-variances of the neutron number as a function of mass alone. These quantities are related to the previous ones by relations such as

$$C(v_1 v_2; m) = \langle \frac{dv_1}{dE_k} \rangle \langle \frac{dv_2}{dE_k} \rangle \sigma^2(E_k) + \frac{m}{E_k} C(v_1 v_2; m E_k)$$

From Fig. 28 it can be seen that the co-variances  $C(v_1, v_2; m)$  are vanishing except for masses between 95 and 105.



#### IV. Some theoretical consequences of the experimental results

We should like to conclude this review of neutron and gamma emission in fission by an evaluation of the information which the experimental results provide for a theory of nuclear fission. We shall first deal with the knowledge of the potential energy surface of the system undergoing fission which can be obtained from the study of the de-excitation of the fragments.

##### 1) Potential energy surface

Studies of the properties of the fission fragments can only provide information on the potential energy near the scission stage of the fission process. It is convenient, at that stage, to split the potential energy of the system in three parts:

The mutual Coulomb interaction energy  $C$

The deformation energies of the two nascent fragments  $D_1$  and  $D_2$

Since the potential energy surface can be considered as the adiabatic ground state of the system for fixed values of a set of shape parameters, the potential energy does not absorb the whole available energy. The remaining energy can also be split into three parts:

The pre-scission kinetic energy  $\epsilon$

The intrinsic excitation energies of the fragments  $X_1$  and  $X_2$

If one neglects the post scission Coulomb effect the experimentally measured quantities can be expressed as a function of the "scission" ones:

The total fragment kinetic energy as

$$E_k = C + \epsilon$$

(IV.1)

The fragments excitation energies as:

$$E_1 = D_1 + X_1$$

(IV.2)

$$E_2 = D_2 + X_2$$

The comparisons<sup>(49,50,51,52)</sup> between potential energy computations and experiment have been based on the average values of kinetic and excitation energies of the fragment. It was, thus, necessary to make assumptions on the magnitude of the pre-scission kinetic energy and intrinsic excitations of the fragments. Those assumptions were, in fact, related to a picture of the dynamics of the fission process. The knowledge of the variances of the fragments excitation energies allow one to avoid the need of such ambiguous assumptions. We can see from Fig. 26 that the representative curves of these variances can be extrapolated to zero. For each mass ratio there are two resulting points characterized by two values of the kinetic energies  $E_k^{(1)}(m)$  and  $E_k^{(2)}(m)$ . For those points the variance  $\sigma^2(E_1: m E_k)$  vanishes. From equation (IV.2) we can write

$$\sigma^2(E_1) = \sigma^2(D_1) + 2C(D_1, X_1) + \sigma^2(X_1)$$

Since

$$|C(D_1, X_1)| \leq \sigma(D_1) \sigma(X_1)$$

the variance  $\sigma^2(E_1)$  can only vanish if both  $\sigma^2(D_1)$  and  $\sigma^2(X_1)$  vanish, or if the deformation and intrinsic energies  $D_1$  and  $E_1$  were totally anticorrelated. The last possibility is obviously unphysical.

When the total intrinsic excitation energy of the system is non-vanishing, one expects that it will be shared in a random manner between the two fragments; this random sharing will produce a non-vanishing value of the variance  $\sigma^2(X_1)$ . Thereby the vanishing value of  $\sigma^2(X_1)$  implies that both intrinsic excitation energies  $X_1$  and  $X_2$  vanish.

Using the formulas of Appendix III one can write that

$$\sigma^2(D_1: E_k m) = \left\langle \frac{dD_1}{d\varepsilon} \right\rangle_{m, E_k} \sigma^2(\varepsilon: E_k m) + \mathcal{M}_\varepsilon \sigma^2(D_1: E_k m) \quad (\text{IV.3})$$

Since we have shown that for the kinetic energies  $E_k^{(1)}(m)$  and  $E_k^{(2)}(m)$   $\sigma^2(D_1: E_k m) = 0$  the two terms of the second member of equation (IV.3) should cancel.

The slope

$$\left\langle \frac{dD_1}{d\varepsilon} \right\rangle_{m, E_k} = - \left\langle \frac{dD_1}{dC} \right\rangle_{m, E_k}$$

has no reason to vanish so that we obtain the result that

$$\sigma^2(\varepsilon: E_k^{(1,2)}(m)) = 0$$

An argument similar to that used for the intrinsic excitation energies shows that this condition can only be fulfilled if  $\varepsilon = 0$ .

An intrinsic understanding of the preceding arguments can be obtained from consideration of Fig. 30.

On the figure we have schematically drawn the minimum potential energy of the system along the scission line (curve A). This curve has been labeled according to the potential Coulomb interaction at each point. We also show the horizontal line corresponding to the total energy available to the system. The shaded area corresponds to the excess energy in the system which can be split more or less at random in pre-scission kinetic energy, additional potential energy or intrinsic excitation energy. For all points between 1 and 2 the system can occupy a whole range of states and thereby the variances of the excitation energies of the fragments should not vanish. At points 1 and 2 all the available energy is necessary to provide the necessary potential energy, and the system has no additional freedom. At these points we can therefore write that

$$C_1 = E_k^{(1)}(m)$$

$$D_1^{(1)} = E_1^{(1)}(m)$$

$$D_2^{(1)} = E_2^{(1)}(m)$$

$$C_2 = E_k^{(2)}(m)$$

$$D_1^{(2)} = E_1^{(2)}(m)$$

$$D_2^{(2)} = E_2^{(2)}(m)$$

The above treatment therefore provides, for each mass ratio of the fragments two points along the minimum potential energy scission line where the Coulomb interaction energy and the fragment's deformation energies are known. Fig. 31 displays the values for these quantities as obtained from the experiment on the spontaneous fission of  $^{252}\text{Cf}$ . It would be interesting to study the behavior of the variances of the excitation energy as a function of the excitation of the nucleus undergoing fission. Such studies could perhaps provide additional points on the potential energy surface. Some additional information can also be obtained using a slightly modified two spheroid model. We assume that the potential energy  $P$  along the scission line has a minimum for a value  $C_0$  of the Coulomb potential. We further assume that the potential energy can be satisfactorily approximated by a parabola so that

$$C_0 = \frac{C_1 + C_2}{2}$$

the potential energy can therefore be written as

$$P = C + D = P_0 + a(C - C_0)^2$$

which gives for the deformation energy

$$D = P_0 + a(C - C_0)^2 - C$$

If  $Q$  is the energy released in the fission we also can write that

$$Q = P_0 + a(C_1 - C_0)^2 = P_0 + a(C_2 - C_0)^2 = P_0 + a\Delta C^2$$

since the points (1) and (2) are such that the potential energy is equal to the energy release, as shown earlier.

We make the further assumption, as in the two spheroids model that there exists a value  $C^*$  where both

$$D(C^*) = 0 \quad \text{and} \quad \left( \frac{dD(C)}{dC} \right)_{C=C^*} = 0$$

These conditions are written:

$$C^* - C_0 = \frac{1}{2a}$$

$$4a^2 \Delta C^2 - 4a(Q - C_0) + 1 = 0$$

We make the further assumption that  $C^* > Q$  (this is equivalent to the assumption that the fragments are always elongated at scission) and obtain that

$$P = Q + \frac{[(C - C_0)^2 - \Delta C^2]}{2 \Delta C^2} \times [Q - C_0 - \sqrt{(Q - C_0)^2 - \Delta C^2}]$$

The maximum energy of the system which is not tied up in potential energy is obtained for  $C = C_0$  and amounts to

$$Q - P(C_0) = \frac{1}{2}((Q - C_0) - \sqrt{(Q - C_0)^2 - \Delta C^2})$$

The variations of this quantity as a function of the mass of the light fragment are shown in Fig. 32. It is an upper limit for both the pre-scission kinetic energy and total intrinsic excitation energy. Also shown in the figure is the second derivative of the potential energy which is equal to

$$\frac{(Q - C_0) - \sqrt{(Q - C_0)^2 - \Delta C^2}}{\Delta C^2}$$

It can be seen on Fig. 31, that the values of the maximum energy which is not tied up in potential energy is surprisingly small. It rises slightly from the most asymmetric splits to the most probable ones where it reaches a value of approximately 7 MeV. Although the error on that number is difficult to estimate, it should not exceed 50%. It appears doubtful that the statistical approach of P. Fong<sup>(42)</sup> could be justified with excitation energies of the fragments as low as 4 MeV. On the other hand, pre-scission kinetic energies of 40 MeV which have been obtained in some computations<sup>(53,54)</sup> seem to be ruled out. In that respect it is worth recalling that the early  $\alpha$  accompanied fission experiments<sup>(55)</sup> which seemed to confirm this high figure have been improved and yield much smaller values.<sup>(56,57)</sup> The study of the even-odd effect reported in Sec. II provides an additional experimental approach to fission dynamics.

2) Even-odd effects and quasiparticle excitations in the fission process

The production of two odd-charge fragments in the fission of an even-charge nucleus requires the breaking of at least one proton-pair bond. For low excitation fission where the nucleus can be considered as cold at the saddle point as well as for spontaneous fission the corresponding two quasiparticles excitation must occur somewhere between saddle and scission. If the time difference between the instant when this excitation takes place and the instant of scission is longer than the characteristic time of a nucleon in the nucleus (approximately  $2.10^{-22}$  s) the two unpaired protons can be freely exchanged between the two nascent fragments before scission takes place. At scission the positions of the two protons can be considered to be uncorrelated. The probabilities to observe two odd-charge or two even-charge fragments will therefore be equal. If two even-charge fragments are observed one of them would have at least one two-quasiparticle excitation. While the excitation energies of the even-Z fragments will be higher by approximately 2.5 MeV than those of the odd-Z ones, the observed total kinetic energies should not differ for the

two cases. The experimental results show that approximately two-thirds of the pairing energy appears as fragment's kinetic energy, in contradiction with the above prediction. We conclude that most of the even-Z fragments are produced in the absence of quasiparticle excitation.

It is known that the yields of odd-Z fragments do not differ markedly from those of even-Z ones. The radiochemical measurements<sup>(58)</sup> appear to show a slight enhancement by approximately 30% of the even-charge elements. In the following we shall assume that this enhancement is 50%. If we again make the hypothesis that the two quasiparticle excitation required to produce odd-Z fragments occurs at a relatively long-time before scission and that the energy of approximately 2.5 MeV, necessary to break the proton-proton bond comes entirely from the kinetic energy of the fragments, an average difference of 1.25 MeV in kinetic energy should be observed between odd-Z and even-Z fragments. This is because half of the even-Z fragments should be formed with at least one two-quasiparticle excitation as explained above. Since the experimental figure is again higher than the predicted one, itself an upper limit, the hypothesis that the quasiparticles excitation occur a long time before scission must be abandoned. It, therefore, appears that quasiparticle excitations occur only at the very late stage of the fission process with a probability close to 0.5.

These findings are contradictory to the basic assumptions of the statistical model of P. Fong.<sup>(42)</sup> They agree well with the calculations of W. Nöremberg<sup>(41)</sup> who found that the probability of level-slipage at the crossing of two levels differing by their number of particle-hole excitations was close to unity. This means that the structure of the level is conserved and, thus, that the probability for quasiparticle excitations from saddle to scission is small.



An interesting check on the ideas just outlined would be to study the even-odd effect on fragments' kinetic energies as a function of the excitation energy of the fissile nucleus. As soon as quasiparticle excitations would be possible at the saddle point this even-odd effect should decrease markedly and eventually vanish.

### 3) Variances of the excitation energies

We have noticed the remarkable experimental result that the co-variance of the excitation energies for a fixed mass ratio  $C(E_1, E_2; m)$  was very close to zero except around mass 100. We now show that this can be expected on the basis of a very schematic two spheroid model with the assumption of equipartition of the energy.

Let  $\alpha$  and  $\beta$  be the deformation parameters of the two fragments. The deformation energies of these fragments are assumed to be

$$D_1 = d_1 \alpha^2$$

$$D_2 = d_2 \beta^2$$

We further assume that around the minimum potential energy of the system the Coulomb energy is a linear function of  $\alpha$  and  $\beta$

$$C = V - K(\alpha + \beta)$$

The potential energy is then equal to

$$P = V - K(\alpha + \beta) + d_1 \alpha^2 + d_2 \beta^2$$

and can be written around the minimum

$$P - P_{\min} = 2 d_1 (\alpha - \alpha_M)^2 + 2 d_2 (\beta - \beta_M)^2$$

If we assume thermal equilibrium the probability to observe a deformation couple  $\alpha, \beta$  is:

$$P(\alpha, \beta) = \exp \frac{P(\alpha, \beta) - P(\alpha_M, \beta_M)}{T} = P(\alpha) P(\beta)$$

it follows that the two deformations behave independently and that

$$C(\alpha, \beta) = 0$$

and also that  $C(D_1, D_2) = 0$ .

We had previously assumed<sup>(59)</sup> that the variances of the deformation energies for a fixed value of the total kinetic energy

$$\sigma^2(D_1: m E_k)$$

could be neglected. The above result shows that this cannot be the case since we have

$$0 = C(D_1, D_2: m) = \left\langle \frac{dD_1}{dE_k} \right\rangle \left\langle \frac{dD_2}{dE_k} \right\rangle \sigma^2(E_k) + \sum_{E_k} C(D_1, D_2: m E_k)$$

and

$$\sum_{E_k} C(D_1, D_2: m E_k) = - \left\langle \frac{dD_1}{dE_k} \right\rangle \left\langle \frac{dD_2}{dE_k} \right\rangle \sigma^2(E_k)$$

contrary to our original assumption<sup>(59)</sup> we find that the variances of the deformation energies are more important than those of the intrinsic excitation energies. Assuming that

$$C(E_1, E_2: m) = C(D_1, D_2: m) = 0$$

we obtain an average value of  $C(E_1, E_2: m E_k)$  of approximately

$$-\frac{\sigma^2(E_k)}{4} = -20 \text{ MeV}^2 = C(E_1, E_2: m E_k) = -\sigma^2(E_1: m, E_k)$$

in good agreement with the experimental values shown on Fig. 26.

The above treatment implied that the fluctuations of the intrinsic excitation energies were small. This is to be expected if the system behaves statistically except when the fluctuations become critical. It is possible that this is the situation when the light fragment has a mass number around 100.

While in the previous sub-section we have shown that almost no quasiparticle excitations occurred in the descent from saddle to scission, we had not ruled out the possibility of a strong coupling of collective states within what W. Nöremberg<sup>(41)</sup> defines as a fission band. W. Nöremberg predicts that such a strong coupling should exist and that a statistical treatment of the system near scission should be adequate. We have shown above that such a treatment predicts, at least qualitatively, the values of the variances of the excitation energy. We have not shown, however, that other models would fail to predict these values. It appears, at this time, that the strongest argument in favor of the "fission band" model comes from another kind of experiments where the total kinetic energies obtained in induced and spontaneous fission of the same nucleus are compared.<sup>(60)</sup> It appears that only a small fraction of the increase of excitation energy of the fissioning system appears in additional kinetic energy. This suggests a strong damping of the fission mode in the first part of the way from saddle to scission.

### Conclusion

In conclusion, we should like to summarize the information which appears to us relevant to the fission theory and has been explained in detail previously. We also wish to suggest some possible future developments as regards the experiments.

The gamma-ray emission by the fission fragments can be explained within the frame of the theory of statistical decay of excited nuclei provided angular momentum effects are included. The anisotropy of the fission  $\gamma$  rays appear to be in contradiction with P. Fong's<sup>(42)</sup> statistical theory of fission. It can be explained, as well as the correlation between total  $\gamma$  ray energies and excitation energies in the frame of the "fission band" model of W. Nöremberg.<sup>(41)</sup>

The experimentally determined variances of the excitation energies of the fragments yield values of the minimum potential energy of the system near scission which are surprisingly high, allowing for less than 10 MeV in pre-scission kinetic energy or internal excitation.

The study of the even-odd fluctuations of the total kinetic energy of the fragments points to a very small probability for two-quasiparticle excitations in the descent from saddle to scission. On the other hand, the comparison between total kinetic energy in induced and spontaneous fission is easily explained in terms of a strong damping of the fission mode into other excitation modes. Those two features are reconciled in the "fission band" model which predicts the right order of magnitude for the variances of the excitation energies.

As far as the experimental situation is concerned, we have seen that some discrepancies remain with respect to a satisfactory account of energy balance in fission. The main cause of uncertainty lies in the kinetic energy measurements; our knowledge of the energy resolution and tailing obtained with fragments detectors needs to be improved. The availability of heavy ion beams or of separated beams of fission fragments should help to obtain this information.

The better accuracy obtained in measurements of average neutron numbers has not been accompanied by a similar progress in obtaining the average neutron kinetic energies; the time has perhaps come to improve on the measurements of H. R. Bowman et al.<sup>(1)</sup> In particular, the question of the isotropic component in the neutron emission remains mostly opened not only with respect to its behavior as a function of the masses and kinetic energies of the fragments but regarding its very existence. A better knowledge of the neutron kinetic and angular distributions could in turn allow an improvement of the neutron variance measurements; it could also help resolve the present discrepancies between variance measurements using large or small detectors, respectively. It is important that this discrepancy be resolved so that the less cumbersome small detector method could be used safely.

The neutron variance measurements, if carried out at varying excitation energies of the fissile nucleus could provide more points on the potential energy surface and perhaps more sensitive tests of models for the fission dynamics.

Regarding the gamma-ray measurements it has usually been assumed that their angular distribution was not significantly perturbed by the hyperfine interaction. It appears\* that such an assumption might not be justified since deorientation effects were very important for highly ionized rare-earth nuclei.

Finally, the study of even-odd effects on kinetic energies as a function of excitation energy of the compound nucleus should be a useful test of the conclusions we have reached here and eventually provide information on the number of 2-quasi-particles excitations at the saddle point.

---

\* F. Stephens, private communication.

Acknowledgements

One of us, H. Nifenecker, has greatly benefited of the hospitality of the Lawrence Berkeley Laboratory. He is greatly indebted to S. G. Thompson, who made available the data used in the study of even-odd effects on the fragments' total kinetic energy, and whose continuous interest has been of great comfort. It is also a pleasure to thank R. C. Jared for his help in sorting out the kinetic energy data. Most fruitful discussions with J. J. Griffin, S. S. Kataria, M. Kleber, H. Krappe, L. Moretto, W. Myers, G. Sussmann, W. Swiatecki, C. F. Tsang, and J. B. Wilhelmy have very much helped in writing this article.

REFERENCES

- [1] BOWMAN, H. R., THOMPSON, S. G., MILTON, J. C. D., SWIATECKI, W. J., Phys. Rev. 126 (1962) 2120.
- [2] MILTON, J. C. D., FRASER, J. S., "Proceedings of the Symposium on Physics and Chemistry of Fission", Vol. II, p. 39, IAEA, Salzburg (1965).
- [3] APALIN, V. F., GRITYUK, Y. N., KUTIKOV, I. E., LEBEDEV, V. I., MIKAELIAN, L. A., Nucl. Phys. 55 (1964) 249.
- [4] WHETSTONE, S. L., Phys. Rev. 100 (1956) 1016.
- [5] MASLIN, E. E., RODGERS, A. L., CORE, W. G. F., Phys. Rev. 164 (1967) 1520.
- [6] BOLDEMAN, J. W., MUSGROVE, A. R. L., WALSH, R. L., Aust. J. Phys. 24 (1971) 821.
- [7] SIGNARBIEUX, C., NIFENECKER, H., POITOU, J., RIBRAG, M., Journal de Physique 33(8-9) C5-1972(I-23).
- [8] GAVRON, A., Correction of Experimental Results in Fission Experiments, to be published.
- [9] TERRELL, J., Phys. Rev. 127 (1962) 880.
- [10] RIBRAG, M, POITOU, J., SIGNARBIEUX, C., MATUSZEK, J., Etude d'un ensemble de detection destiné à mesurer la multiplicité de l'emission neutronique dans les réactions nucléaires, Internal Report, CEA, SMPNF/853/71.
- [11] BOLDEMAN, J. W., DALTON, A. W., (1962) AAEC/E172.
- [12] MACKLIN, R. L., GLASS, F. M., HALPERIN, J., ROSEBERRY, R. T., SCHMITT, H. W., STOUGHTON, R. W., TOBIAS, M., Nucl. Instr. Methods 102 (1972) 181.
- [13] GAVRON, A., FRAENKEL, Z., unpublished.
- [14] POITOU, J., NIFENECKER, H., SIGNARBIEUX, C., unpublished.
- [15] SKARSVÄG, K., BERGHEIM, K., Nucl. Phys. 45 (1963) 72.
- [16] KAPOOR, S. S., RAMANNA, R., RAMA RAO, D. N., Phys. Rev. 131 (1963) 283.
- [17] NIFENECKER, H., SIGNARBIEUX, C., RIBRAG, M., POITOU, J., MATUSZEK, J., Nucl. Phys. A189 (1972) 285.

- [18] MAIER-LEIBNITZ, H., SCHMITT, H. W., ARMBRUSTER, P., "Proceeding of the Symposium on Physics and Chemistry of Fission", Vol. II, p. 143, IAEA, Salzburg (1965).
- [19] PLEASANTON, F. FERGUSON, R. L., SCHMITT, H. W., Phys. Rev. C 6 3 (1972) 1023.
- [20] ARMBRUSTER, P. LABUS, H., REICHELT, K., Z. Naturforsch 26a (1971) 512.
- [21] WILHELMY, J. B., CHEIFETZ, E., JARED, R. C., THOMPSON, S. G., BOWMAN, H. R., RASMUSSEN, J. O., Phys. Rev. C 5 6 (1972) 2041.
- [22] HOFFMAN, M. M., Phys. Rev. 133 (1964) B714.
- [23] IVANOV, O. I., KUSHNIR, Y. A., SMIRENKIN, G. N., ZhETF Pis'ma 6 10 (1967) 898.
- [24] JOHANSSON, S. A. E., Nucl. Phys. 60 (1964) 378.
- [25] ALBINSSON, H., Physica Scripta 3 (1971) 113.
- [26] ALBINSSON, H., Energies and Yields of Prompt Gamma Rays from Fragments in Slow Neutron Induced Fission of  $^{235}\text{U}$ , Internal Report n° AE-420.
- [27] CHEIFETZ, E., JARED, R. C., THOMPSON, S. G., WILHELMY, J. B., Phys. Rev. Letters 25 (1970a) 38.
- [28] JOHN, W., WESOLOWSKI, J. J., GUY, F., Phys. Letters 30B (1969) 340.
- [29] VERBINSKY, V. V., WEBER, H., SUND, R. E., "Physics and Chemistry of Fission", Proc. Symp. Vienna, 1969 (IAEA, Vienna 1969), p. 929.
- [30] MEHTA, G., POITOU, J., RIBRAG, M., SIGNARBIEUX, C., Phys. Rev. C 7 (1973) 373.
- [31] NARDI, E., MORETTO, L. G. THOMPSON, S. G., Phys. Letters 43B (1973) 259.
- [32] ALBINSSON, H., LINDOW, L., Prompt Gamma Radiation from Fragments in the Thermal Fission of  $^{235}\text{U}$ , Internal Report AE-398.
- [33] ALBINSSON, H., Yield of Prompt Gamma Radiation in Slow Neutron Induced Fission of  $^{235}\text{U}$  as a Function of the Total Fragment Kinetic Energy, Internal Report AE-417.
- [34] VAL'SKII, G. V., PETROV, G. A., PLEVA, Y. S., Sov. J. Phys. 8 (1969) 171.
- [35] NIFENECKER, H., SIGNARBIEUX, C., RIBRAG, M., POITOU, J., MATUSZEK, J., Nucl. Phys. A189 (1972) 285.



- [36] GARVEY, G. T., GERACE, W. J., JAFFEE, R. L., TALMI, I., KELSON, I., Rev. Mod. Phys. 41 (1969) S1.
- [37] WILKINS, B. D., FLUSS, M. J., KAUFMAN, S. B., GROSS, C. E., STEINBERG, E. P., Nucl. Instr. Methods 92 (1971) 381.
- [38] SCHMITT, H. W., PLEASANTON, F., Nucl. Instr. Methods 40 (1966) 204.
- [39] MORETTO, L. G., Nucl. Phys. A182 (1972) 641.
- [40] RASMUSSEN, J. O., NÖREMBERG, W., MANG, H. J., Nucl. Phys. A136 (1969) 465.
- [41] NÖREMBERG, W., "Zur mikroskopischen Beschreibung der Kernspaltung", Habilitationsschrift, Heidelberg University (1970).
- [42] FONG, P., Phys. Rev. 102 (1956) 434.
- [43] NIFENECKER, H., Nucl. Instr. Methods 81 (1970) 45.
- [44] GAVRON, A., FRAENKEL, Z., Phys. Rev. Letters 27 (1971) 1148.
- [45] BABINET, R., NIFENECKER, H., POITOU, J., SIGNARBIEUX, C., this conference SM-174/41.
- [46] REISDORF, W., UNIK, J. P., GRIFFIN, H. C., GLENDENIN, L. E., Nucl. Phys. A177 (1971) 337.
- [47] NIFENECKER, H., Thesis, CEA R4121.
- [48] SIGNARBIEUX, C., POITOU, J., RIBRAG, M., MATUSZEK, J., Phys. Letters 39B (1972) 503.
- [49] TERRELL, J., "Physics and Chemistry of Fission", Vol. II, p. 3, IAEA, Salzburg (1965).
- [50] VANDENBOSCH, R., Nucl. Phys. 46 (1963) 129.
- [51] DICKMANN, F., DIETRICH, K., Nucl. Phys. A129 (1969) 241.
- [52] SCHMITT, H. W., "Physics and Chemistry of Fission", IAEA, Vienna (1969), p. 67.
- [53] NIX, J. R., SWIATECKI, W. J., Nucl. Phys. 71 (1965) 1.
- [54] HASSE, R. W., "Physics and Chemistry of Fission", IAEA, Vienna (1969), p. 33.
- [55] BONEH, Y., FRAENKEL, Z., NEBENZAHL, I., Phys. Rev. 156 (1962) 1305.
- [56] RAJAGOPALAN, M., THOMAS, T. D., Phys. Rev. C 5 (1972) 2064.
- [57] FLUSS, M. J., KAUFMAN, S. B., STEINBERG, E. P., WILKINS, B. D., Phys. Rev. C 7 (1973) 353.

- [58] WAHL, A. C., "Physics and Chemistry of Fission", IAEA, Salzburg (1965), p. 317.
- [59] NIFENECKER, H., BABINET, R., SIGNARBIEUX, C., Journal de Physique 33(8-9) C5-1972, Vol. II (I.24).
- [60] DERUYTTER, A. J., this conference SM-174/35.

## Appendix I

Effect of an isotropic component on the determination of the average number of neutrons emitted by the fission fragments

We consider a fission event in which  $v_1$  neutrons are emitted by fragment 1,  $v_2$  by fragment 2 and assume  $v_a$  scission neutrons. When fragment 1 flies towards the neutron detector the average number of detected neutrons will be

$$g_1 = \epsilon v_1 + r v_2 + a v_a$$

where  $\epsilon$  is the efficiency for neutrons emitted by fragments flying towards the detector,  $r$  the efficiency for neutrons emitted by the complementary fragment and  $a$  the efficiency for detecting scission neutrons. We assume that  $\epsilon$  and  $r$  are independent of the fragment's characteristics. Then, when fragment 2 flies towards the neutron detector we have

$$g_2 = \epsilon v_2 + r v_1 + a v_a$$

and

$$g_1 + g_2 = (\epsilon + r)(v_1 + v_2) + 2a v_a$$

When we neglect the pre-scission component we assume that  $n_1$  and  $n_2$  neutrons are emitted by the two fragments so that

$$g_1 = \epsilon^1 n_1 + r^1 n_2$$

$$g_2 = \epsilon^1 n_2 + r^1 n_1$$

the efficiencies  $\epsilon^1$  and  $r^1$  are assumed to be proportional to  $\epsilon$  and  $r$

$$\epsilon^1 = \alpha \epsilon \quad r^1 = \alpha r$$

as explained in the main article the proportionality constant is determined by writing that

$$g_1 + g_2 = (\epsilon^1 + r^1)(n_1 + n_2) = \alpha(\epsilon + r)(n_1 + n_2)$$

with

$$n_1 + n_2 = v_1 + v_2 + v_a = v_T$$

so that

$$\alpha(\epsilon + r)(v_1 + v_2 + v_a) = (\epsilon + r)(v_1 + v_2) + 2a v_a$$

from which we obtain

$$\alpha = 1 + \frac{v_a}{v_T} \left( \frac{2a}{\epsilon + r} - 1 \right)$$

and

$$n_1 = \frac{1}{2} \left[ v_1 \left( 1 + \frac{1}{\alpha} \right) + v_2 \left( 1 - \frac{1}{\alpha} \right) + v_a \right]$$

$$n_2 = \frac{1}{2} \left[ v_2 \left( 1 + \frac{1}{\alpha} \right) + v_1 \left( 1 - \frac{1}{\alpha} \right) + v_a \right]$$

We now consider two limiting cases. In the first one a large neutron detector is seen from the source through an angle of  $90^\circ$ . Then, if one assumes that all efficiencies are proportional to the related solid angles, obviously

$$\frac{2a}{\epsilon + r} = 1 \quad \text{and} \quad \alpha = 1$$

so that

$$n_{(1,2)} = v_{(1,2)} + \frac{v_a}{2}$$

We see that in this case, the assumption that all neutrons are emitted by the fragments is equivalent to an equal sharing of the pre-scission component between the two fragments. Furthermore, the condition  $n_1 + n_2 = v_T$  is always fulfilled. In the second case we consider a low efficiency detector. We, thereby, can neglect  $r$  and

$$\alpha = 1 + \frac{v_a}{v_T} \left( \frac{2a}{\epsilon} - 1 \right) \quad (\text{A.I.1})$$

Assuming a Maxwellian shape for the center of mass fragment's neutrons spectrum we have

$$\frac{\epsilon}{a} = 2 \sqrt{\frac{E_0}{\pi T}} e^{-\frac{E_0}{T}} + \left( 1 + P \left( \sqrt{\frac{2E_0}{T}} \right) \right) \left( 1 + \frac{2E_0}{T} \right) \quad (\text{A.I.2})$$

where  $E_0$  is the energy per nucleon of the fission fragment,  $T$  is the neutron spectrum temperature and

$$P \left( \sqrt{\frac{2E_0}{T}} \right) = \frac{1}{\sqrt{2\pi}} \int_{-\sqrt{\frac{2E_0}{T}}}^{+\sqrt{\frac{2E_0}{T}}} e^{-\frac{t^2}{2}} dt$$

Typical values of  $\frac{E_0}{T}$  are around 0.5. Then

$$\frac{\epsilon}{a} \# 4$$

and

$$\alpha \# 1 - \frac{v_a}{v_T} \times 0.5$$

From equation (A.I.1) it can be seen that the value of  $\alpha$  which ensures that the condition  $n_1 + n_2 = v_T$  is fulfilled will depend on the fission event's characteristics with respect to both the value of  $\frac{v_a}{v_T}$  and that of  $\frac{a}{\epsilon}$ . Alternatively, if one uses the value of  $\alpha$  obtained for the average characteristics of the fission fragments one obtains

that

$$n_1^1 + n_2^1 = v_T + 2 v_a a \left( \frac{1}{\epsilon} - \frac{1}{\epsilon'} \right)$$

where  $n_1^1 + n_2^1$  represents the average total number of neutrons as obtained with the assumption that there are no pre-scission neutrons,  $\epsilon$  and  $\epsilon'$  are the efficiencies computed for the average and the specific fission events, respectively. In particular,

one obtains for the slopes with respect to  $E_k$

$$\left\langle \frac{d(n_1^1 + n_2^1)}{dE_k} \right\rangle = \left\langle \frac{dv_T}{dE_k} \right\rangle + 2 \frac{v_a a^2}{\epsilon^2} \left\langle \frac{d\epsilon(E_k)/a}{dE_k} \right\rangle$$

With typical values of the variations of  $\frac{E_D}{T}$  in equation (A.I.2) one obtains a relative increase in the slopes of the variation of the average total number of neutrons as a function of  $E_k$  of a few percent. The error on  $v_T$  itself is of the order of 0.1 neutron.

## Appendix II

A study of two causes of systematic errors in the measurement of neutron number variances1) Recoil effect

A. Gavron<sup>(8)</sup> has pointed out that the hypothesis of isotropic emission of the neutrons, usually made to obtain pre-neutron masses and kinetic energies from the post-neutron energies of the fission fragments, was no more valid when the neutrons were detected with small detectors. We first recall the treatment given by A. Gavron in the case of average neutron number measurements. We then extend his treatment to the measurement of co-variances of the neutron distributions.

Using the notations of A. Gavron,  $V_F$  is the velocity of the fragment before the detected neutron is emitted,  $V_F^1$  its velocity after emission of the neutron,  $V^1$  and  $\theta^1$  are the velocities and angle of emission of the neutron in the fragment frame,  $V$  and  $\theta$  the corresponding quantities in the laboratory system.

The final energy of the fragment when a neutron is detected at the angle  $\theta$  will differ from that of the isotropic case, when no neutron is detected, by :

$$e_{1F}(\theta) - e_{1F}(is) = - \frac{2e_1}{m_1} \left( \frac{V \cos \theta}{V_F} - 1 \right)$$

where  $e_{1F}(\theta)$  is the final energy of the fragment when a neutron is detected at angle  $\theta$ ,  $e_{1F}(is)$  the same energy in the isotropic case,  $e_1$  and  $m_1$  the pre-neutron emission kinetic energy and mass of the fragment.

The pre-neutron energy of the fragment is then equal to

$$e_1 = e_{1F} \left( 1 + \frac{\bar{v}(m,e)}{m_1} \right) - 2 e_{1F} \left( \frac{V \cos \theta}{V_F} - 1 \right) / m_1$$

when the recoil effect is not taken into account the pre-neutron energy is written

$$e_1^1 = e_{1F} \left( 1 + \frac{\bar{v}(m_1, e)}{m_1} \right)$$

$\bar{v}_1(m, e)$  is the average number of neutrons emitted by the fragment of mass  $m_1$  and for a total kinetic energy  $e$ .

The average neutron number is given by the ratio of two counting rates. The numerator is proportional to the number of triple coincidences between the fragments and neutron detectors, the denominator to the number of double coincidences between the fragments detectors. When the recoil correction is not included one obtains :

$$\bar{v}_1(e) = \frac{N_C(e, m_1)}{N_T(e, m)}$$

when it is included one should write :

$$\bar{v}_1^1 = \frac{N_C(e^1, m^1)}{N_T(e, m)}$$

A. Gavron has shown that the error made in assuming that  $m = m^1$  was not great. If we make a first order development in  $e$  we obtain

$$\begin{aligned} \bar{v}_1^1 - \bar{v}_1 &= \frac{1}{N_T(e, m)} (e^1 - e) \frac{d N_C(e, m)}{de} = \frac{1}{N_T(e, m)} (e^1 - e) \frac{dv_1 N_T}{de} \\ &= (e^1 - e) \frac{dv_1}{de} + \frac{1}{N_T(e, m)} \bar{v}_1 (e^1 - e) \frac{dN_T}{de} \end{aligned}$$

We now assume that  $N_T(e, m)$  is a gaussian function of the total kinetic energy so that

$$\frac{dN_T/de}{N_T} = - \frac{(e - \bar{e})}{\sigma^2}$$



where  $\bar{e}$  is the most probable value of  $e$ .

The difference  $e^1 - e$  arises only from the difference between  $e_1$  and  $e_1^1$ . We then obtain

$$\bar{v}_1^1 - \bar{v}_1 = \frac{2m_2}{m_1(m_1 + m_2)} \left( \frac{v \cos\theta}{v_F} - 1 \right) e \left( \frac{d\bar{v}_1}{de} - \frac{\bar{v}_1(e - \bar{e})}{\sigma^2} \right) \quad (\text{A.II.1})$$

this expression also allows the study of the difference in slope between the corrected and uncorrected data. We neglect the second derivative  $\frac{d^2\bar{v}_1}{de^2}$  so that :

$$\frac{d\bar{v}_1^1}{de} - \frac{d\bar{v}_1}{de} = \frac{2m_2}{m_1(m_1 + m_2)} \left( \frac{d\bar{v}_1}{de} - \frac{\bar{v}_1(e - \bar{e})}{\sigma^2} - \frac{\bar{v}_1 e}{\sigma^2} - \frac{e(e - \bar{e})}{\sigma^2} \frac{d\bar{v}_1}{de} \right) \left( \frac{v \cos\theta}{v_F} - 1 \right) \quad (\text{A.II.2})$$

the dominant term in the parenthesis is  $-\frac{\bar{v}_1 e}{\sigma^2}$ . Setting in A.II.2,  $\cos\theta = 1$ ,  $\frac{v}{v_F} = 2$  and writing the same equation for the complementary fragment one obtains an estimate of the difference in the slopes of the total number of neutrons variations

$$\frac{d\bar{v}_T^1}{de} - \frac{d\bar{v}_T}{de} = - 0.07$$

For example, if the true value  $\left( \frac{d\bar{v}_T^1}{de} \right)^{-1}$  is 8.3 MeV, the uncorrected value would yield 5.26 MeV.

In the small neutron detector measurements of the co-variances the quantity

$$M(e) = \frac{N_4(e)}{N_1^C(e) N_2^C(e)}$$

is provided by the experiment, the co-variance being given by

$$\frac{C(v_1 v_2)}{\bar{v}_1 \bar{v}_2} = M - 1$$

Here the quantity  $N_4(e)$  is proportional to the number of quadruple coincidences between two neutron detectors and two fragments detectors while  $N_1^C(e)$  and  $N_2^C(e)$  are proportional to the number of triple coincidences between one of the neutron detectors and the two fragment detectors. Using the definitions of  $\bar{v}_1$  and  $\bar{v}_2$  we also can write that

$$C(v_1 v_2) = \frac{N_4(e)}{N_1^C(e) N_2^C(e)} \bar{v}_1 \bar{v}_2 - \bar{v}_1 \bar{v}_2 = \frac{N_4(e)}{N_T^2(e)} - \bar{v}_1 \bar{v}_2$$

We define

$$P(e) = \frac{N_4(e)}{N_T^2(e)}$$

The errors made in neglecting the recoil effect will then be

$$\Delta P = \frac{N_4(e^1) - N_4(e)}{N_T^2(e)}$$

and

$$\Delta C = \Delta P - \bar{v}_1 \Delta \bar{v}_2 - \bar{v}_2 \Delta \bar{v}_1$$

where  $\Delta \bar{v}_1$  and  $\Delta \bar{v}_2$  have been computed above.

We express  $\Delta P$

$$\begin{aligned} \Delta P &= \frac{1}{N_T^2(e)} \frac{dN_T(e)}{de} (e^1 - e) = \frac{1}{N_T^2} \frac{dP(e) N_T^2(e)}{de} (e^1 - e) \\ &= \left[ \frac{dP(e)}{de} + 2P(e) \frac{dN_T(e)/de}{N_T(e)} \right] (e^1 - e) \\ &= \left[ \frac{dP(e)}{de} - 2P(e) \frac{e - \bar{e}}{\sigma^2} \right] \left[ e_1^1 + e_2^1 - e_1 - e_2 \right] \end{aligned}$$

The quantity  $P(e)$  is very nearly equal to  $\bar{v}_1 \bar{v}_2$  since  $C(v_1, v_2)$  is a small quantity so that :

$$\Delta P = \left[ \bar{v}_1 \frac{dv_2}{de} + \bar{v}_2 \frac{dv_1}{de} - 2\bar{v}_1 \bar{v}_2 \frac{e - \bar{e}}{\sigma^2} \right] \left[ e_1^1 + e_2^1 - e_1 - e_2 \right]$$

From A.II.1 we also have

$$\Delta v_1 = \left[ \frac{dv_1}{de} - \frac{(e - \bar{e})\bar{v}_1}{\sigma^2} \right] (e_1^1 - e_1)$$

and

$$\Delta v_2 = \left[ \frac{dv_2}{de} - \frac{(e - \bar{e})\bar{v}_2}{\sigma^2} \right] (e_2^1 - e_2)$$

We then obtain :

$$\Delta C = (e_1^1 - e_1) \left( \bar{v}_1 \frac{dv_2}{de} - \bar{v}_1 \bar{v}_2 \frac{(e - \bar{e})}{\sigma^2} \right) + (e_2^1 - e_2) \left( v_2 \frac{dv_1}{de} - \bar{v}_1 \bar{v}_2 \frac{(e - \bar{e})}{\sigma^2} \right)$$

$$= \frac{e_1^1 - e_1}{e_2^1 - e_2} \bar{v}_1 \Delta \bar{v}_2 + \frac{e_2^1 - e_2}{e_1^1 - e_1} \bar{v}_2 \Delta \bar{v}_1$$

inserting typical values of  $V$ ,  $V_F \sigma^2$  we obtain

$$\Delta v_1 \# 1.4 \left( 0.1 - \frac{(e - \bar{e})}{40} \right)$$

$$\# 0.14 - \frac{(e - \bar{e})}{26}$$

and

$$\Delta C \# 0.56 - \frac{(e - \bar{e})}{26} 0.14$$

The correction is of the same order of magnitude of the co-variances themselves.

It has usually a tendency to yield positive correlations.

## 2) Variations of the efficiencies with neutron multiplicity

We shall consider, as an example, the obtention of co-variances with small neutron detectors. The measured quantity  $M$  is equal to

$$M = \frac{\overline{\epsilon_1 v_1 \epsilon_2 v_2}}{\overline{\epsilon_1 v_1} \overline{\epsilon_2 v_2}}$$

and it is assumed that  $\epsilon_1$  and  $\epsilon_2$  do not depend on  $v_1$  and  $v_2$ . In that case

$$M = \frac{\overline{v_1 v_2}}{\bar{v}_1 \bar{v}_2}$$

However, even for fixed masses and total kinetic energies of the fragments it must be expected that the center of mass velocities of the neutrons will depend on their multiplicity. Therefore, the efficiencies should themselves depend on the neutron multiplicity. To first order we write

$$\epsilon_1(v_1) = \epsilon_1 + k_1 \epsilon_1 (v_1 - \bar{v}_1)$$

and similarly

$$\epsilon_2(v_2) = \epsilon_2 + k_2 \epsilon_2 (v_2 - \bar{v}_2)$$

it is expected that the values of the efficiencies should decrease with neutron numbers so that  $k_1$  and  $k_2$  should be negative. For the sake of simplicity we assume that  $k_1 = k_2$ . Then, to first order

$$M = \frac{\epsilon_1(1 + k(v_1 - \bar{v}_1))v_1 v_2(1 + k(v_2 - \bar{v}_2))\epsilon_2}{\epsilon_1(1 + k(v_1 - \bar{v}_1))v_1 \epsilon_2(1 + k \epsilon_2(v_2 - \bar{v}_2))v_2}$$

$$= \frac{\overline{v_1 v_2} + k[v_1 v_2 (v_1 - \bar{v}_1) + v_1 \bar{v}_2 (v_2 - \bar{v}_2)]}{\bar{v}_1 \bar{v}_2 + k[v_1 (v_1 - \bar{v}_1) \bar{v}_2 + v_2 (v_2 - \bar{v}_2)] \bar{v}_1}$$

We assume that since the total kinetic energy and masses of the fragments are fixed  $v_1 + v_2 = v_T = \bar{v}_1 + \bar{v}_2$  it then comes that:

$$M = \frac{\overline{v_1 v_2}}{\bar{v}_1 \bar{v}_2 \left( 1 + k \left( \frac{\sigma^2(v_1)}{\bar{v}_1} + \frac{\sigma^2(v_2)}{\bar{v}_2} \right) \right)}$$

and since  $v_1 + v_2 = v_T$

$$\sigma^2(v_1) = \sigma^2(v_2) = -C(v_1, v_2)$$

so that

$$M = \frac{\overline{v_1 v_2}}{\overline{v_1} \overline{v_2} \left( 1 - k \frac{C(v_1, v_2) v_T}{\overline{v_1} \overline{v_2}} \right)}$$

which leads to

$$\frac{C(v_1, v_2)}{\overline{v_1} \overline{v_2}} (1 + k M v_T) = M - 1$$

If the variations of the efficiency had not been taken into account we would have

$$\frac{C^1(v_1, v_2)}{\overline{v_1} \overline{v_2}} = M - 1$$

so that  $C^1 - C = \Delta C = k M v_T$ . The quantity  $M$  is close to one and  $v_T$  to four so that  $\Delta C \approx 4 k$ . Values of  $k$  of the order of  $-0.2$  appear possible and in that case  $\Delta C \approx -0.8$ .

This is again of the same order of magnitude as the observed quantities.

Appendix III

Recalls on regression analysis

In the following we derive some useful relations between the conditional moments of multi-variate distributions. Similar relations can be found in the article of J. Terrell<sup>(49)</sup> and in H. Nifenecker.<sup>(47)</sup>

We consider a 4-dimensional probability distribution

$$P(x,y,z,t)$$

The first and second moments of this distribution are given by

$$\bar{x} = \langle x \rangle = \int x P(x,y,z,t) dx dy dz dt$$

$$\sigma^2(x) = \int x^2 P(x,y,z,t) dx dy dz dt - \langle x \rangle^2$$

$$\begin{aligned} C(x,y) &= \int (x - \langle x \rangle)(y - \langle y \rangle) P(x,y,z,t) dx dy dz dt \\ &= \langle xy \rangle - \langle x \rangle \langle y \rangle \end{aligned}$$

and similar relations for the other variables.

We also consider the marginal probability distribution of z and t

$$g(z,t) = \iint P(x,y,z,t) dx dy$$

and the conditional moments as for example

$$\begin{aligned} C(x,y: zt) &= \frac{\iint xy P(x,y,z,t) dx dy}{g(z,t)} - \frac{\iint x P(x,y,z,t) dx dy}{g(z,t)} \frac{\iint y P(x,y,z,t) dx dy}{g(z,t)} \\ &= \langle xy \rangle_{zt} - \langle x \rangle_{zt} \langle y \rangle_{zt} \end{aligned} \tag{A.III.1}$$

The regression coefficient of  $y$  on  $x$ , written  $\langle \frac{dy}{dx} \rangle$ , is defined as the coefficient of the linear term of the straight line  $ax + b$  which minimizes the average value of the square  $(y - ax - b)^2$ .

We must therefore minimize the expression

$$A = \int (y - ax - b)^2 P(x,y,z,t) dx dy dz dt$$

we have

$$\frac{\partial A}{\partial b} = -2 \int (y - ax - b) P(x,y,z,t) dx dy dz dt = 0 \quad (\text{A.III.2})$$

or

$$b = \langle y \rangle - a \langle x \rangle$$

substituting  $b$  in the second relation

$$\frac{\partial A}{\partial a} = -2 \int x(y - ax - b) P(x,y,z,t) dx dy dz dt = 0 \quad (\text{A.III.3})$$

one obtains

$$\int x(y - \langle y \rangle) P(x,y,z,t) dx dy dz dt = a \int x(x - \langle x \rangle) P(x,y,z,t) dx dy dz dt$$

and thus

$$\langle \frac{dy}{dx} \rangle = a = \frac{C(x,y)}{\sigma^2(x)} \quad (\text{A.III.4})$$

Such a relation evidently holds for the conditional moments as well. For example:



$$\left\langle \frac{dy}{dx} \right\rangle_{zt} = \frac{C(xy: zt)}{\sigma^2(x: zt)}$$

a consequence of this relation is that  $\left\langle \frac{dx}{dy} \right\rangle$  is not equal to  $\left\langle \frac{dy}{dx} \right\rangle^{-1}$  rather :

$$\left\langle \frac{dx}{dy} \right\rangle = \frac{C(x,y)}{\sigma^2(y)} = \left\langle \frac{dy}{dx} \right\rangle \frac{\sigma^2(x)}{\sigma^2(y)}$$

it is also possible to write :

$$\left\langle \frac{dx}{dy} \right\rangle = \left\langle \frac{dx}{dy} \right\rangle^{-1} \frac{C(x,y)^2}{\sigma^2(x) \sigma^2(y)} = \left\langle \frac{dx}{dy} \right\rangle^{-1} p^2(x,y)$$

where the correlation coefficient  $p(x,y)$  is defined as

$$p(x,y) = \frac{C(x,y)}{\sigma(x) \sigma(y)}$$

and is only equal to 1 when  $x$  and  $y$  are completely correlated.

Another definition of the regression coefficient is often used. Let us define the conditional average of  $y$

$$\left\langle y \right\rangle_x = \frac{\iiint y P(x,y,z,t) dy dz dt}{\iiint P(x,y,z,t) dy dz dt}$$

and the marginal distribution of  $x$

$$\rho(x) = \iiint P(x,y,z,t) dy dz dt$$

The regression coefficient  $\langle \frac{dy}{dx} \rangle$  is also the slope of the straight line obtained by the least square fit of the curve  $\langle y \rangle_x$ .

In that case we minimize the expression

$$\int (\langle y \rangle_x - ax - b)^2 \rho(x) dx$$

we obtain the two equations

$$\int \langle y \rangle_x \rho(x) dx = a \int x \rho(x) dx + b \int \rho(x) dx \quad (\text{A.III.5})$$

$$\int x(\langle y \rangle_x - ax - b) \rho(x) dx = 0 \quad (\text{A.III.6})$$

Equation (A.III.5) is equivalent to equation (A.III.2) and yields the same result:

$$b = \langle y \rangle - a \langle x \rangle$$

equation (A.III.6) can be written

$$\int x(\langle y \rangle_x - \langle y \rangle) \rho(x) dx = a \sigma^2(x)$$

or

$$\int x \langle y \rangle_x \rho(x) dx - \langle x \rangle \langle y \rangle = a \sigma^2(x)$$

and using the definitions of  $\langle y \rangle_x$  and  $\rho(x)$

$$\iiiii x y P(x,y,z,t) dx dy dz dt - \langle x \rangle \langle y \rangle = a \sigma^2(x)$$

which yields

$$a = \left\langle \frac{dy}{dx} \right\rangle = \frac{C(x,y)}{\sigma^2(x)}$$

as in equation (A.III.4).

We now turn to the conditional co-variance of  $x$  and  $y$  and see, from its definition that

$$\begin{aligned} \iint C(x,y; z,t) g(z,t) dz dt &= \int xy P(x,y,z,t) dx dy dz dt \\ &\quad - \iint \langle x \rangle_t \langle y \rangle_t g(z,t) dz dt \\ &= C(x,y) + \langle x \rangle \langle y \rangle - \iint \langle x \rangle_{zt} \langle y \rangle_{zt} g(z,t) dx dt \end{aligned} \quad (\text{A.III.7})$$

To first order we can write that

$$\langle x \rangle_{zt} = \frac{\partial \bar{x}(zt)}{\partial t} (t - \bar{t}) + \frac{\partial \bar{x}(zt)}{\partial z} (z - \bar{z}) + \langle x \rangle_{z \bar{t}} \quad (\text{A.III.8})$$

and

$$\langle y \rangle_{zt} = \frac{\partial \bar{y}(zt)}{\partial t} (t - \bar{t}) + \frac{\partial \bar{y}(zt)}{\partial z} (z - \bar{z}) + \langle y \rangle_{z \bar{t}}$$

where the partial derivatives are expressed for the value  $\bar{z} \bar{t}$ . By a weighted integration of A.III.7 we obtain for example :

$$\int \langle x \rangle_{zt} g(z,t) dz dt = \overline{\langle x \rangle_{z \bar{t}}} = \langle x \rangle$$

Substituting A.III.8 into A.III.7 we obtain to first order :

$$C(x,y) = \frac{\partial \bar{x}(z,t)}{\partial t} \frac{\partial \bar{y}(z,t)}{\partial t} \sigma^2(t) + \frac{\partial \bar{x}(z,t)}{\partial z} \frac{\partial \bar{y}(z,t)}{\partial z} \sigma^2(z) + \left( \frac{\partial \bar{x}(z,t)}{\partial t} \frac{\partial \bar{y}(z,t)}{\partial z} + \frac{\partial \bar{x}(z,t)}{\partial z} \frac{\partial \bar{y}(z,t)}{\partial t} \right) C(z,t) + \mathcal{M}_{zt} C(x,y: zt) \quad (\text{A.III.9})$$

where

$$\mathcal{M}_{zt} C(xy: zt) = \iint C(xy: zt) g(z,t) dz dt$$

In the main article we consider several limiting cases of equation (A.III.9):

1) If we assume that  $\bar{x}(z,t)$  is independent of  $t$  and  $\bar{y}(z,t)$  is independent of  $z$  we obtain

$$C(x,y) = \frac{\partial \bar{x}(z,t)}{\partial z} \frac{\partial \bar{y}(z,t)}{\partial t} C(z,t) + \mathcal{M}_{zt} C(x,y: zt)$$

and, in that case, using the properties of  $\langle \frac{dx}{dz} \rangle$  and  $\langle \frac{dy}{dt} \rangle$

$$C(x,y) = \langle \frac{dx}{dz} \rangle \langle \frac{dy}{dt} \rangle C(z,t) + \mathcal{M}_{zt} C(xy: zt) \quad (\text{A.III.10})$$

2) If we deal with a three variate distribution  $P(x y t)$  formula A.III.9 can be used by considering  $z$  to be fixed and therefore that

$$\sigma^2(z) = C(z,t) = 0$$

thus in that case

$$C(x,y) = \left\langle \frac{dx}{dt} \right\rangle \left\langle \frac{dy}{dt} \right\rangle \sigma^2(t) + \mathcal{M}_t C(xy: t) \quad (\text{A.III.11})$$

If we consider the variances of x and y we have

$$C(x,x) = \sigma^2(x)$$

so that

$$\sigma^2(x) = \left\langle \frac{dx}{dt} \right\rangle^2 \sigma^2(t) + \mathcal{M}_t \sigma^2(x: t) \quad (\text{A.III.12})$$

## FIGURE CAPTIONS

Fig. 1. Variations of the average neutron number  $\bar{\nu}(m)$  with the fragment mass as obtained in different experiments

(a) For the slow neutron induced fission of  $^{235}\text{U}$

- $\Delta$  Maslin et al. (5)
- Boldeman et al. (6)
- $\square$  Milton et al. (2)
- $\nabla$  Apalin et al. (3)

This figure is taken from Ref. 6.

(b) For the spontaneous fission of  $^{252}\text{Cf}$

- $\blacktriangle$  Bowman et al. (1)
- Signarbieux et al. (7)

Fig. 2. Variations of the total neutron number  $\bar{\nu}_T(E_k)$  with fragments' total kinetic energy for the  $^{252}\text{Cf}$  spontaneous fission

- $\Delta$  Bowman et al. (1)
- $\nabla$  Whetstone (3)
- Our results

Fig. 3. Effects of neutron recoil correction on the average neutron number measured with low efficiency detectors

- a. On  $\bar{\nu}_1(m)$  results
- b. On  $\bar{\nu}_T(E_k)$  results
  - Uncorrected results
  - o Corrected results

The continuous line denotes the input data. This figure is taken from Ref. 8.

Fig. 4. Variations of the "invariant"  $R = \frac{\sigma^2(q)}{q^2} - \frac{1}{q}$  as a function of efficiency in an actual  $4\pi$  neutron detection system.

Fig. 5. Experimental and calculated energies carried away per neutron. The experimental values were obtained from  $\langle \frac{dv_T}{dE_k} \rangle^{-1}$ . The calculated values were obtained from

$$\bar{B} + \bar{\eta} + 0.75$$

- Calculated values for each fragment mass
- ▲ Calculated values for a fragment pair
- △ Experimental values for a fragment pair

Fig. 6. Variations of the average number of neutrons emitted per fragment as a function of the total kinetic energy of the fragments for a range of fragment masses

- Light fragment
- Heavy fragment

Fig. 7. Anisotropy of the  $\gamma$  quanta yield versus fragment kinetic energy in the fission of  $^{235}\text{U}$

- a) For different fragment mass ratios:  $\square \frac{m_1}{m_2} = 1.1-1.25$ ,  $\Delta \frac{m_1}{m_2} = 1.25-1.35$ ,  
 ●  $\frac{m_1}{m_2} = 1.35-1.45$ ,  $\nabla \frac{m_1}{m_2} = 1.45-1.65$ ,  $\diamond \frac{m_1}{m_2} = 1.65-1.9$

b) For all realized mass ratios. The solid curve shows the fragment kinetic energy distribution

This figure is taken from Ref. 23.

Fig. 8. Anisotropy of the prompt radiation as a function of fragment mass  $A_{ex}$ :

- (a) Anisotropy without collimator: the contributions of the two fragments are not separated.
- (b) Anisotropy with collimator selecting  $\gamma$  quanta in the time region (10-100) psec after fission

This figure is taken from Ref. 20.

Fig. 9.  $\gamma$  ray yield per fragment versus fragment mass in the  $^{252}\text{Cf}$  spontaneous fission.

Figure taken from Ref. 24.

Fig. 10.  $\gamma$  ray yield per fragment versus fragment mass in the slow neutron induced fission of  $^{235}\text{U}$

- Data taken from Ref. 19
- $\Delta$  Data taken from Ref. 32

Fig. 11. Observed correlation between the values of  $\gamma$  ( $\bar{N}_\gamma(m)$ ) and neutron ( $\bar{\nu}(m)$ ) multiplicities

- (a) In the case of the induced fission of  $^{235}\text{U}$
- (b) In the case of the spontaneous fission of  $^{252}\text{Cf}$

Fig. 12. Variations of total  $\gamma$  energy  $E_\gamma(E_k)$  as a function of total fragment kinetic energy

- (a) In the induced fission of  $^{235}\text{U}$
- (b) In the spontaneous fission of  $^{252}\text{Cf}$

Fig. 13. Correlation between the total  $\gamma$  ray energy  $\bar{E}_\gamma(E_k)$  and the neutron multiplicity  $\bar{\nu}(E_k)$

- (a) In the induced fission of  $^{235}\text{U}$
- (b) In the spontaneous fission of  $^{252}\text{Cf}$

Fig. 14. Variations of the total  $\gamma$  ray energy as a function of the total kinetic energy of the fragments for different light fragment masses ( $^{252}\text{Cf}$ )

- Direct measurement
- o Results obtained from energy balance considerations

Fig. 15. (a) Slopes  $\left\langle \frac{dE_\gamma}{dE_k} \right\rangle_m$  of the variations of the total  $\gamma$  ray energy versus the total kinetic energy of the fragments as a function of light fragment's mass ( $^{252}\text{Cf}$ )

- Direct measurement
- o Results obtained from energy balance considerations
- (b) Total  $\gamma$  ray energy as a function of the light fragment mass ( $^{252}\text{Cf}$ )



Fig. 16. Slice plots at constant mass  $m_1^*$  in the 3 MeV  $\times$  3 amu array  $\bar{E}_\gamma(E_k^*, m_1^*)$ .

Figure taken from Ref. 19.

Fig. 17. (A) Fission x-ray spectrum  $N(\chi_1)$

(B) Average value of the  $\gamma$  pulse height as a function of x-ray detector pulse-height  $\bar{E}_\gamma(\chi_1)$  ( $^{252}\text{Cf}$  fission)

Fig. 18. Average total  $\gamma$  ray energy emitted as a function of the

- Light fragment's charge
- $\Delta$  Heavy fragment's charge ( $^{252}\text{Cf}$  fission)

Fig. 19. Average neutron number as a function of the

- Mass of the fragments
- $\Delta$  Charge of the fragments ( $^{252}\text{Cf}$  fission)

Fig. 20. Average kinetic energies as a function of

- Light fragment's charge
- $\Delta$  Heavy fragment's charge

Fig. 21. Best average neutron number as a function of charge of the binary fission fragments ( $^{252}\text{Cf}$  fission).

Fig. 22. Best average total kinetic energy as a function of charge of the fission fragments. The continuous line shows the value of average total kinetic energy as a function of mass of the fragments. The mass and charge scales reflect the charge to mass ratios of the fragments.

Fig. 23. Experimental and calculated values of the average center of mass kinetic energy of the neutrons  $\bar{\eta}$ . Typical experimental errors are shown by full dots with error bars. The theoretical values were obtained including pairing in the level densities. Figure taken from Ref. 31.

Fig. 24. • Variations of the variance of the total number of neutrons as a function of mass of the light fragment  $\sigma^2(v_T: m)$

○ Average value over the total kinetic energy of the conditional variances  $\overline{\sigma^2(v_T: m E_k)}$  as a function of the mass of the light fragment

Fig. 25. Variances of the total kinetic energy

- As obtained directly from the kinetic energies
- As obtained from the neutron variances

The full lines give an idea of the errors on the experimental values.

Fig. 26. Variations of the excitation energy variances  $\sigma^2(E_1: m E_k)$  as a function of  $E_k$  for a number of masses of the light fragment.

Fig. 27. • Variations of the excitations energy variances  $\overline{\sigma^2(E_1: m E_k)}$  averaged over  $E_k$  as a function of light fragment mass

○ Variations of the maximum observed energy variance as a function of fragment mass

The full lines give an idea of the errors.

Fig. 28. • Variations of the variances of the total number of neutrons  $\sigma^2(v_T: m)$  as a function of fragment mass

Δ Variations of the sum of the two neutron variances for complementary fragments  $\sigma^2(v_1: m) + \sigma^2(v_2: m)$  as a function of fragment mass

○ Variation of the co-variance of the neutron distribution as a function of fragment mass

$$C(v_1 v_2: m) = \frac{\sigma^2(v_1: m) - \sigma^2(v_1: m) - \sigma^2(v_2: m)}{2}$$

The quantity shown on the figure is  $-C(v_1 v_2: m)$  for the sake of convenience.

Fig. 29. Observed relative intra-ground state band transition intensities for fission fragments (triangles) and for (charged particle, x n) reactions (lines). The reaction data are labeled with the average angular momentum of the reaction as calculated from optical model codes. Figure taken from Ref. 21.

Fig. 30. Schematic representation of the minimum potential energy and "free energy" along the scission line

Abscissa: Coulomb interaction energy C

Curve A: Minimum potential energy

Curve C: Total energy of the fissioning system

Points 1 and 2: Points where the minimum potential energy is equal to the total available energy

The shaded area shows the amount of free energy.

Fig. 31. (a) ● Values of the maximum Coulomb energy at scission  $E_k^{(1)}(m)$  as a function of light fragment mass

○ Values of the minimum Coulomb energy at scission  $E_k^{(2)}(m)$  as a function of light fragment mass

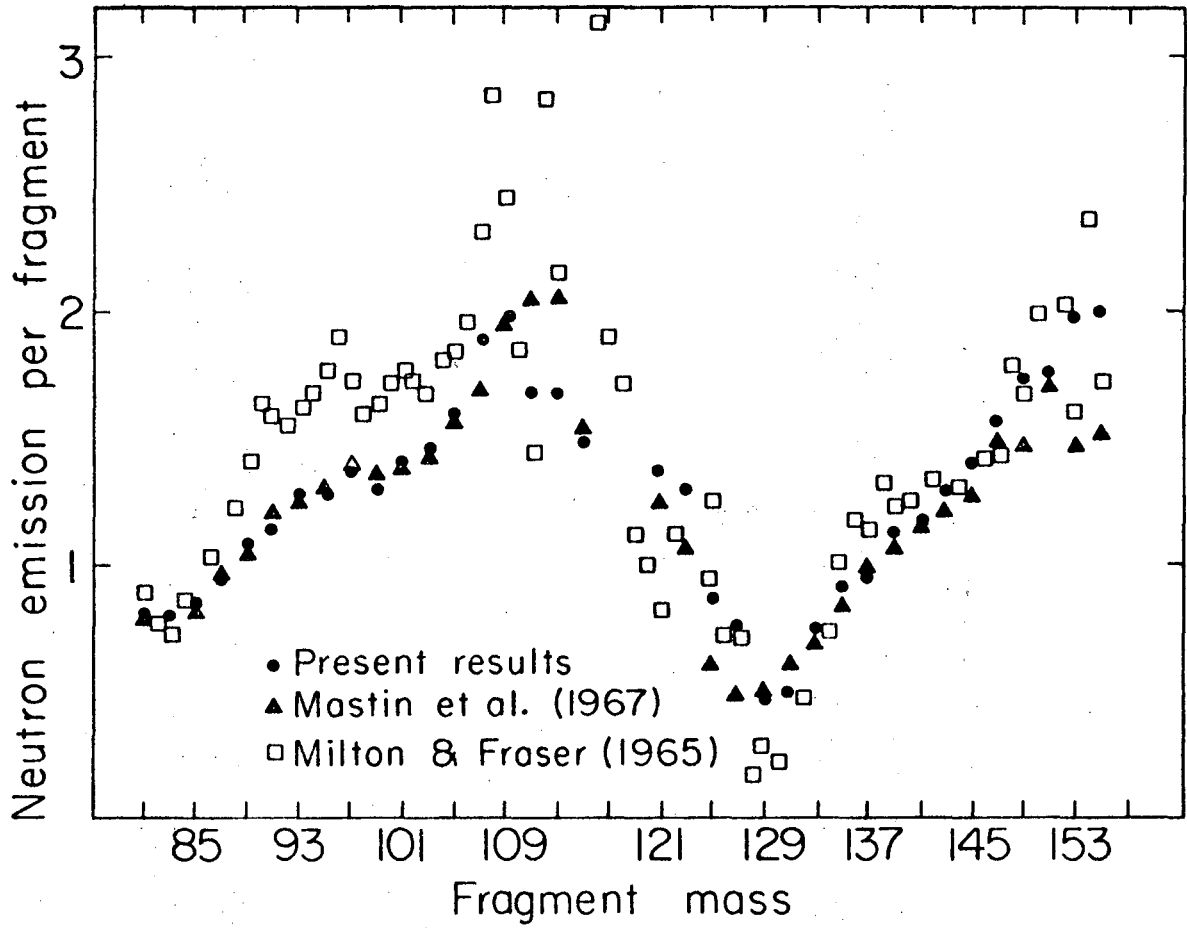
(b) ● Values of the deformation energies of the fragments corresponding to the minimum Coulomb energy

The shaded area represents the range of possible values of the deformation energies for the maximum Coulomb energy configuration. The full lines give an idea of the errors.

Fig. 32. (a) Maximum "free energy" available at scission as a function of light fragment mass

(b) Second derivative of the minimum potential energy curve

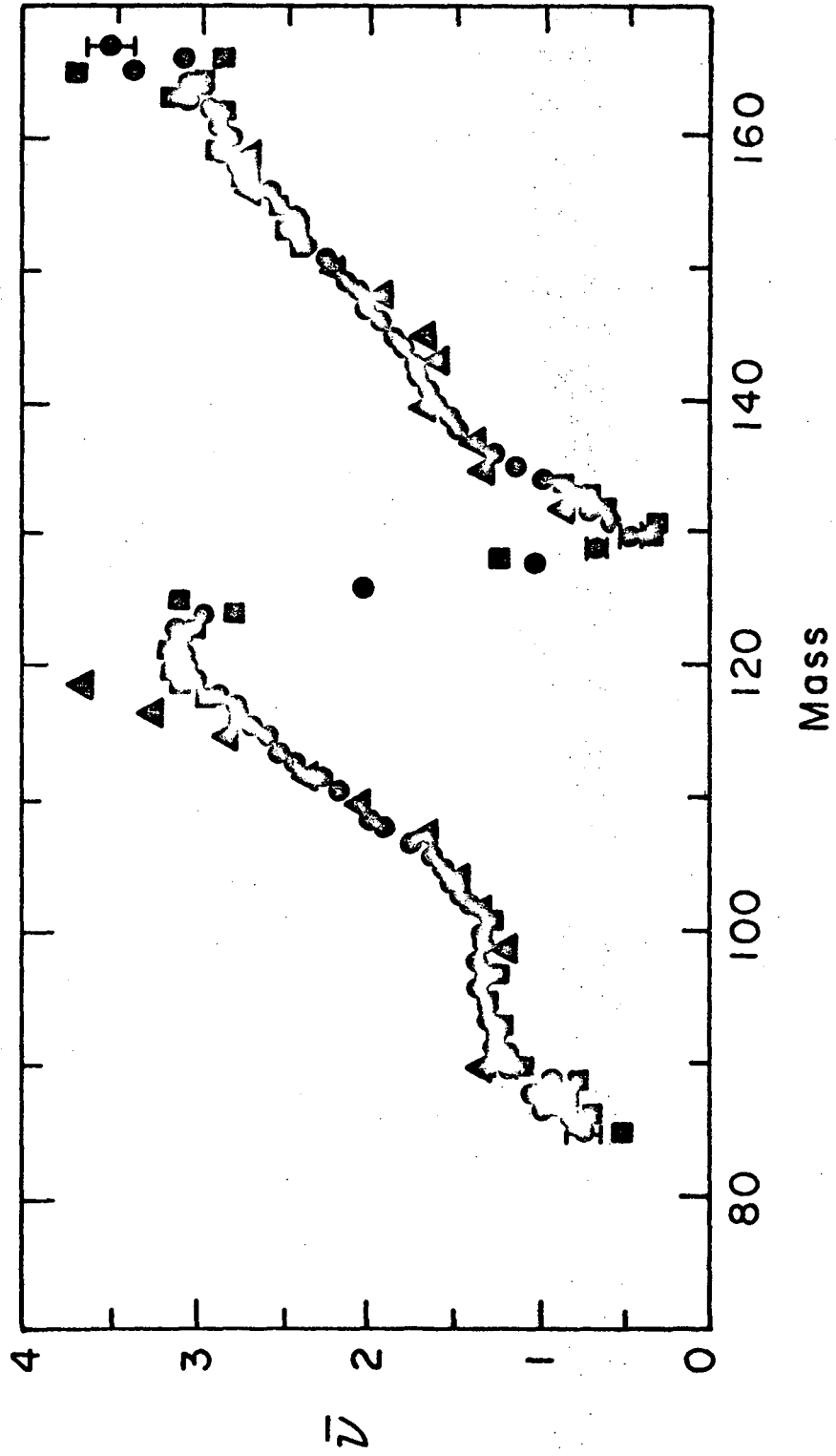
The full lines give an idea of the errors.



XBL737-3479

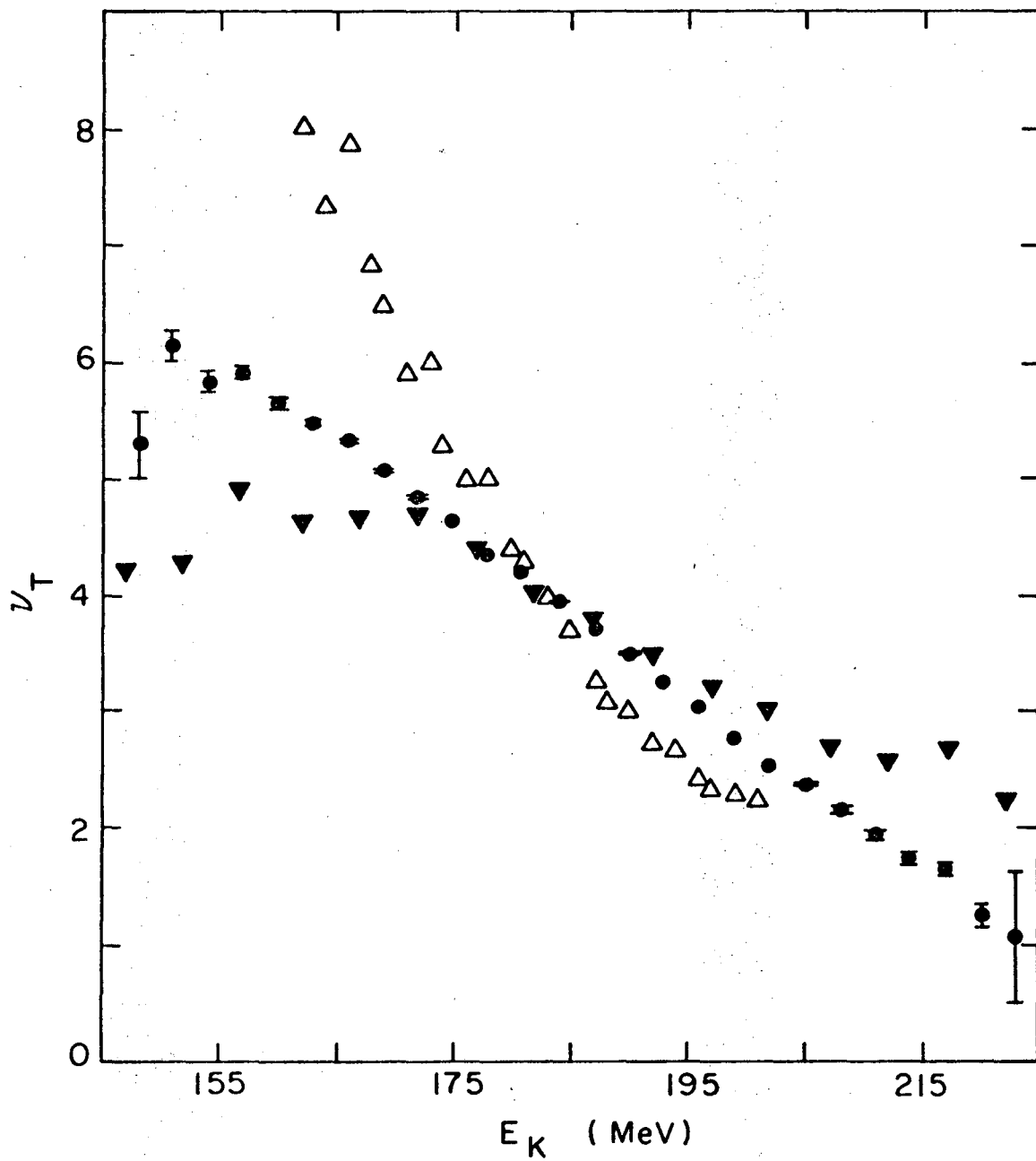
Fig. 1a

Spontaneous fission of  $^{252}\text{Cf}$



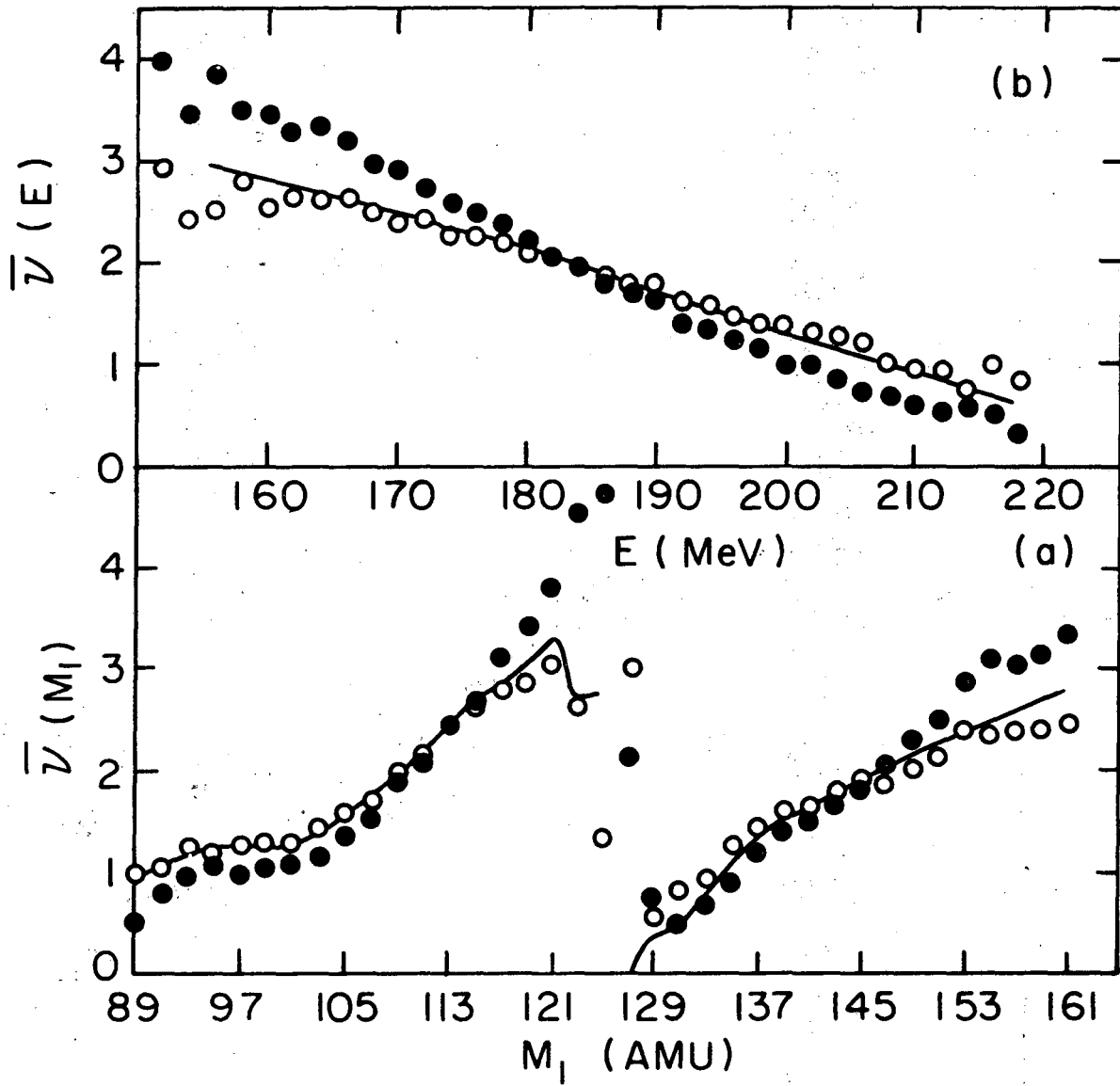
XBL 737-3485

Fig. 1b



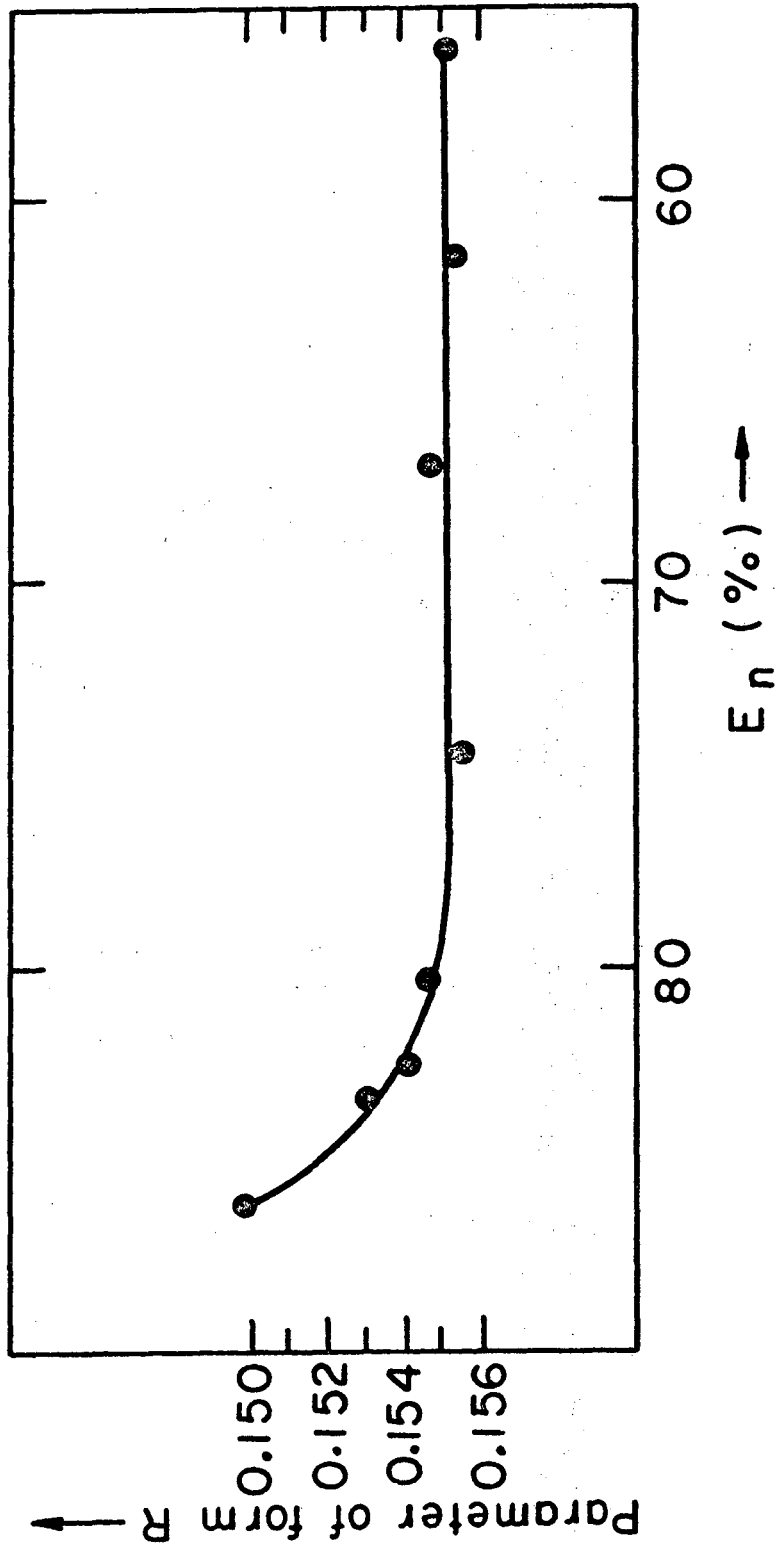
XBL737-3484

Fig. 2



XBL737-3486

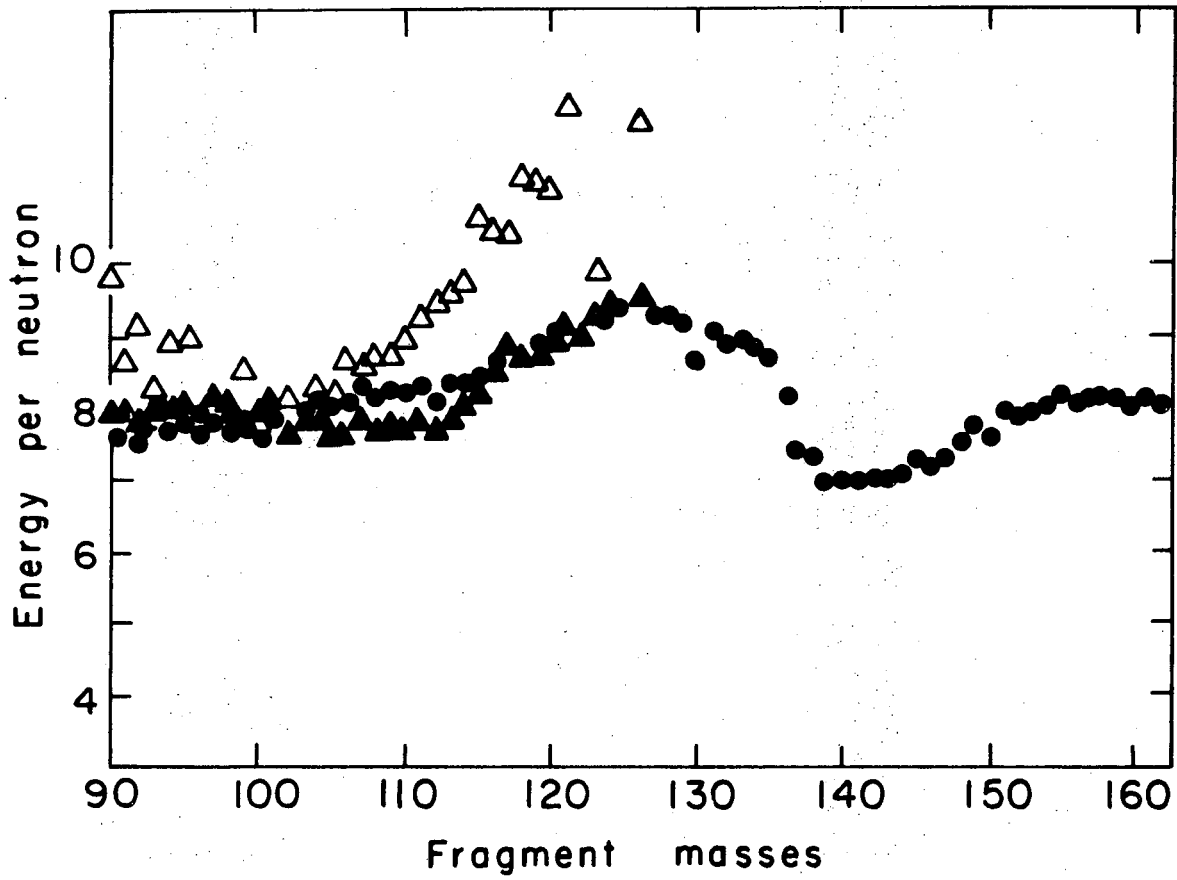
Fig. 3



XBL737-3387

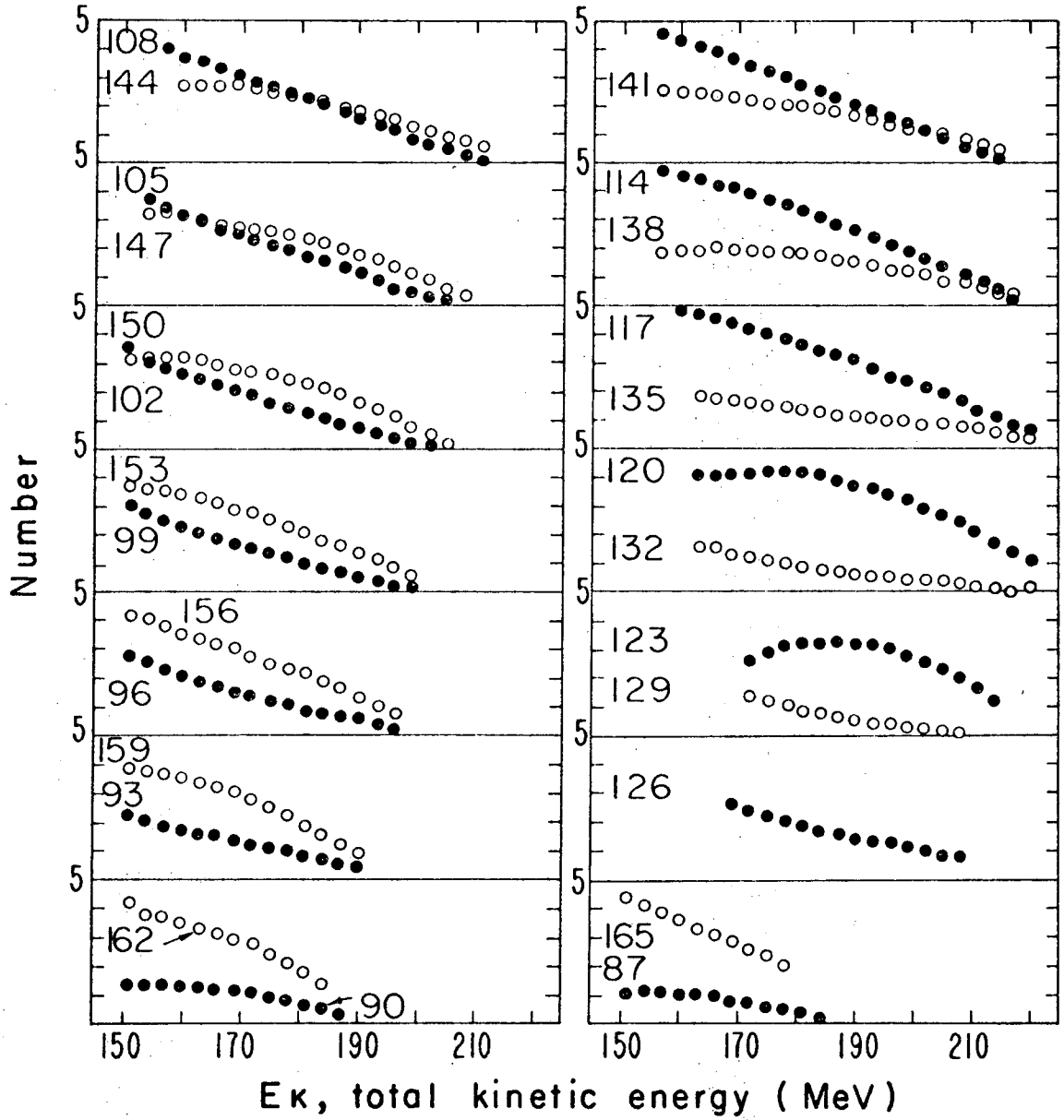
Fig. 4





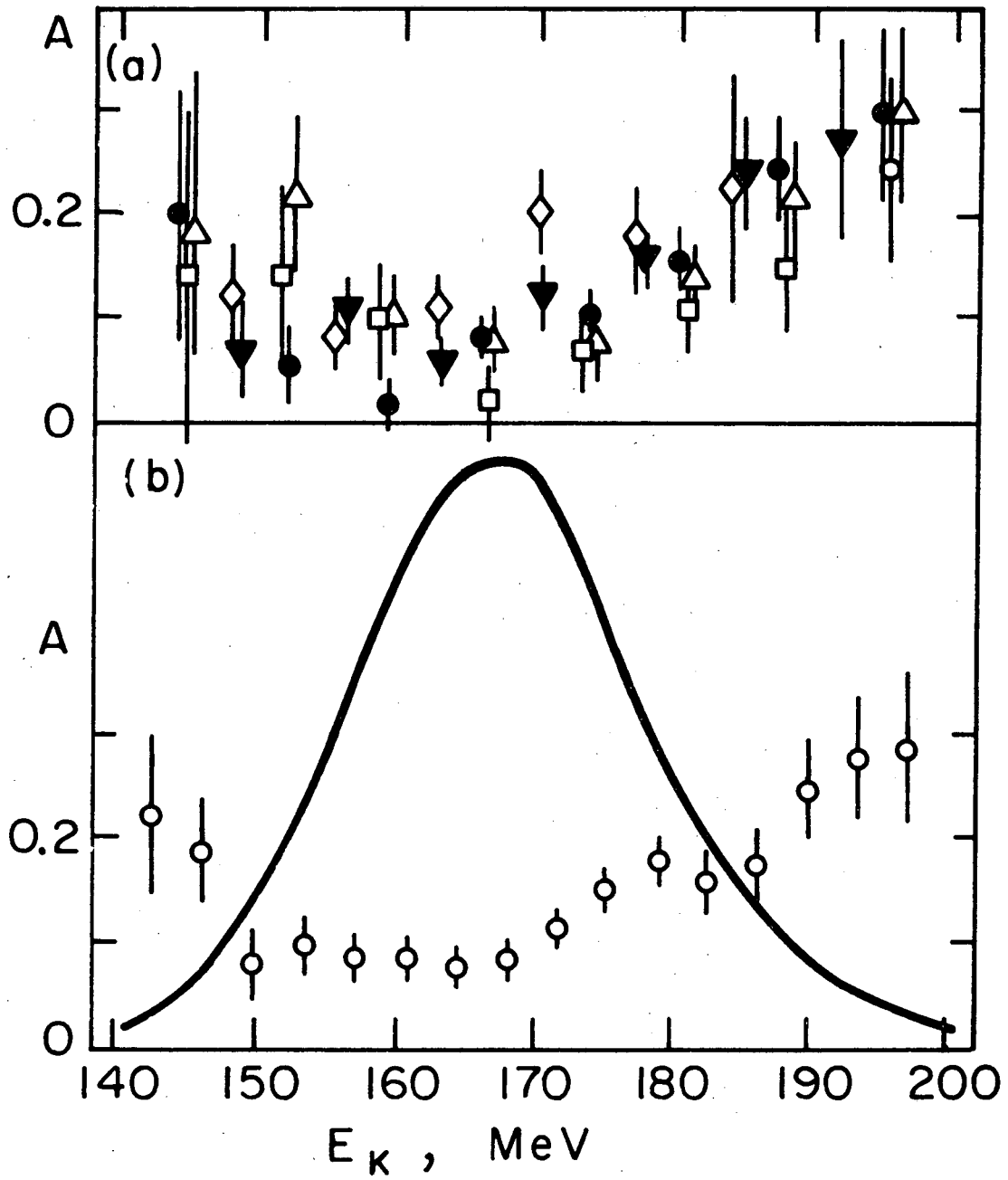
XBL737-3466

Fig. 5



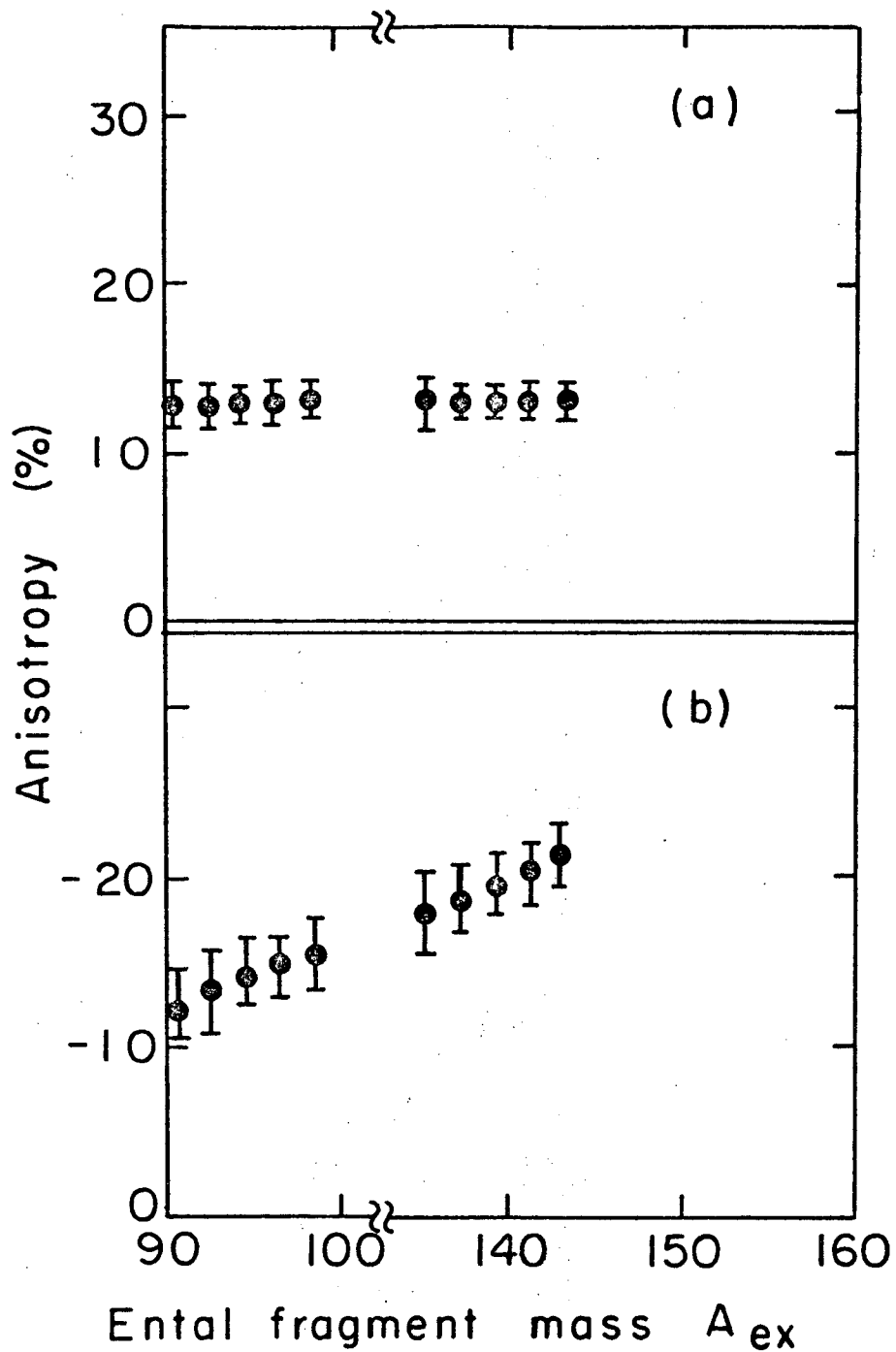
XBL 737-3491

Fig. 6



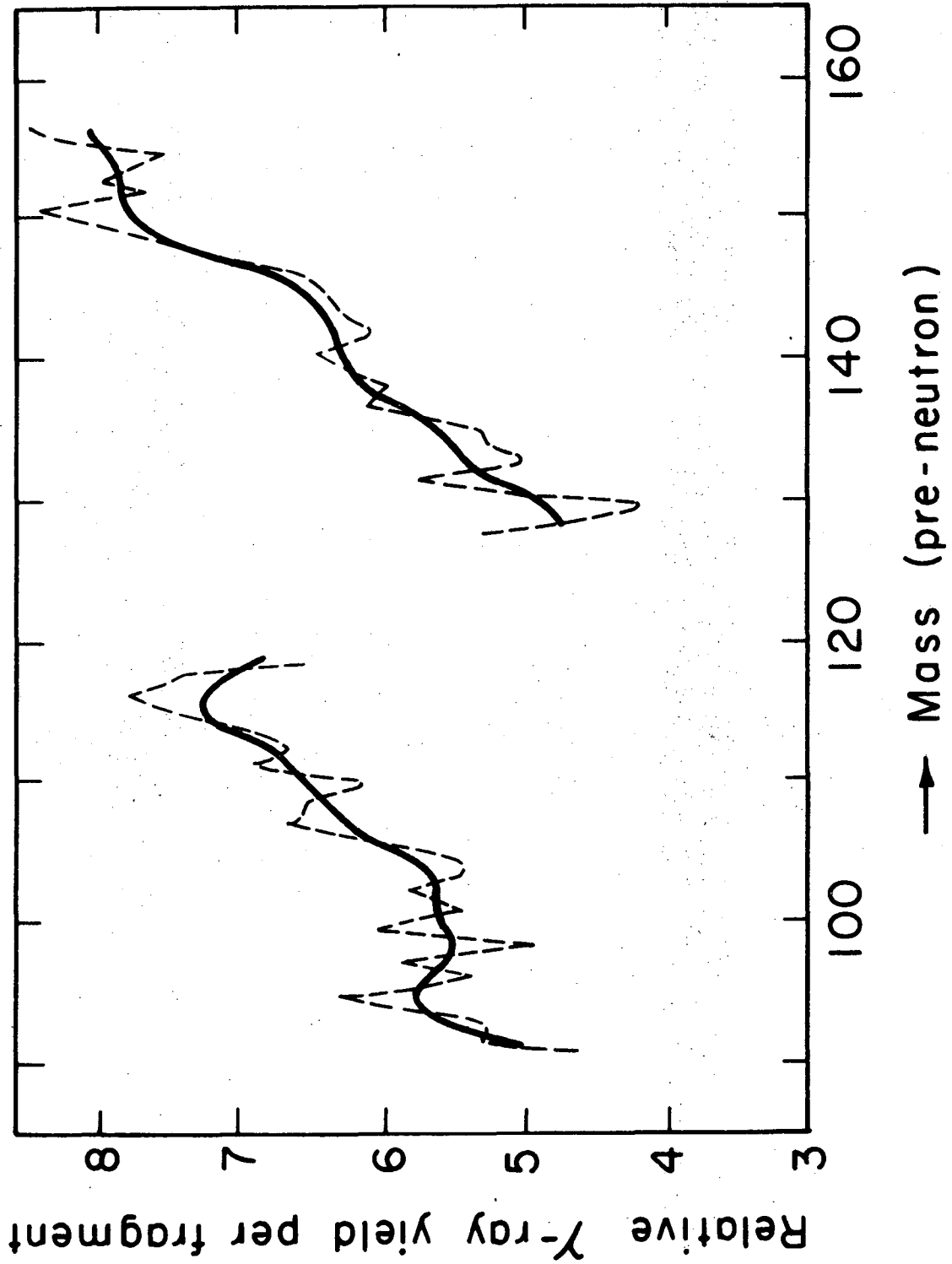
XBL 737-3480

Fig. 7



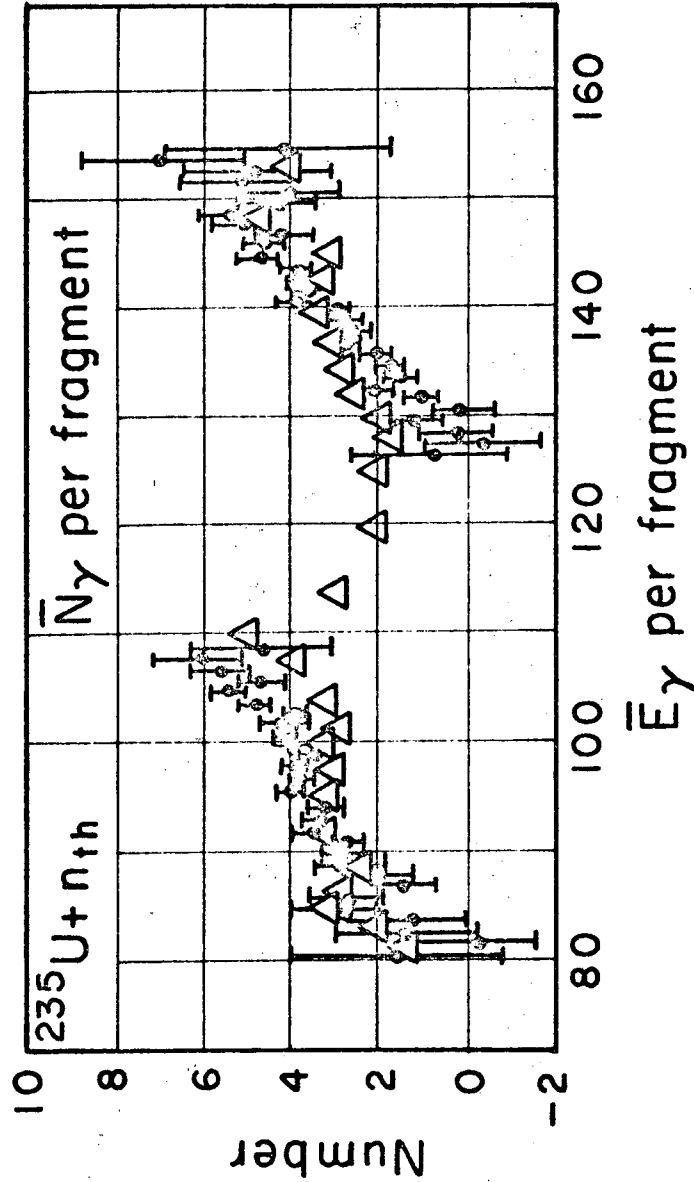
XBL737-3476

Fig. 8



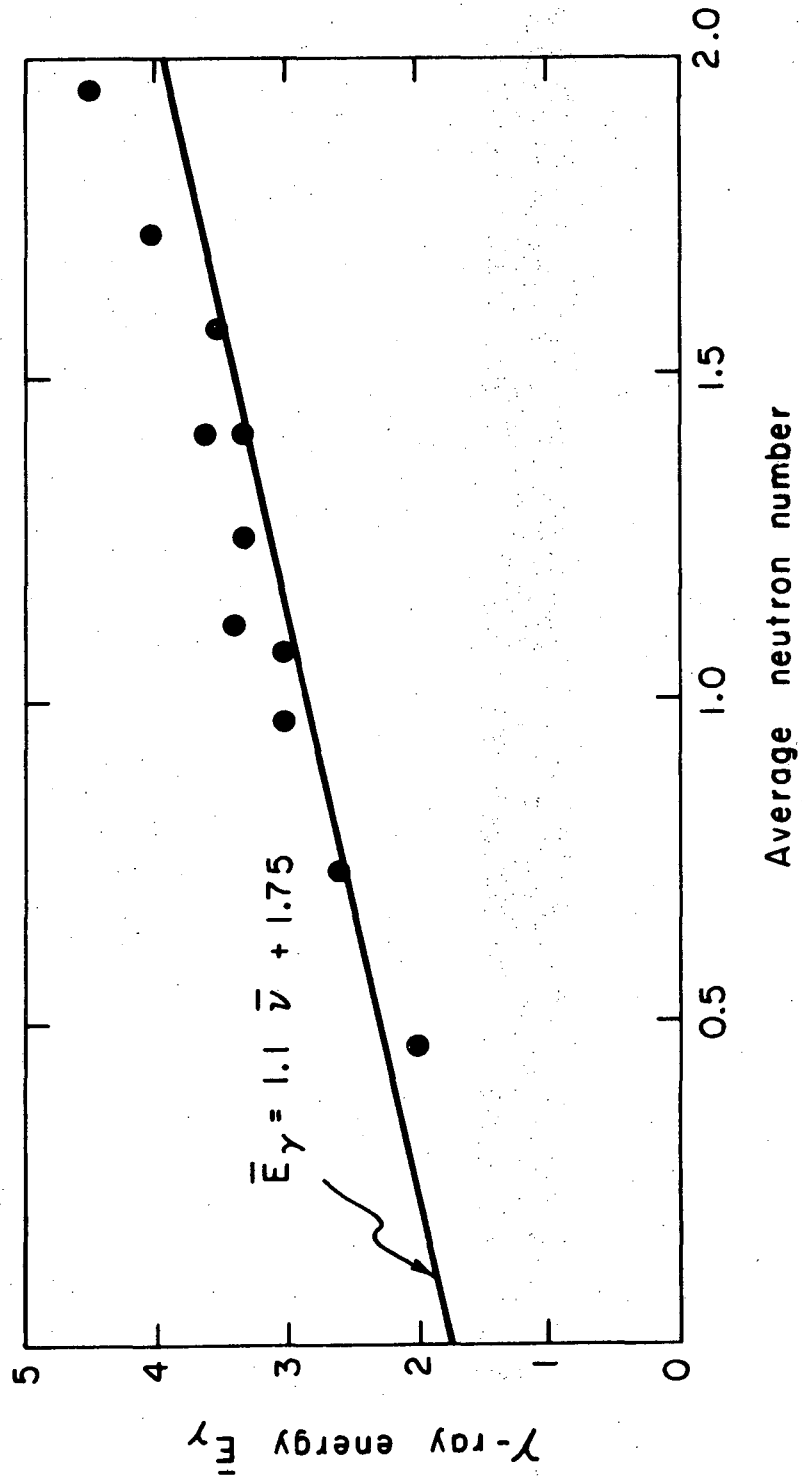
XBL737-3487

Fig. 9



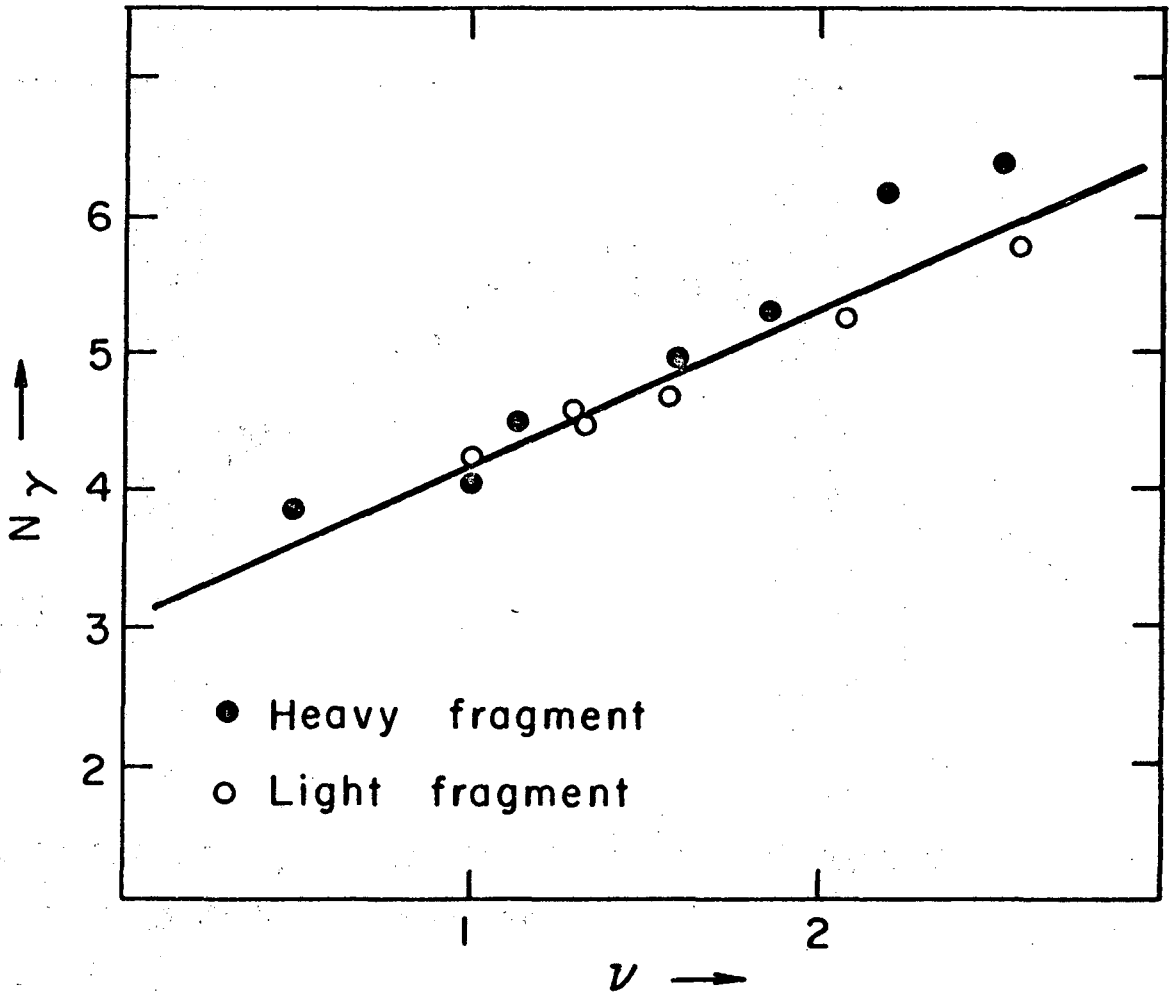
XBL737-3481

Fig. 10



xBL737-3468

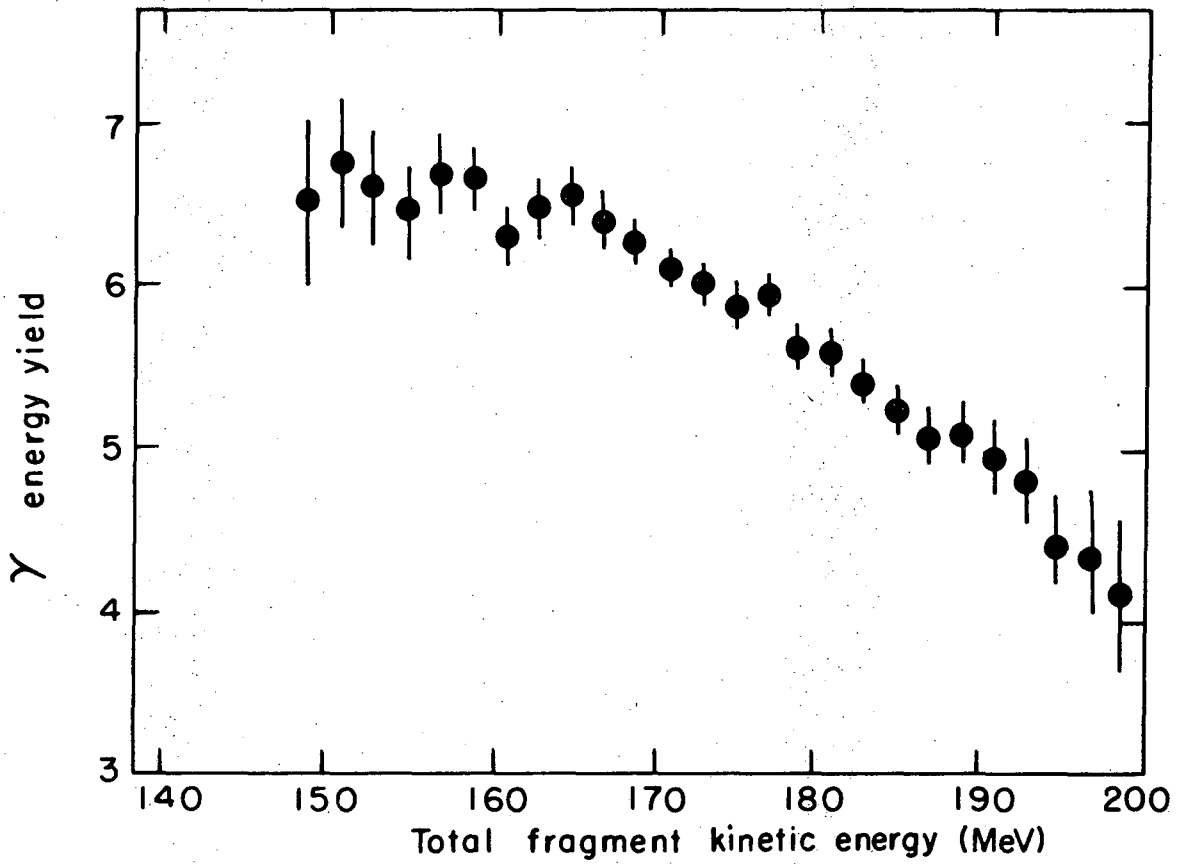
Fig. 11a



XBL737-3386

Fig. 11b





XBL737-3388

Fig. 12a

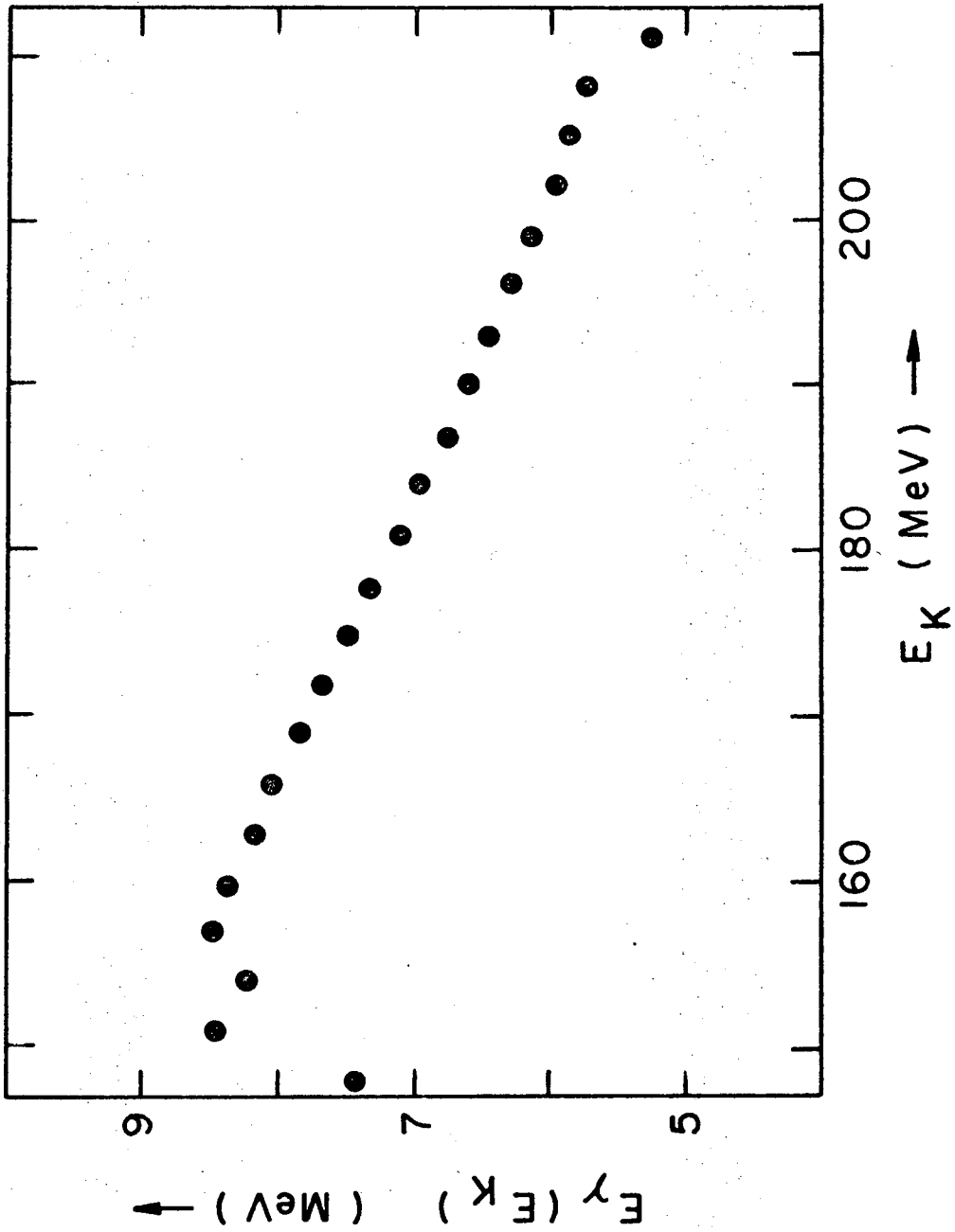
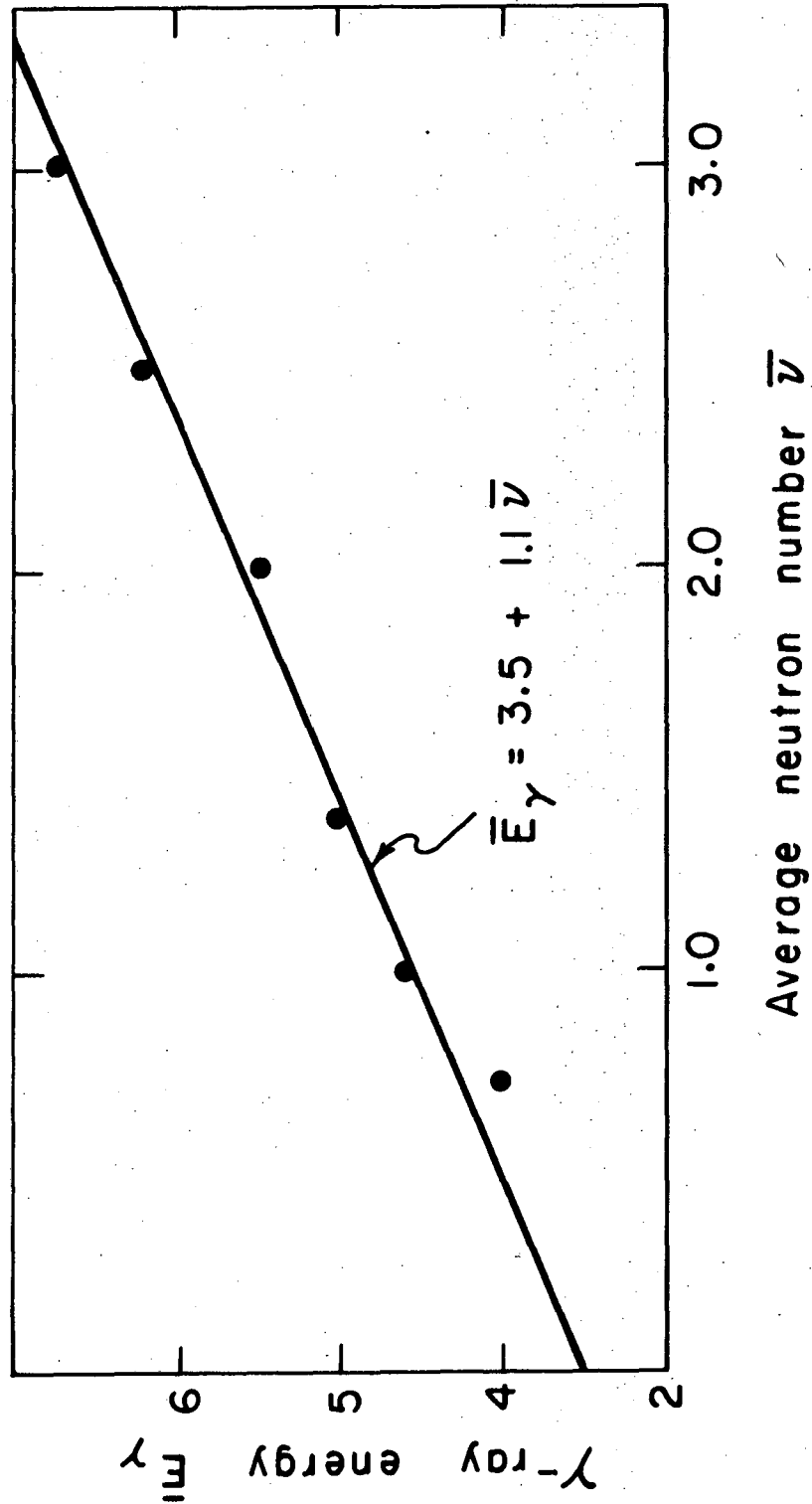


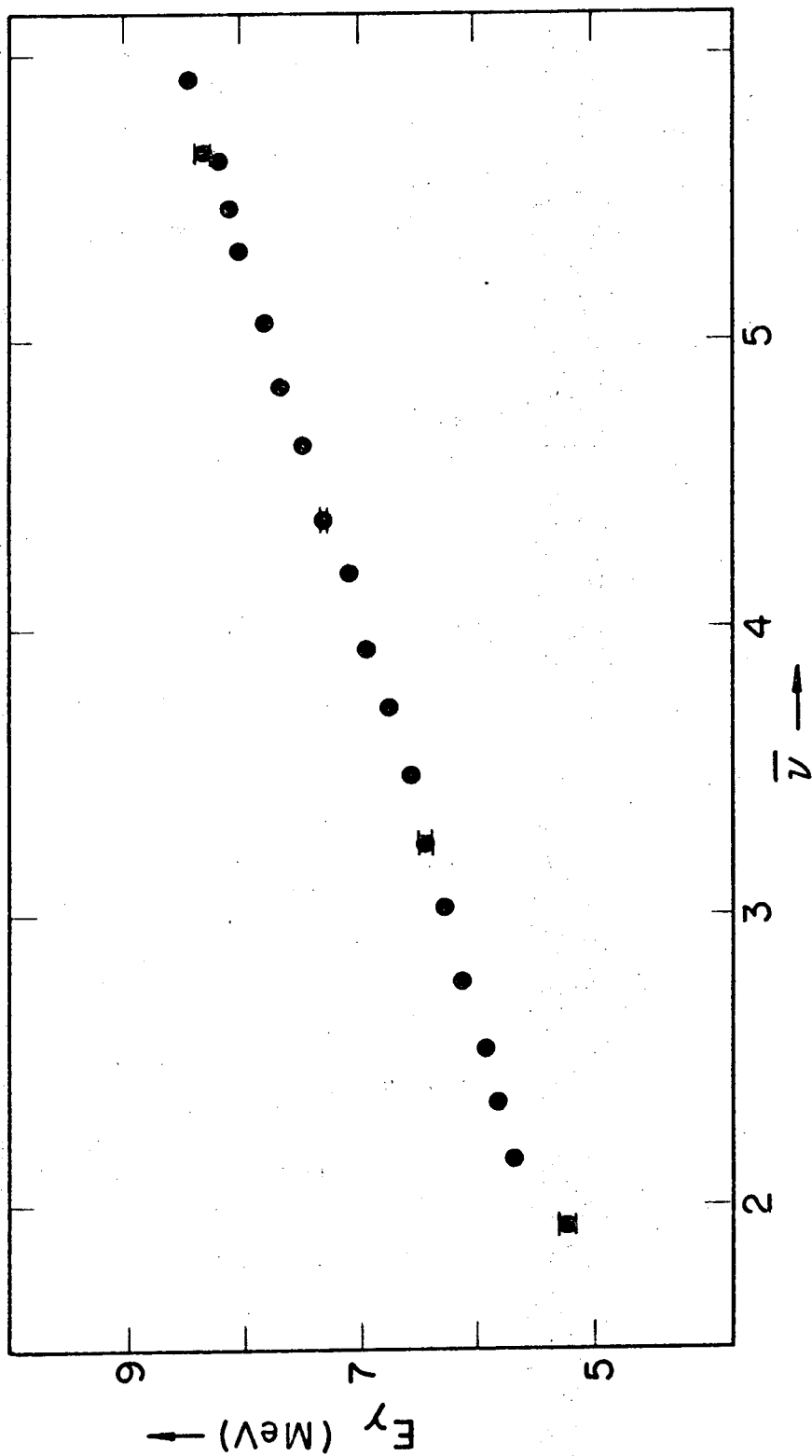
Fig. 12b

XBL737-3389



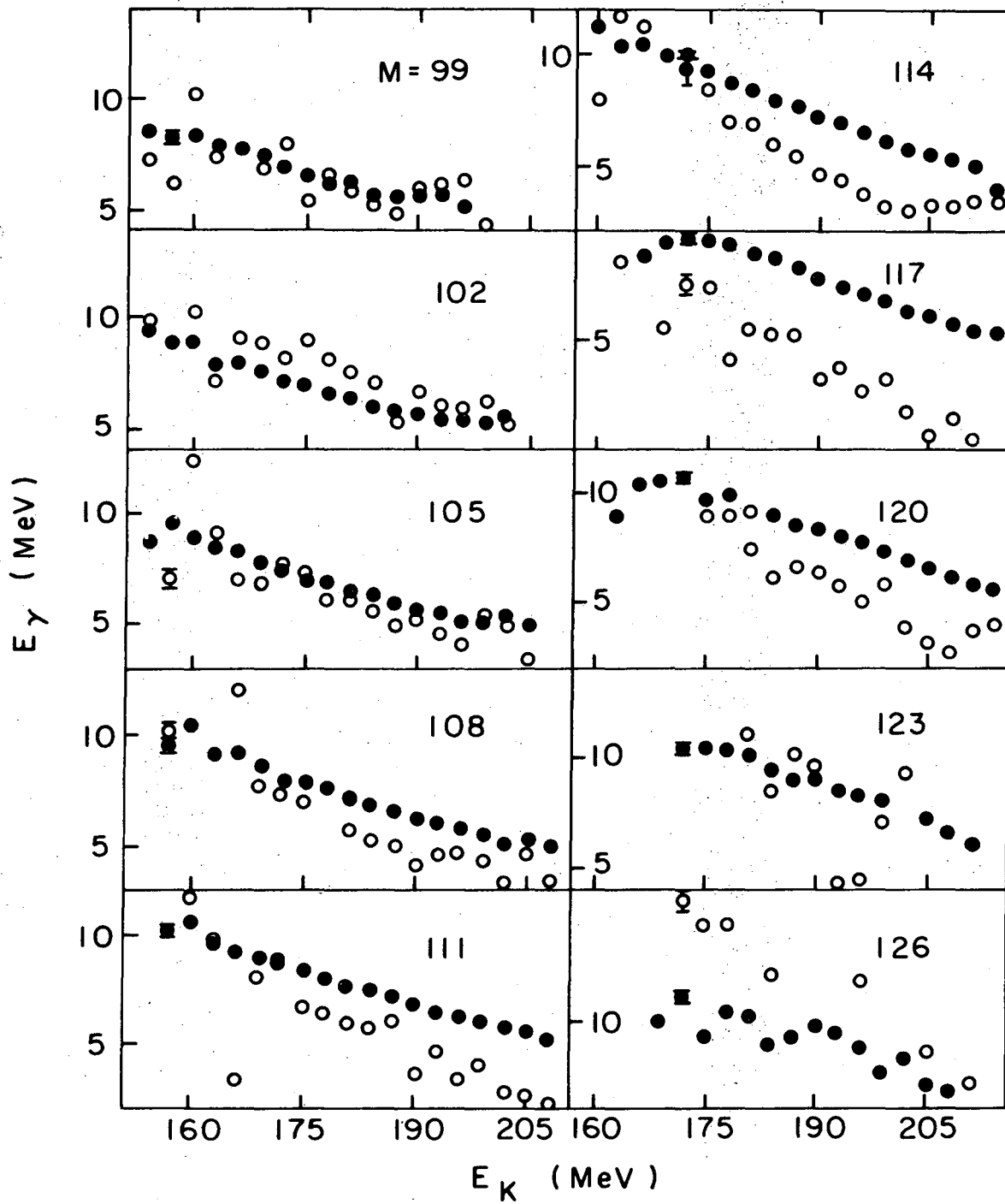
XBL737-3467

Fig. 13a



XBL737-3391

Fig. 13b



XBL737-3482

Fig. 14

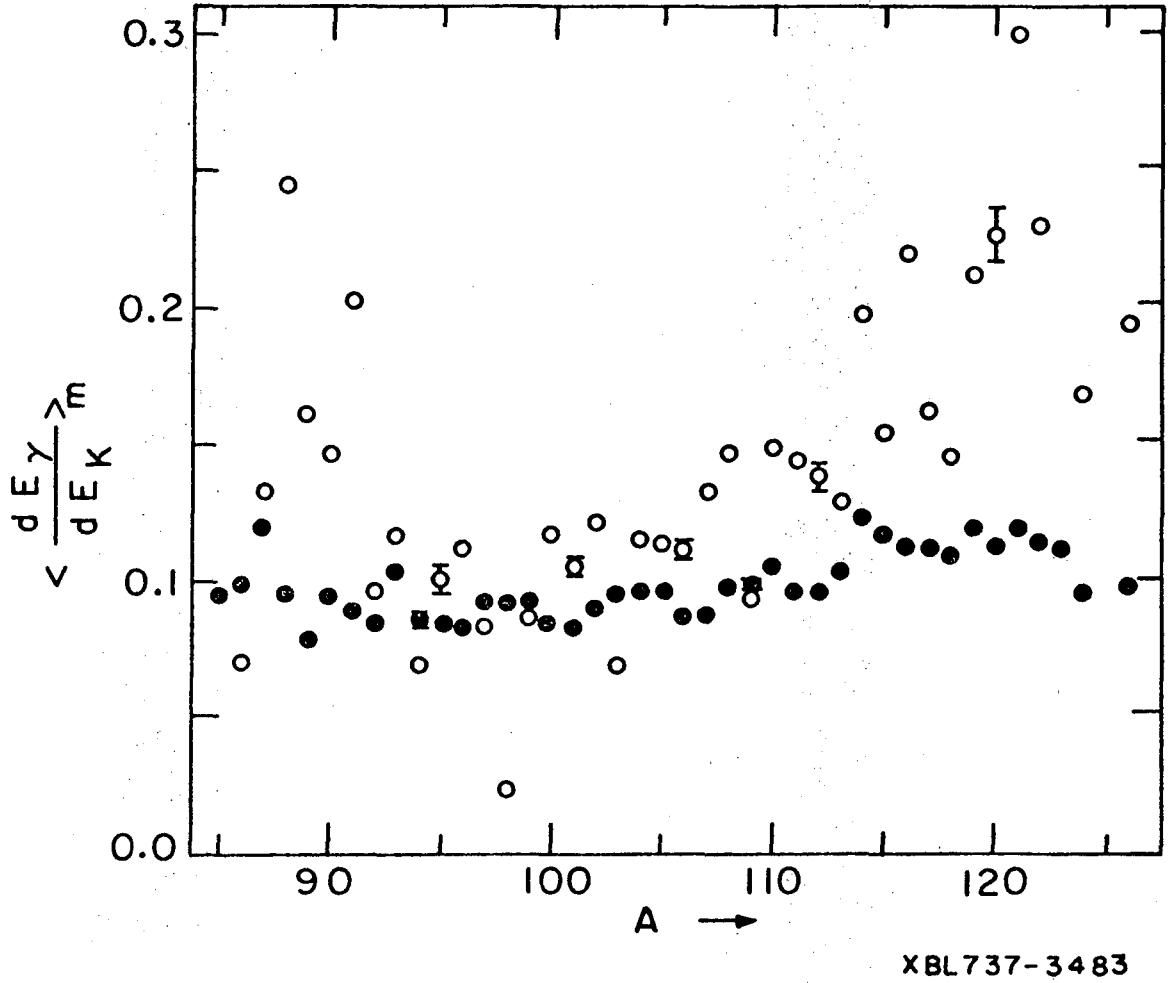
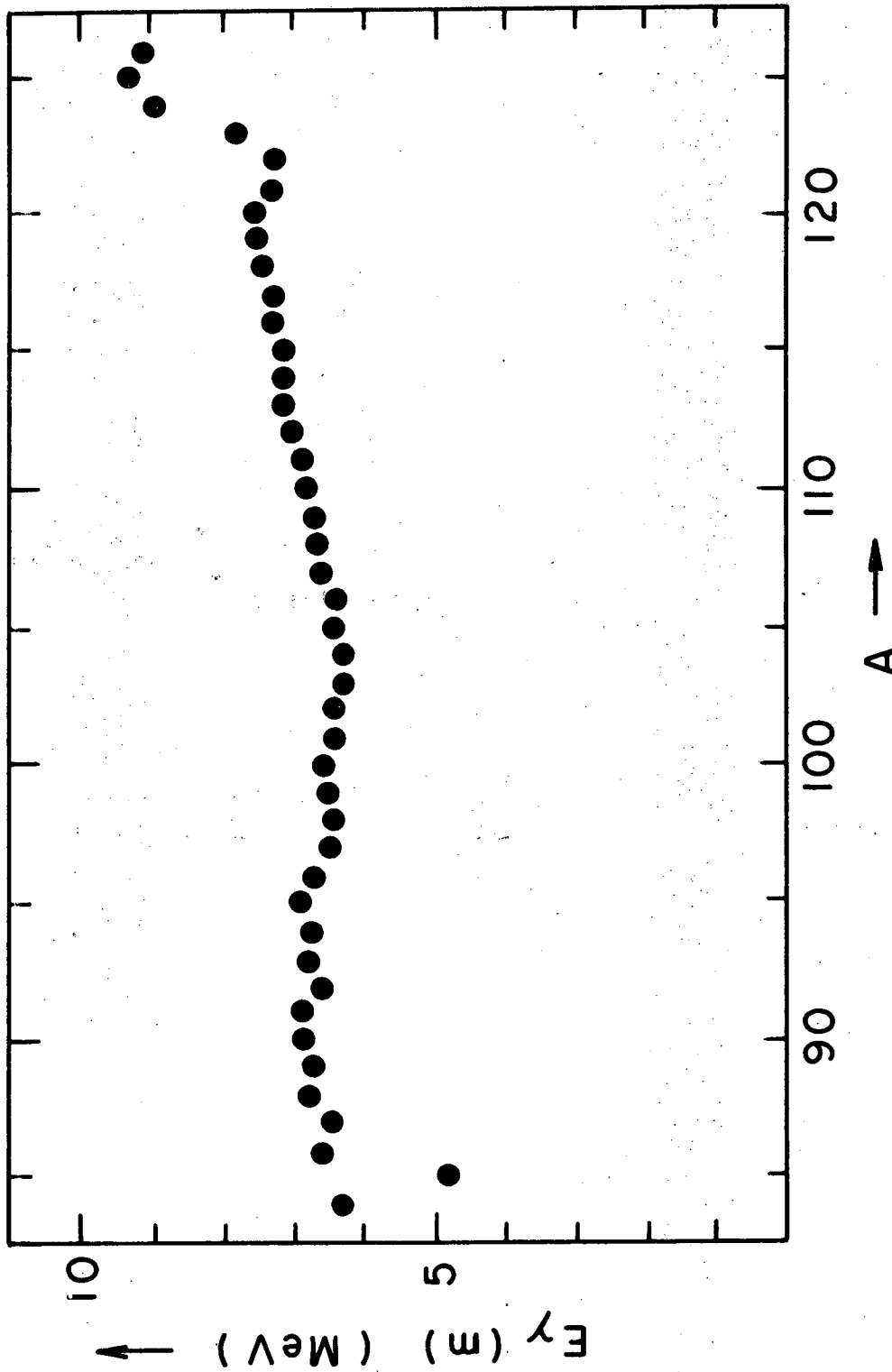
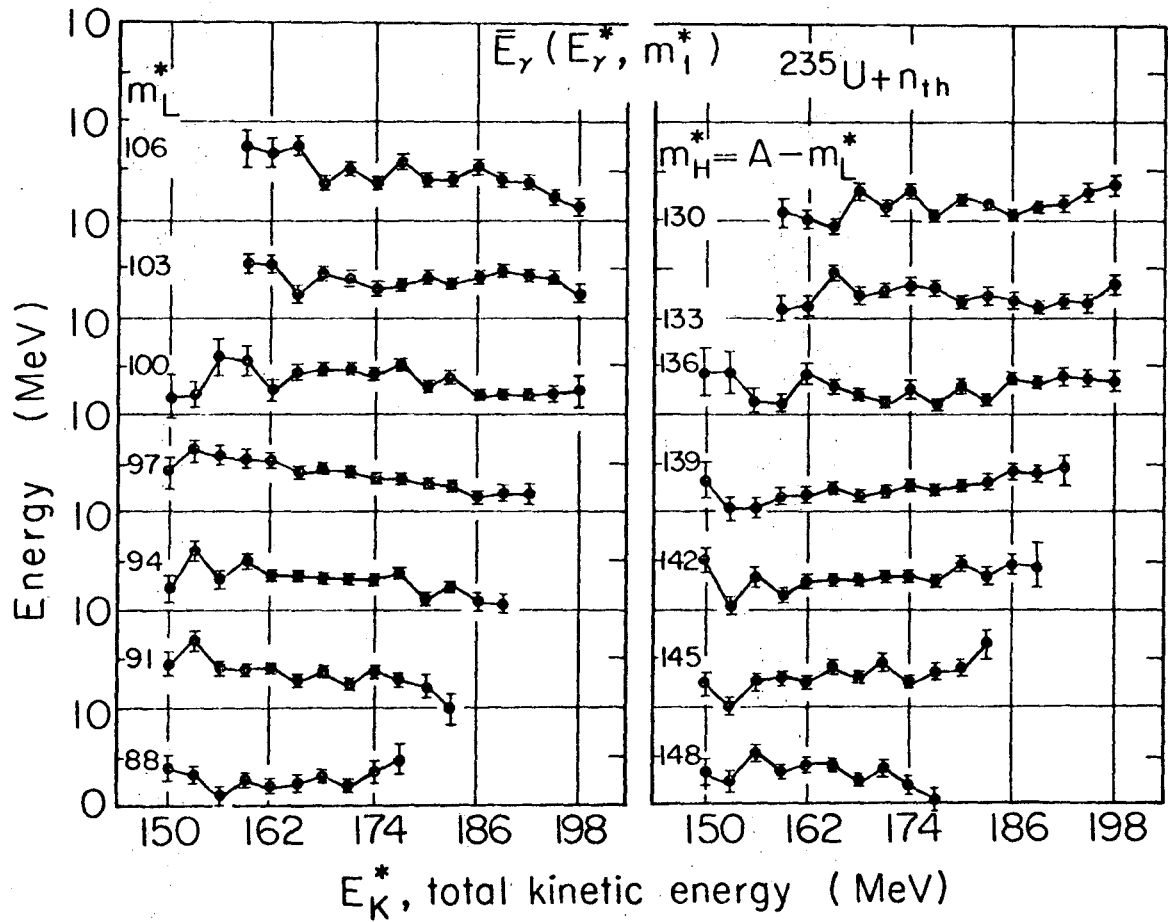


Fig. 15a



XBL737-3390

Fig. 15b

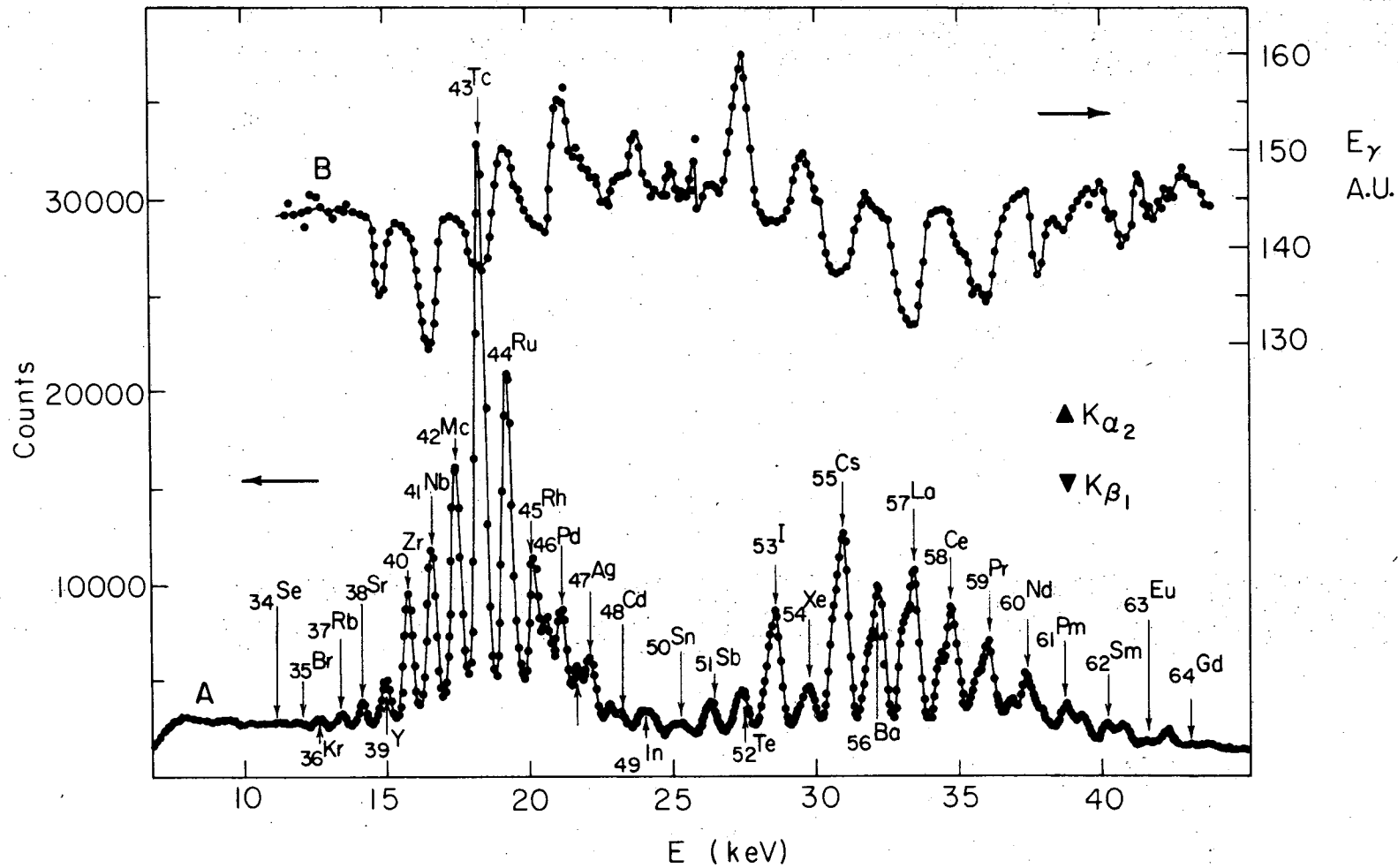


XBL737-3478

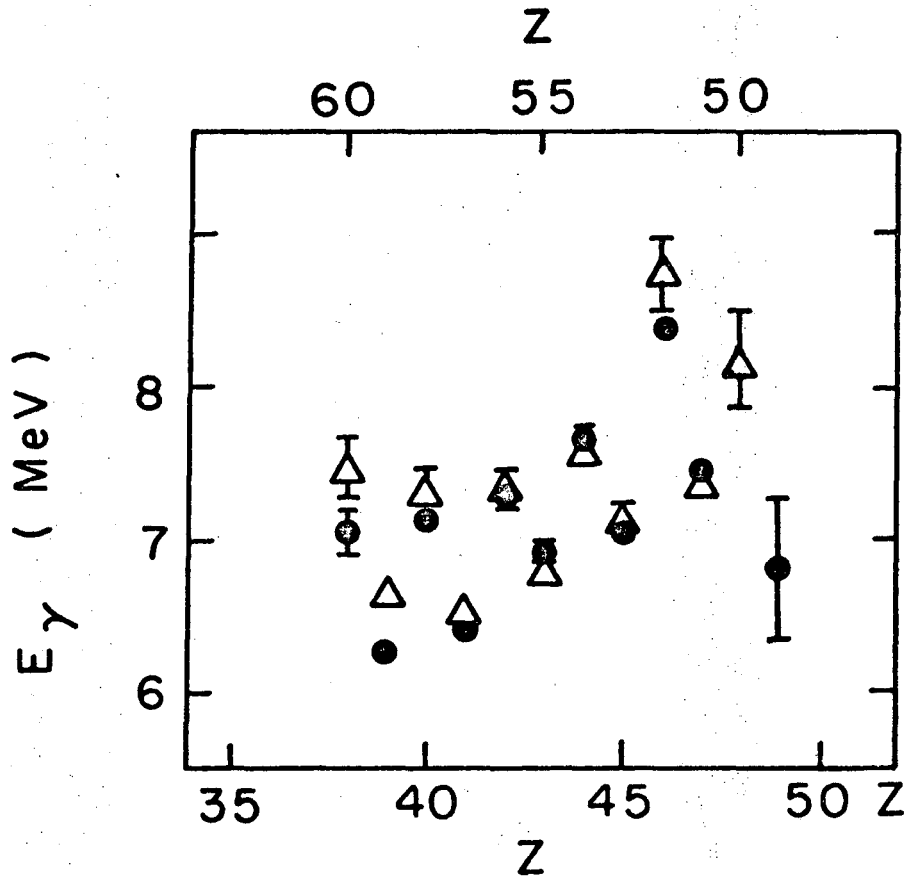
Fig. 16



Fig. 17

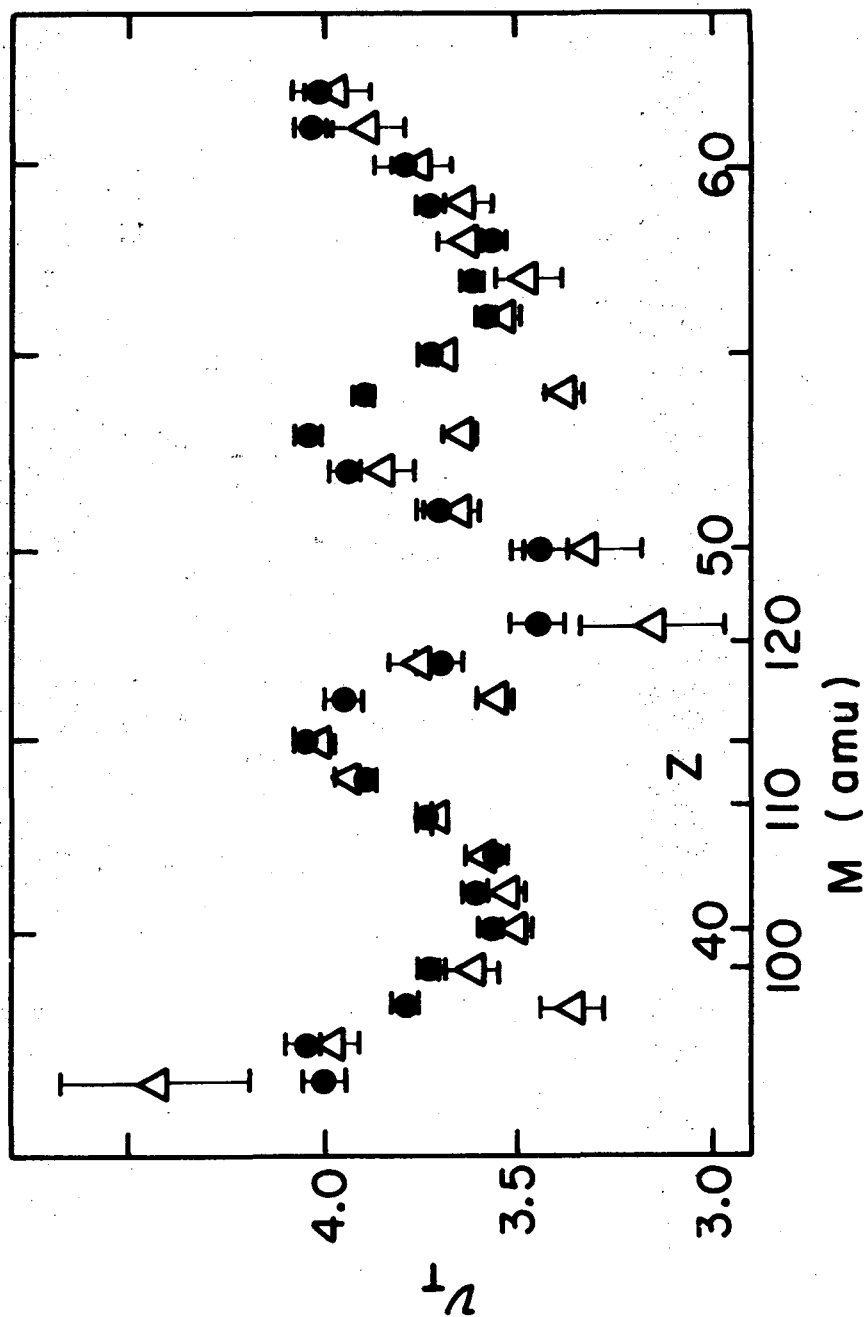


XBL737- 3488



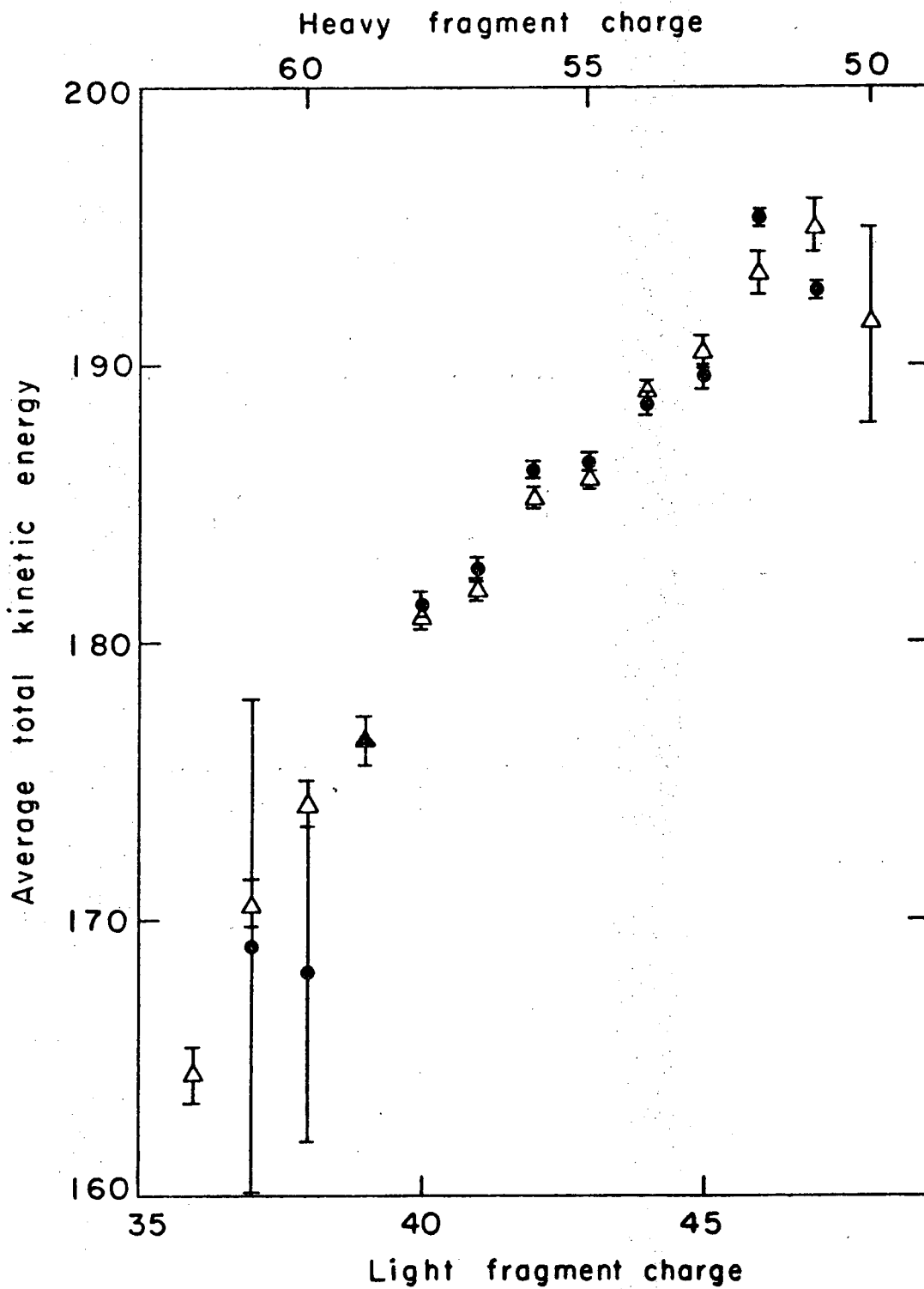
XBL737-3395

Fig. 18



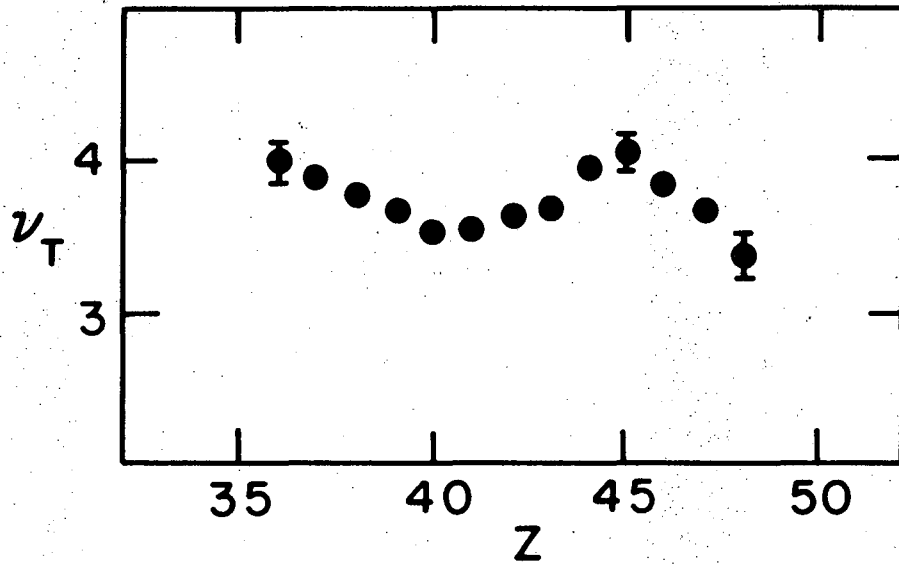
XBL737 - 3394

Fig. 19



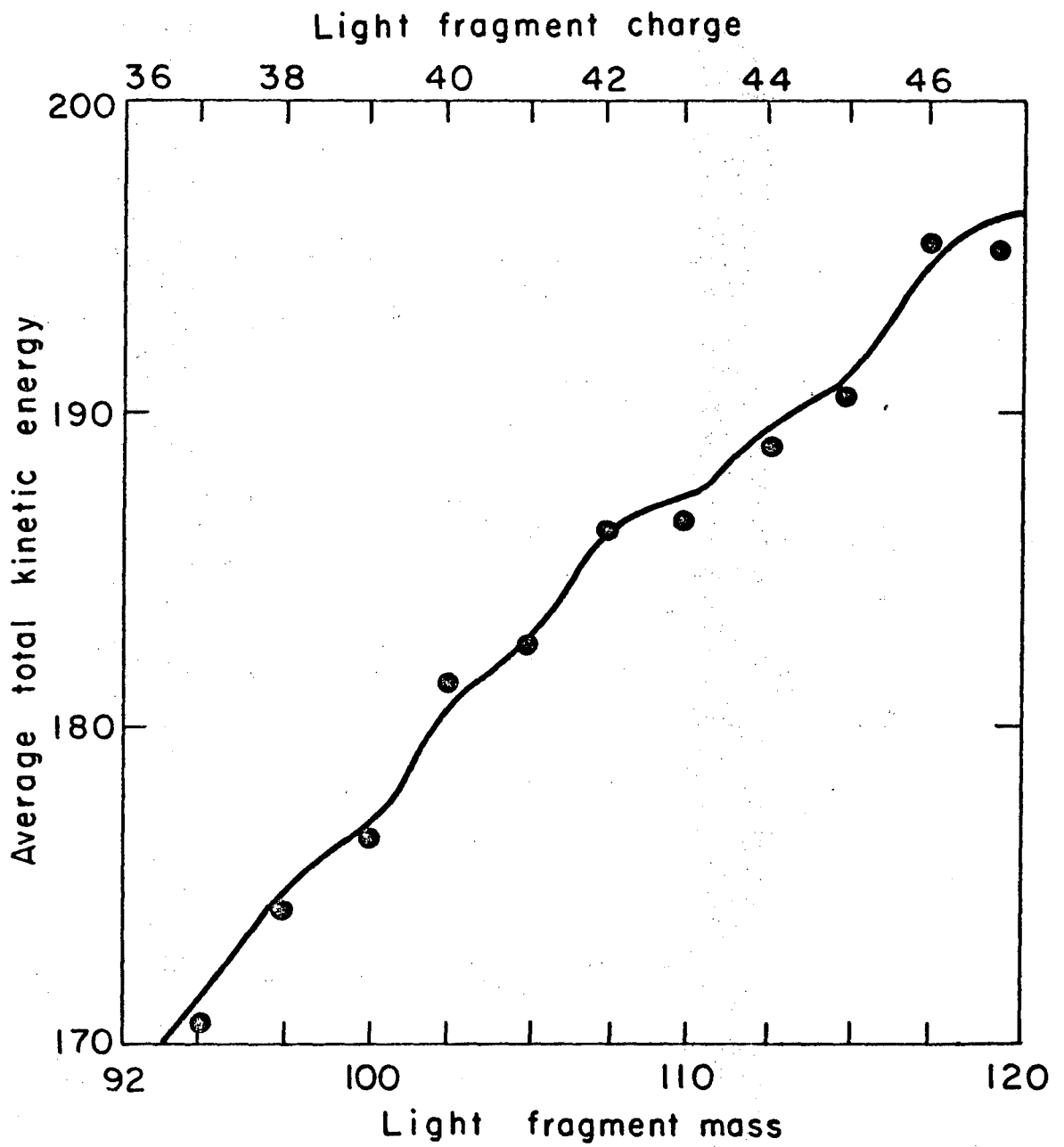
XBL737-3469

Fig. 20



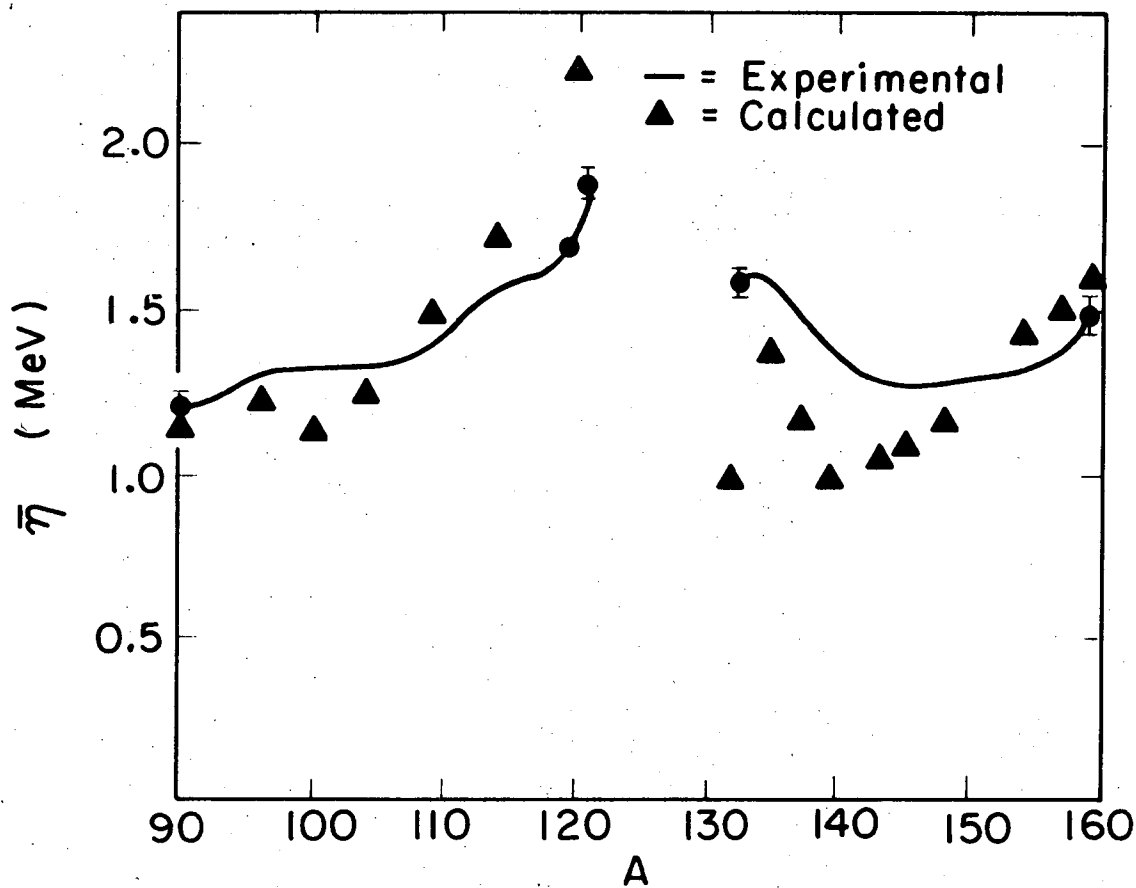
XBL 737- 3393

Fig. 21



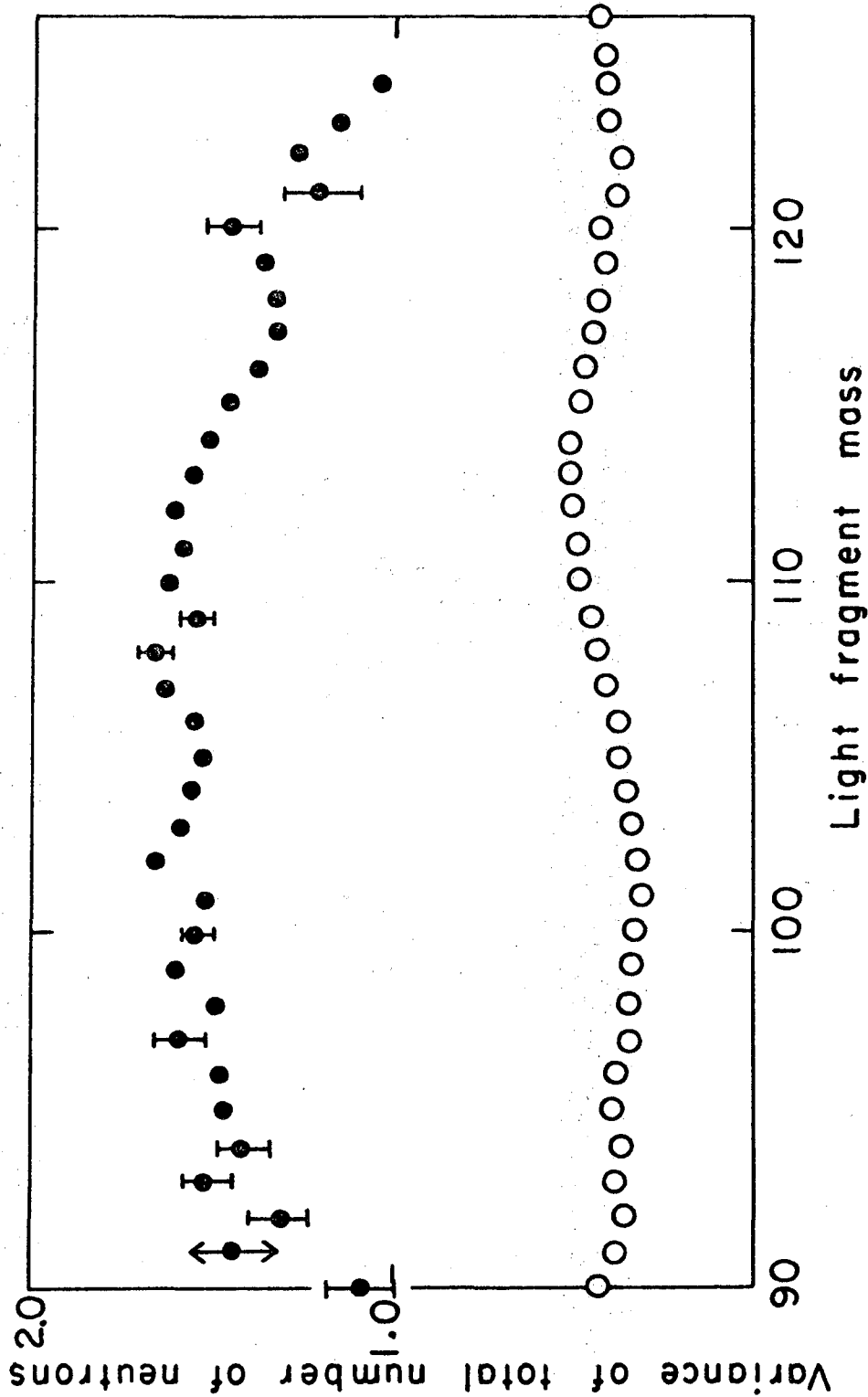
XBL737-3464

Fig. 22



XBL737-3392

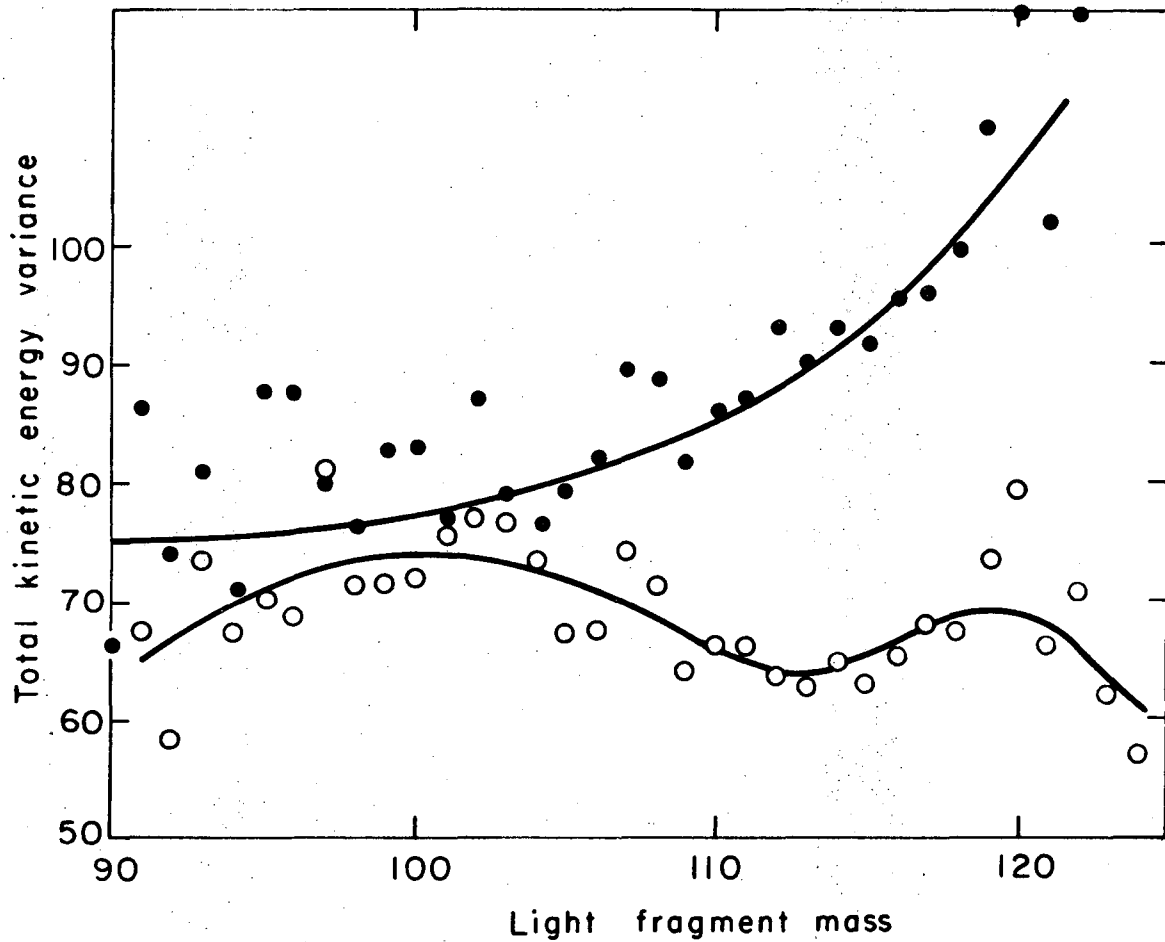
Fig. 23



XBL737-3465

Fig. 24





XBL737-3472

Fig. 25

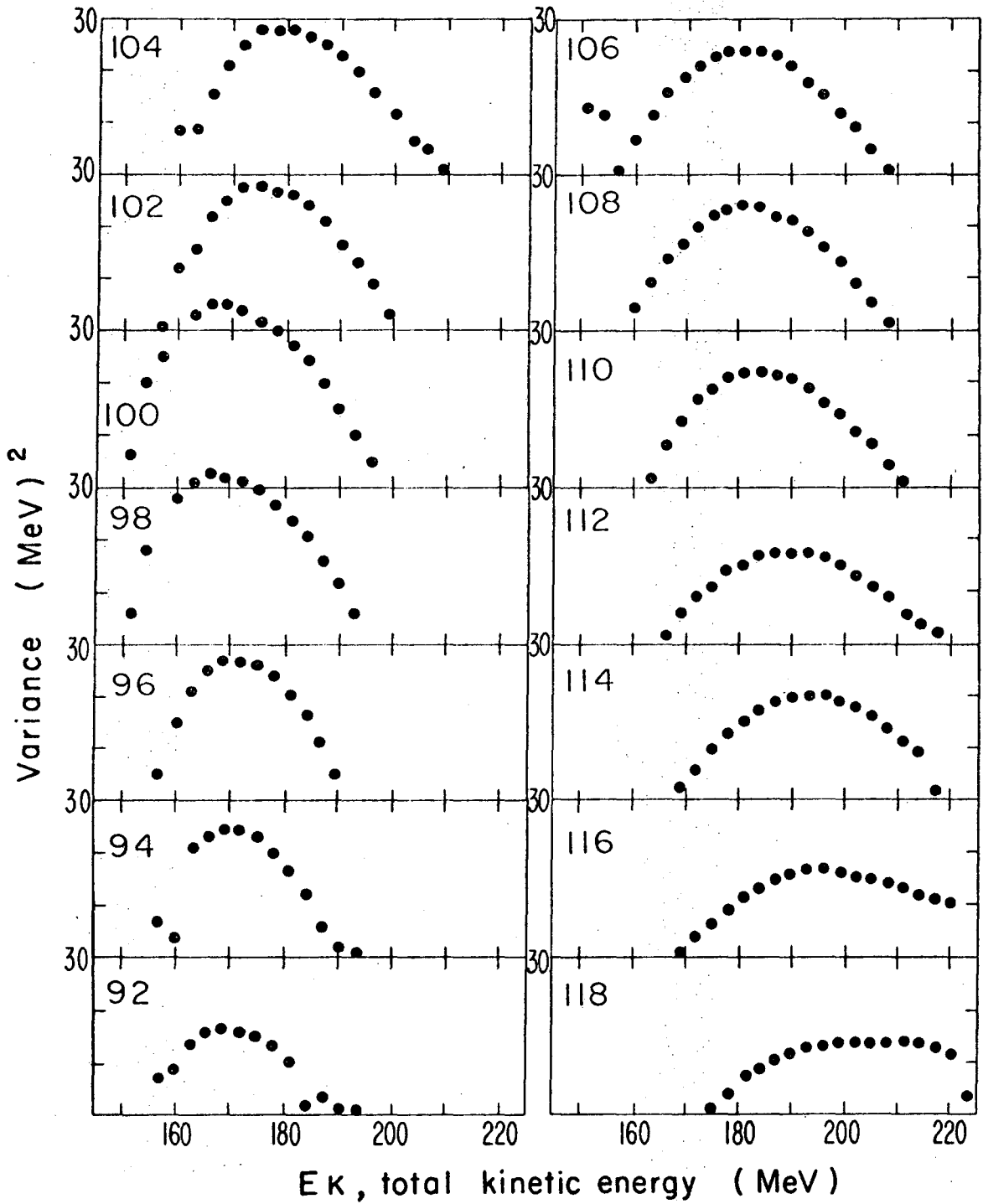
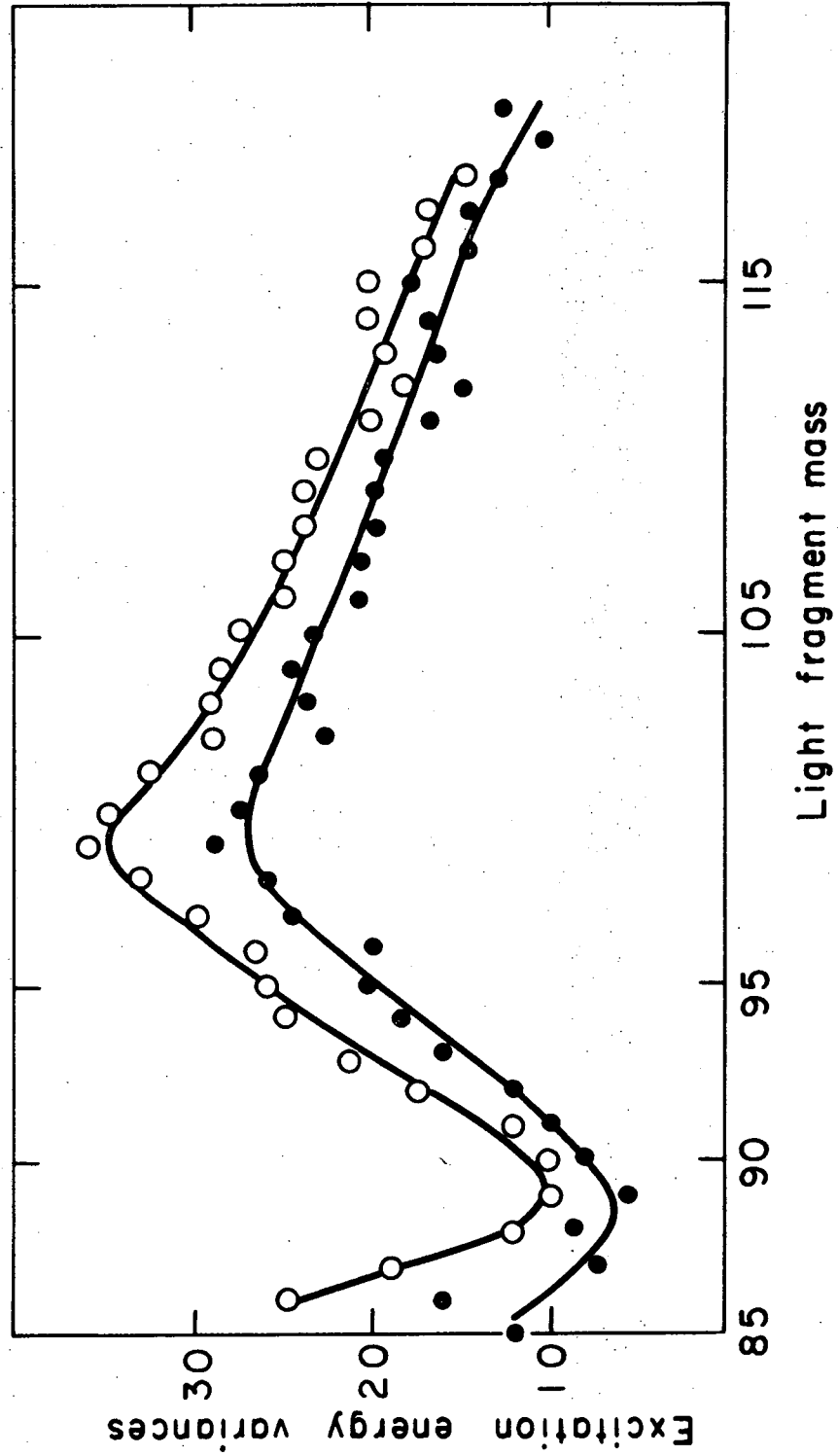
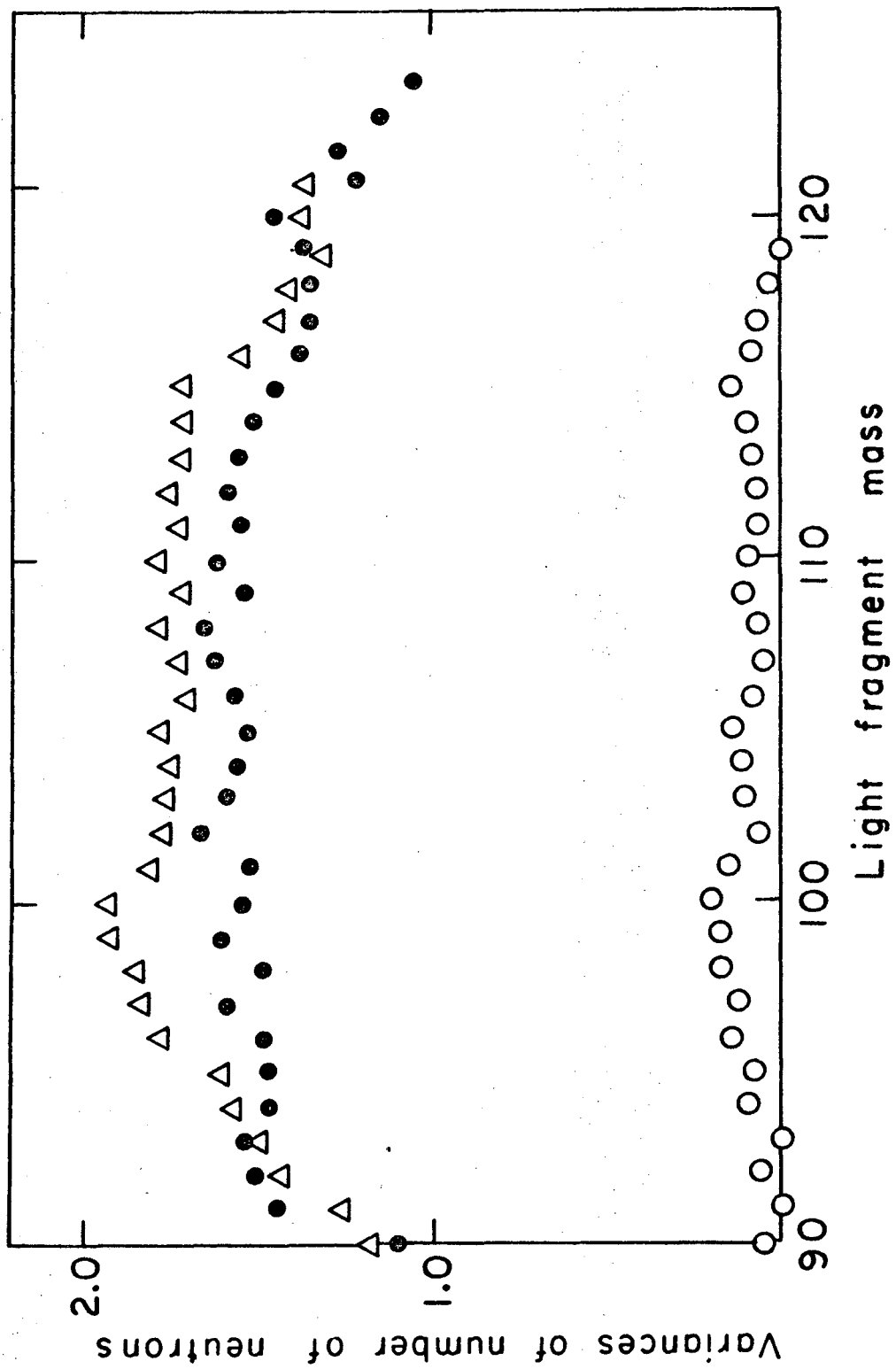


Fig. 26



XBL737-3463

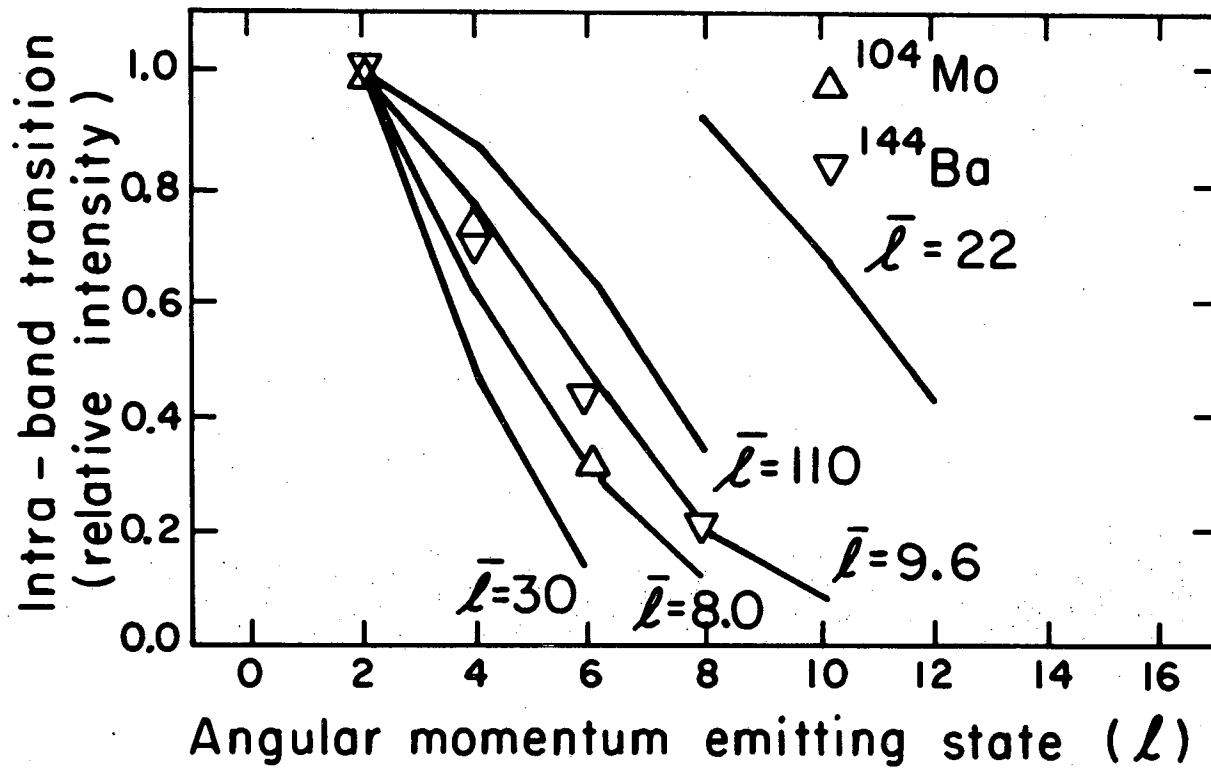
Fig. 27



XBL737-3489

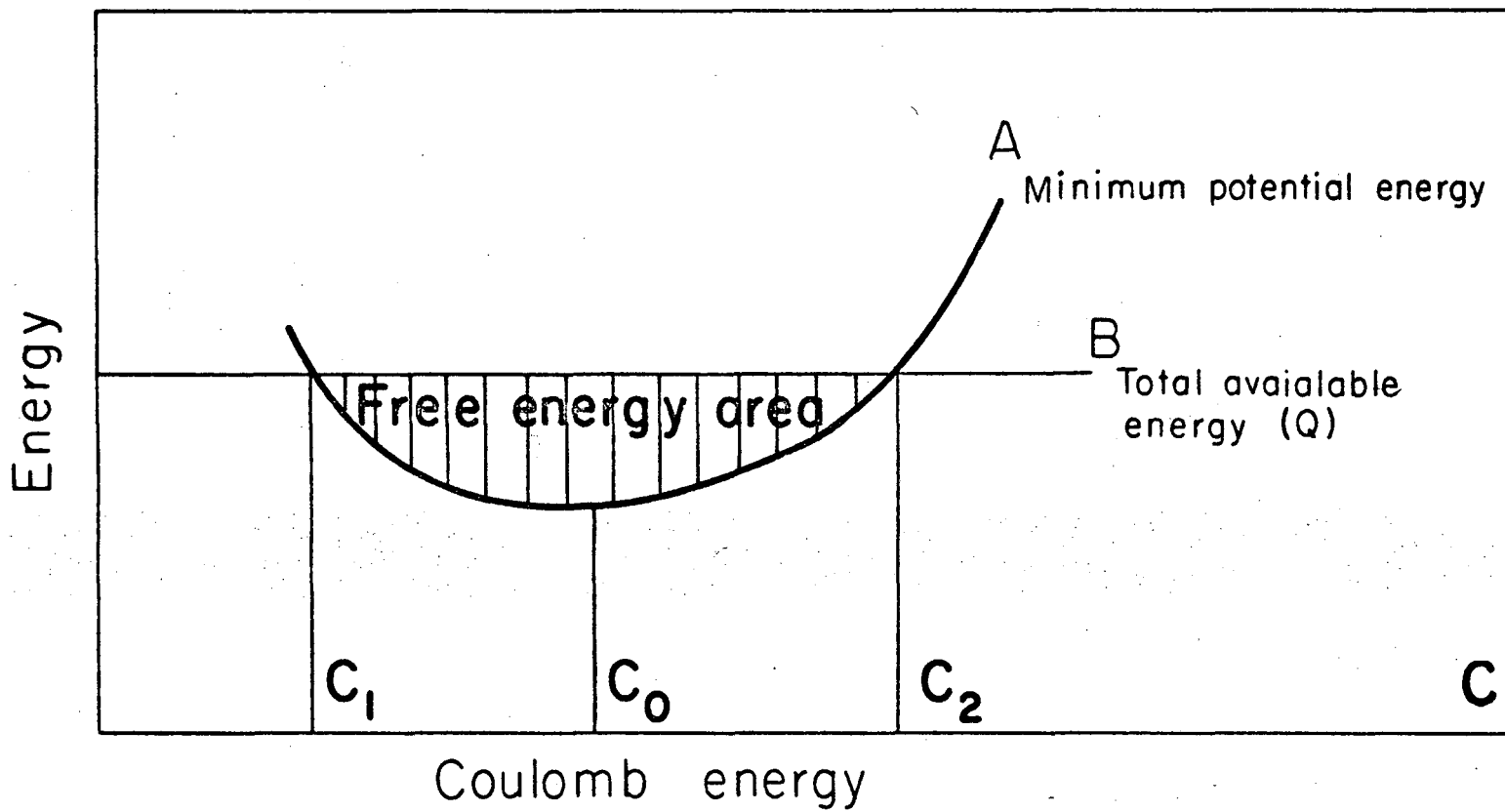
Fig. 28

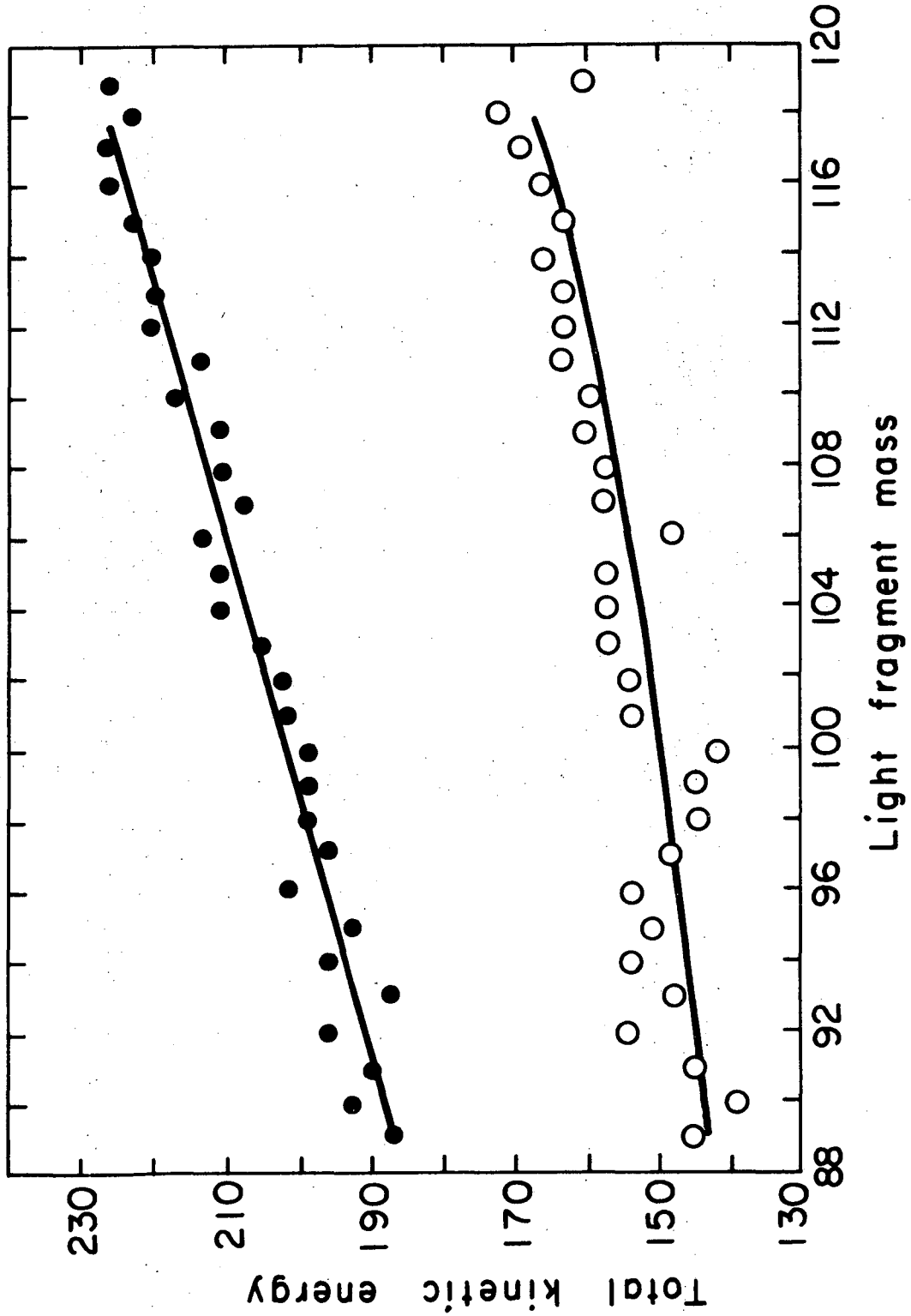
FIG. 29



XBL737-3473

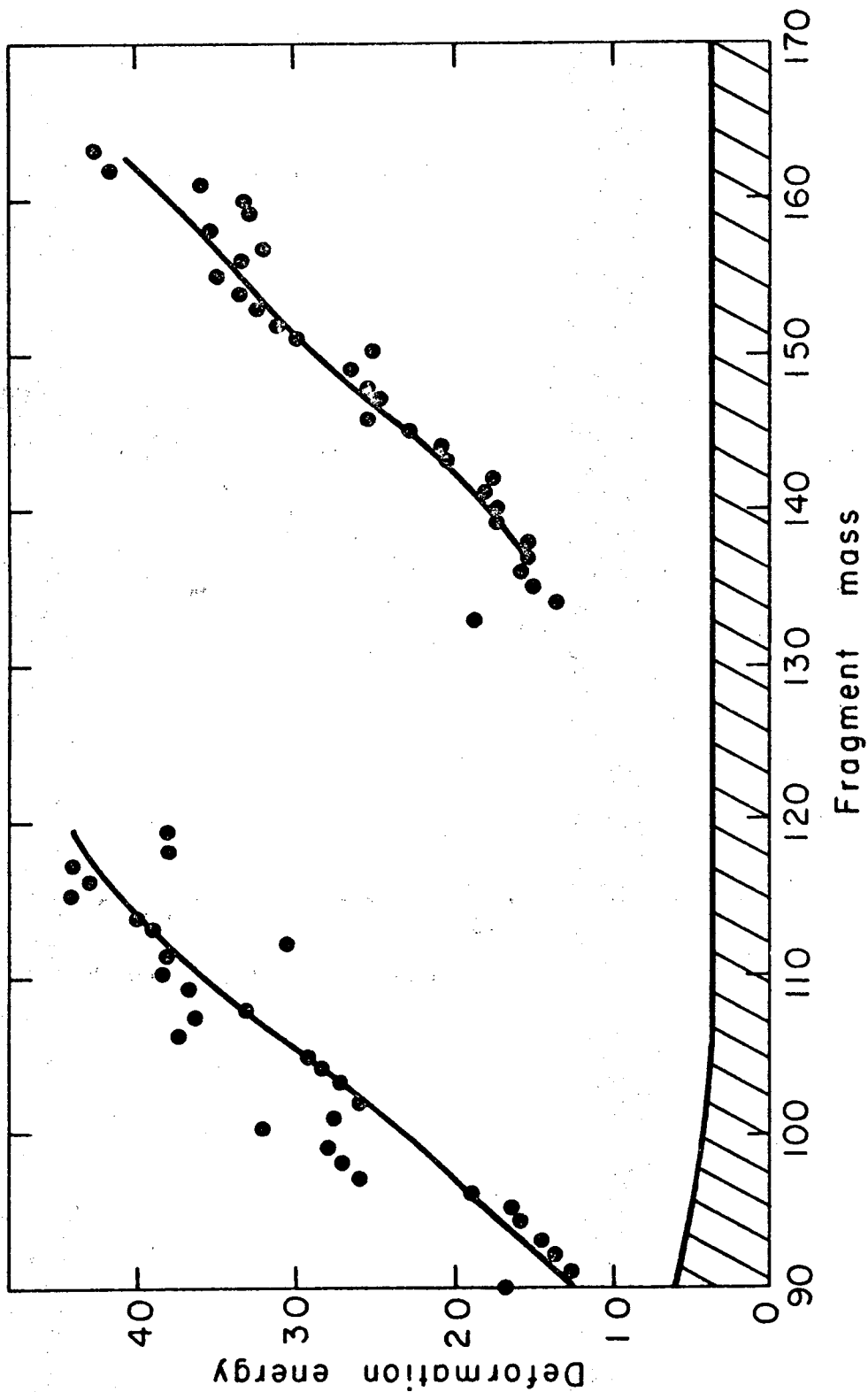
Fig. 30





XBL737-3470

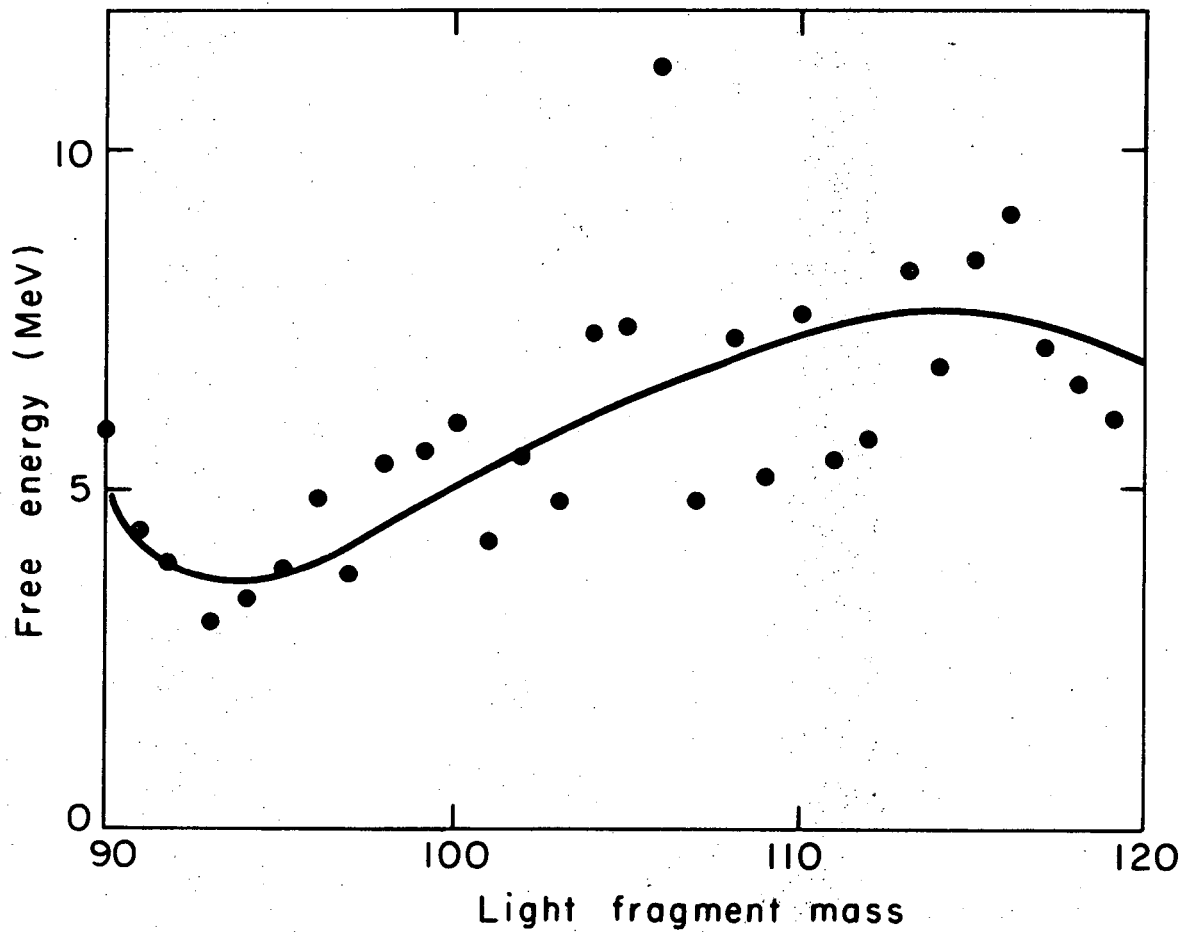
Fig. 31a



XBL737-3474

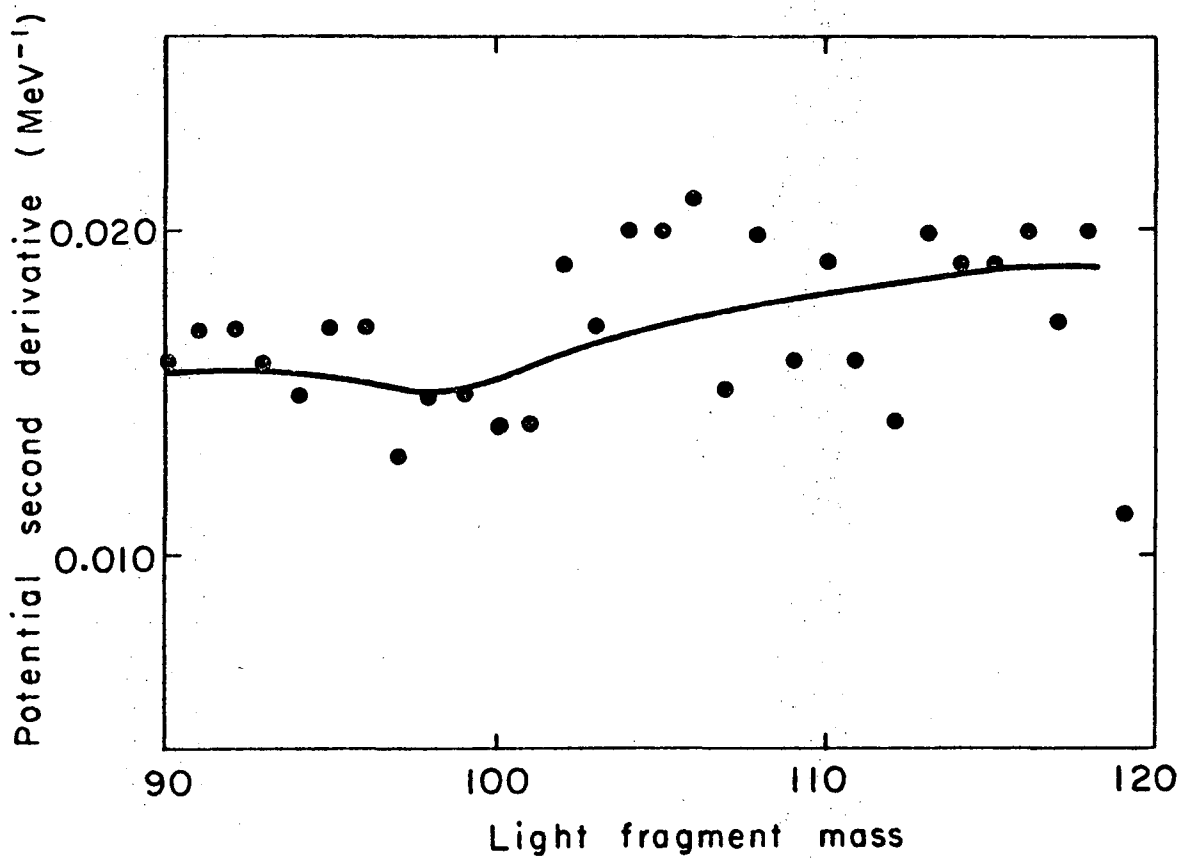
Fig. 3lb





XBL737-3475

Fig. 32a



XBL737-3471

Fig. 32b

LEGAL NOTICE

*This report was prepared as an account of work sponsored by the United States Government. Neither the United States nor the United States Atomic Energy Commission, nor any of their employees, nor any of their contractors, subcontractors, or their employees, makes any warranty, express or implied, or assumes any legal liability or responsibility for the accuracy, completeness or usefulness of any information, apparatus, product or process disclosed, or represents that its use would not infringe privately owned rights.*

TECHNICAL INFORMATION DIVISION  
LAWRENCE BERKELEY LABORATORY  
UNIVERSITY OF CALIFORNIA  
BERKELEY, CALIFORNIA 94720